

**Genesis of Tin - Tungsten Deposits and their Associated  
Granitoids**

**Proceedings of Joint Meeting of Working Groups 2 & 4  
IGCP Project 220**

**" Correlation and Resource Evaluation of Tin/ Tungsten Granites  
in Southeast Asia and the Western Pacific Region "**

**30th June - 2nd July, 1986, Canberra, Australia.**

**Bureau of Mineral Resources Record 1986/10**



**\* R 8 6 0 1 0 0 1 \***

© Commonwealth of Australia, 1990

This work is copyright. Apart from any fair dealing for the purposes of study, research, criticism or review, as permitted under the Copyright Act, no part may be reproduced by any process without written permission. Inquiries should be directed to the Principal Information Officer, Bureau of Mineral Resources, Geology and Geophysics, GPO Box 378, Canberra, ACT 2601.

# CONTENTS

	Page
<b>Conference Programme</b> .....	i
<b>Anderson J. A.</b> The geology and geochemistry of the Zeehan sulphide-tin deposits, NW Tasmania. (Australia).....	1
<b>Anderson J. A.</b> The granitoid association of scheelite mineralisation in the Ardlethan-Kikoira district, central NSW. (Australia).....	3
<b>Andrew A. S</b> , Pollard P.J. & Taylor R.G. . Closed -system behaviour for the tin-tungsten system at Zaaipplaats, South Africa. ....	5
<b>Bai Zhenghua</b> , Zhang Zheru, Zhang Zhengen, Yan Rongxiu Thermodynamic analysis of ore-forming conditions and the sulfur isotope system in the Dachang ore field, China. ....	7
<b>Blevin P.</b> Geometry of the Bamford Hill granite-hosted greisen system, North Queensland. (Australia).....	8
<b>Blevin P.</b> Behaviour of the K-feldspars in the Bamford Hill W-Mo-Bi granite-hosted mineralising system, North Queensland , Australia.....	10
<b>Collins P L.F.</b> Two contrasting tin-tungsten metallogenic provinces in Tasmania. (Australia).....	12
<b>Creech M</b> , Sangameshwar S & Marshall B. Silixite geology and mineralisation. ....	14
<b>Eadington P.</b> Some hydrothermal reactions that contribute to the mineral composition of tin ores in granites . ....	16
<b>Eggleston T</b> & Norman D . The Taylor Creek Tin Deposits (USA): Products of magmatic processes. ....	18
<b>Etminan H.</b> & Higgins N.C. The composition of ore fluids in the Mt Paynter tin/tungsten deposit, NSW. (Australia).....	20
<b>Haapala I.</b> On the origin of albite in mineralized granites. ....	22
<b>Hajataheri J.</b> & Solomon M. Emplacement and chemical evolution of the Heemskirk granite and associated tin and tungsten deposits . (Australia).....	24

<b>Halley S., Walshe J.L. &amp; Solomon M.</b> Skarn paragenesis and cassiterite precipitation at Mt Bischoff, Tasmania. (Australia).....	25
<b>Heinrich C.</b> Some thermodynamic and mass-balance considerations on the hydrothermal precipitation of cassiterite.....	26
<b>Higgins N.C. &amp; Forsythe D.F.</b> Paragenesis and mineral zoning in the Mt Carbine tungsten deposit, Nth Queensland. (Australia).....	28
<b>Higgins N.C. &amp; Solomon M.</b> The genesis of the clay deposits of N.E. Tasmania (Australia): A product of low temperature hydrothermal alteration ?.....	30
<b>Holyland P.</b> Interconnected hydrothermal drainage of the Pine Hill Intrusive Group. (W. Tasmania, Australia).....	32
<b>Kigai I.N.</b> Some geologic constraints of genetic concepts for tin deposits. ....	34
<b>Kigai I.N. &amp; Baskina V.A.</b> Tin and tungsten deposits of the Soviet Far East and their relationship to granitoids. ....	36
<b>Kwak T.</b> Granites associated with W-Sn skarns. ....	38
<b>Large R.R.</b> Integration of Geology and Geophysics in the development of exploration models for massive sulphide tin deposits in Western Tasmania. (Australia).....	40
<b>Liu Chanshi, Zhu Jinchu &amp; Cai Dekun.</b> Lancang River granitoid belt and its tin mineralisation, Western Yunnan, China.....	41
<b>MacKenzie D.</b> Magmatic evolution of the Poimena Granite and associated tin-bearing alkali feldspar granites, N.E. Tasmania (Australia)...	43
<b>Minlu Fu</b> .The sources of ore forming elements in the Dachang Tin field, China. ....	45
<b>Moon K.J.</b> Tungsten mineralization in South Korea. ....	47
<b>Neiva A.M.R.</b> Geochemistry of micas from Portuguese tin and tungsten deposits. ....	49
<b>Norman D.I. &amp; Mearns E.</b> Genesis of the Mayo-Darle Sn deposit, Cameroon. ....	51
<b>Nozawa T.</b> Asymmetry of centred plutons in Japan. ....	52

<b>Partington G.A.</b> The tectonic controls on the intrusion of specialized pegmatites in the Greenbushes pegmatite district, Western Australia. ....	53
<b>Partington G.A.</b> Geochronology of the Balingup metamorphic belt: Constraints on the Temporal Evolution of the Greenbushes pegmatite district.(W.Australia) .....	55
<b>Pei Rongfu</b> , Wu Liangshi, Zhao Yu: Tectonic environment and features of granite emplacement and related mineralization in South China..	57
<b>Praditwan J.</b> Mineral distribution study for cassiterite and associated heavy minerals in Phuket, Thailand. ....	59
<b>Putthapiban P.</b> The possible age of the maximum Sn/W mineralization on Phuket Island, Thailand. ....	61
<b>Ren S.K &amp; Walshe J.L.</b> Geology , brecciation and paragenesis of the Ardlethan tin field. (NSW,Australia) .....	63
<b>Sato K &amp; Shibata K.</b> Oxidised and reduced granitoids from the Kofu complex, central Japan. ....	65
<b>Schwartz M.O &amp; Surjuno.</b> Geochemistry of the Nam Salu horizon, Kelapa Kampit, Belitung, Indonesia. ....	67
<b>Scott K</b> Phyllosilicate and rutile chemistry as indicators of Sn-specialization in SE Australian granitoids. ....	69
<b>Sun S-S, Higgins N.C. &amp; McCulloch M.T.</b> Nd and Sr isotope study of granitoids of the Blue Tier and Eddystone Batholiths, N.E. Tasmania, (Australia) and associated Sn-W mineralisation. ....	71
<b>Trudu A.G. &amp; Clark A.H.</b> The evolution of the K-1 orebody (western sector) and the origin of the Felbertal (Mittersill) tungsten deposit.(Austria).....	73
<b>Tulloch A.J. &amp; MacKenzie I.F.</b> Tin-tungsten mineralised granites in New Zealand. ....	75
<b>Wyborn D.</b> Fractionation and mineralisation in the Boggy Plains zoned pluton. (NSW, Australia).....	77
<b>Wyborn L.A.I , Chappell B.W &amp; Wyborn D.</b> Primary magmatic control on the distribution of Sn deposits of the Lachlan fold belt in N.S.W and Victoria. (Australia).....	78

<b>Xu Keqin</b> , Sun Mingzhi & Cheng Hai. A general survey of tungsten deposits of China. ....	80
<b>Zaw K</b> . Geological, petrological and geochemical characteristics of granitoid rocks in Burma, with special reference to the emplacement of W-Sn mineralisation. ....	82
<b>Zhu Jinchu</b> , Xu Keqin, & Zhu Zhengshu. Preliminary studies on geology and geochemistry of two types of porphyry tin deposits in Southern China. ....	84

1

## **IGCP 220 Conference Programme**

**Monday 30th June**

**Venue: Haydon-Allen Lecture Theatre, ANU**

**8.30-8.45 AM Opening Address**

**Chairman : M. Solomon**

**8.45-9.30 AM Keynote Address**

**Xu Keqin**, Sun Mingzhi & Cheng Hai. A general survey of tungsten deposits of China.

### **Session 1A: Petrology of Mineralised Granitoids**

**9.30-10.00 AM**

**Nozawa T.** Asymmetry of centred plutons in Japan.

**10.00-10.30 AM**

**Sato K & Shibata K.** Oxidised and reduced granitoids from the Kofu complex, central Japan.

**Morning Tea**

**11.00-11.30 AM**

**Kwak T.** Granites associated with W-Sn Skarns

**11.30-12.00 AM**

**Creech M**, Sangameshwar S & Marshall B. Silicite geology and mineralisation.

**12.00-12.30 PM**

**Wyborn L.A.I**, Chappell B.W & Wyborn D. Primary magmatic control on the distribution of Sn deposits of the Lachlan fold belt in N.S.W and Victoria (Australia).

**Lunch**

**Chairman : R.G. Taylor**

**1.30-2.00 PM**

**Anderson J. A.** The granitoid association of scheelite mineralisation in the Ardlethan-Kikoira district, central NSW (Australia).

**2.00-2.30 PM**

**Blevin P.** Behaviour of the K-feldspars in the Bamford Hill W-Mo-Bi granite - hosted mineralising system, North Queensland, Australia.

**2.30-3.00 PM**

**MacKenzie D.** Magmatic evolution of the Poimena Granite and associated tin-bearing alkali feldspar granites, N.E. Tasmania (Australia).

**Afternoon Tea****3.30-4.00 PM**

**Sun S-S, Higgins N.C. & McCulloch M.T.** Nd and Sr isotope study of granitoids of the Blue Tier and Eddystone Batholiths, N.E. Tasmania, (Australia) and associated Sn-W mineralisation.

**4.00-4.30 PM**

**Andrew A. S. , Pollard P.J. & Taylor R.G. .** Closed -system behaviour for the tin-tungsten system at Zaaipplaats, South Africa.

**4.30-5.00 PM**

**Haapala I.** On the origin of albite in mineralized granites.

**5.00-5.30 PM**

**Hajataheri J. & Solomon M.** Emplacement and chemical evolution of the Heemskirk granite (Australia) and its associated tin and tungsten deposits.



**Monday, 30th June**

**Venue: Lecture Theatre G27 , Haydon-Allen Building**

**Chairman: P. Pollard**

**Session : 1B -General**

**9.30-10.00 AM**

**Kigai I.N.** Some geologic constraints of genetic concepts for tin deposits

**10.00-10.30 AM**

**Pei Rongfu**, Wu Liangshi, Zhao Yu: Tectonic environment and features of granite emplacement and related mineralization in South China.

**Morning Tea**

**10.30-11.00 AM**

**Putthapiban P.** The possible age of the maximum Sn/W mineralization on Phuket Island, Thailand.

**11.30-12.00 AM**

**Collins P L.F.** Two contrasting Tin-Tungsten metallogenic provinces in Tasmania (Australia).

**12.00-12.30 PM**

**Large R.R.** Integration of Geology and Geophysics in the development of exploration models for massive sulphide tin deposits in Western Tasmania, (Australia)

**Lunch**

**1.30-2.00 PM**

**Praditwan J.** Mineral distribution study for cassiterite and associated heavy minerals in Phuket, Thailand.

**2.00-2.30 PM**

**Wyborn D.** Fractionation and mineralisation in the Boggy Plains zoned pluton (NSW, Australia)

**2.30-3.00 PM**

**Scott K.** Phyllosilicate and rutile chemistry as indicators of Sn-specialization in SE Australian granitoids.

**Afternoon Tea**

**3.30-4.00 PM**

**Moon K.J.** Tungsten mineralization in South Korea.

**4.00-4.30 PM**

**Zaw K.** Geological, petrological and geochemical characteristics of granitoid rocks in Burma, with special reference to the emplacement of W-Sn mineralisation.

**4.30-5.00 PM**

**Liu Chanshi, Zhu Jinchu & Cai Dekun.** Lancang River granitoid belt and its tin mineralisation, Western Yunnan, China.

**5.00-5.30 PM**

**Tulloch A.J. & MacKenzie I.F.** Tin-tungsten mineralised granites in New Zealand.

**Tuesday, 1st July**

**Venue: Haydon-Allen Lecture Theatre, ANU**

**Chairman: N.C. Higgins**

**8.45-9.30 AM Keynote Address**

**Kigai I.N. & Baskina V.A.** Tin and tungsten deposits of the Soviet Far East and their relationship to granitoids.

**Session 2: Tin/Tungsten Ore Deposits**

**9.30-10.00 AM**

**Partington G.A.** The tectonic controls on the intrusion of specialized pegmatites in the Greenbushes pegmatite district, Western Australia.

**10.00-10.30 AM**

**Partington G.A.** Geochronology of the Balingup metamorphic belt: Constraints on the Temporal Evolution of the Greenbushes pegmatite district (Western Australia).

**Morning Tea**

**11.00-11.30 AM**

**Blevin P.** Geometry of the Bamford Hill granite-hosted greisen system, North Queensland, (Australia)

**11.30-12.00 AM**

**Higgins N.C. & Forsythe D.F.** Paragenesis and mineral zoning in the Mt Carbine tungsten deposit, Nth Queensland, (Australia).

**12.00-12.30 PM**

**Eggleston T & Norman D.** The Taylor Creek Tin Deposits (USA): Products of magmatic processes.

**Lunch**

**Chairman: T. Kwak**

**1.30-2.00 PM**

**Norman D.I. & Mearns E.** Genesis of the Mayo-Darle Sn deposit, Cameroon.

**2.00-2.30 PM**

**Anderson J. A.** The geology and geochemistry of the Zeehan sulphide-tin deposits, NW Tasmania, (Australia)

**2.30-3.00 PM**

**Ren S.K & Walshe J.L.** Geology , brecciation and paragenesis of the Ardlethan tin field, (NSW, Australia)

**Afternoon Tea****3.30-4.00 PM**

**Minlu Fu** .The sources of ore forming elements in the Dachang tin field, China

**4.00-4.30 PM**

**Neiva A.M.R.** Geochemistry of micas from Portuguese tin and tungsten deposits.

**4.30-5.00 PM**

**Trudu A.G. & Clark A.H.** The evolution of the K-1 orebody (western sector) and the origin of the Felbertal (Mittersill) tungsten deposit (Austria)

**5.00-5.30 PM**

**Schwartz M.O & Surjuno.** Geochemistry of the Nam Salu horizon, Kelapa Kampit, Belitung, Indonesia.

**6.00 PM Conference Dinner**

Bus leaves the corner of Childers St and University Ave for 'The Carrington' at Bungendore, returning at 11 PM approximately.

**Wednesday, 2nd July**

**Venue: Haydon-Allen Lecture Theatre, ANU**

**Chairman: P.J. Eadington**

**8.45-9.30 AM Keynote Address**

**Zhu Jinchu**, Xu Keqin, & Zhu Zhengshu. Preliminary studies on geology and geochemistry of two types of porphyry tin deposits in Southern China.

**Session 3: Fluid / granite interaction and metal transport**

**9.30-10.00 AM**

**Bai Zhenghua**, Zhang Zheru, Zhang Zhengen, Yan Rongxiu. Thermodynamic analysis of ore-forming conditions and the sulfur isotope system in the Dachang ore field, China.

**10.00-10.30 AM**

**Eadington P.** Some hydrothermal reactions that contribute to the mineral composition of tin ores in granites

**Morning Tea**

**11.00-11.30 AM**

**Heinrich C.** Some thermodynamic and mass-balance considerations on the hydrothermal precipitation of cassiterite.

**11.30-12.00 AM**

**Holyland P.** Interconnected hydrothermal drainage of the Pine Hill Intrusive Group (W Tasmania, Australia).

**12.00-12.30 PM**

**Halley S.**, Walshe J.L. & Solomon M. Skarn paragenesis and cassiterite precipitation at Mt Bischoff, Tasmania, (Australia).

**Lunch**

**Chairman P.L.F. Collins**

**1.30-2.00 PM**

**Etminan H.** & Higgins N.C. The composition of ore fluids in the Mt Paynter tin/tungsten deposit, NSW, (Australia)

**2.00-2.30 PM**

**Higgins N.C.** & Solomon M. The genesis of the clay deposits of N.E. Tasmania (Australia): A product of low temperature hydrothermal alteration ?

**2.30-3.00 PM**

**Mahawat C.** Tin-tungsten mineralization in Northern Thailand.

**Afternoon Tea**

**3.30-5.00 PM** Business and Discussion and closing remarks.

## THE GEOLOGY OF THE ZEEHAN CASSITERITE-SULPHIDE DEPOSITS, TASMANIA

J.A. Anderson

Department of Geology and Geophysics, University of New England, 2351  
(on leave from Aberfoyle Resources Limited)

Three unexploited bodies of cassiterite-sulphide mineralisation (Queen Hill, Montana and Severn) were discovered beneath the flanks of Queen Hill during 1969-1976. The geological resource is estimated as 7.3 million tonnes averaging 0.7 % Sn. The bodies are central to the defunct Zeehan mining field which produced 15,000 tonnes of stannite ore, 200,000 tonnes Pb and 84,000 kg Ag from narrow pyrite siderite quartz galena lodes.

The three bodies have similar tabular morphologies with NE or E plunges resulting from easterly-dipping NW or NNE feeder fractures intersecting NE-striking host stratigraphies. Cassiterite is present as 20-70 micron disseminations in stockworks (Queen Hill, Severn) or massive replacements (Montana) by siderite quartz chlorite pyrite pyrrhotite, lesser sellaite fluorite tourmaline phlogopite sericite apatite galena sphalerite arsenopyrite marcasite and local minor stannite and silver sulphosalts. There is an upward and outward zonation from sellaite tourmaline pyrrhotite arsenopyrite (minor pyrite marcasite topaz) to siderite fluorite pyrite (minor pyrrhotite) to siderite pyrite galena sphalerite (minor stannite) in each body, reflecting the general paragenetic sequence. Pyrite is the dominant sulphide as pyrrhotite has undergone a substantial pyrite/marcasite retrogression such that the core of the larger Severn body produced the only magnetic signature.

An interbedded sequence ('Queen Hill Beds') of sideritised evaporite laminates, dolomicrites, framboidal pyrite laminates, shales and tilloidal diamictites hosts the Queen Hill body on the W side of the hill. The sequence is incorporated within splititised basaltic lavas and tuffs of the Montana Volcanics. The gypsum evaporites are bottom-nucleated, upright palmate and 'grassy' bladed forms characteristic of sea-marginal ponds (e.g. Friedman, 1980). The sideritisation of the evaporites is early diagenetic as it delicately replaces the gypsum blades, preserves interblade pyrite framboids, is cut by stylolites and remains as siderite outside the hydrothermal zone. Stromatolites are not yet recognised although there is an abundance of pre-graphite pyrobitumen which shows diagenetic and hydrothermally remobilised characteristics. The variety of lithologies represents rapidly fluctuating evaporitic, euxinic and deeper (glacio-?) marine conditions, similar to those demonstrated elsewhere in the Late Proterozoic (e.g. Walter and Bauld, 1983).

On the NE side of Queen Hill, the Montana mineralisation replaces massive dolomites within a 45m thick sequence ('Poverty Point Beds') including shales and interlaminated sandstone/siltstone. The Poverty Point Beds are correlated with the Success Creek Group as the sequence is conformably overlain by the shales and volcanoclastic wackes of the Cambrian Crimson Creek Formation and is considered to unconformably overlie the Oonah Quartzite and Slate (Brown, 1982; c.f. Blissett, 1962). A NNE fault disrupted the Poverty Point Beds and provided a locus for the Severn mineralisation within the hangingwall of Crimson Creek Formation, which was dragged into pseudo-conformity with the Oonah Quartzite and Slate along the fault. No evaporite and only minor possible syngenetic pyrite are evident in the Poverty Point Beds and the local Crimson Creek Formation.

A Late Proterozoic age is proposed for the Queen Hill sequence in contrast with the model of Lutley (1975), who correlated the Montana Volcanics with the Crimson Creek Formation and the Queen Hill Beds with the Poverty Points Beds by proposing an anticlinal closure over Queen Hill. Although evaporites and dropstones indicate a W-facing for the Queen Hill Beds as required by Lutley's model, the Queen Hill sequence is

part of the Oonah because:- 1) the spilites that host the Queen Hill Beds are a recognised regional component of the upper Oonah Quartzite and Slate, 2) the Oonah Quartzite and Slate contains thin evaporite beds in the vicinity of the Queen Hill Beds and 3) the different lithological and structural characters of the Queen Hill and Poverty Point sequences cannot be explained by facies changes over the proposed anticline. Structural investigation of any such mega-fold is hampered by the intense faulting, shearing and rafting of competent blocks in the phyllitic sections of the Oonah Quartzite and Slate.

An epigenetic hydrothermal origin for the cassiterite mineralisation is evidenced by the varying environments and ages of the host sediments, the overprinting and fault-controlled nature of the mineralisation and the similar vertical zonations of the mineralisation within the different hosts.

An underlying granitoid cupola is the likely source and pathway of the mineralisation as was proposed by Both and Williams (1968) to explain the stannite-bearing pyrite lodes which constitute an anomalous outlier to the regional zoning pattern. Although no dyke was intersected by the drilling to 450m depth and only one of the quartz porphyries reported by Waller (1903) is a likely source-related leucocratic granitoid, three coincident features which are centred on Queen Hill, support the cupola model. The features are:- 1) the three clustered cassiterite bodies, 2) an 8 square km Rb drainage anomaly and 3) a 130nT 1.8 km diameter magnetic anomaly. The latter is interpreted to be sourced by a 200m thick horizontal body which is likely to be a contact metamorphic aureole to a 600m diameter, 900m deep granitoid cupola. Additionally, the small siderite veins in the vicinity of the cassiterite deposits become pyrite dominant with depth, similar to the regional change towards the Heemskirk Granite.

#### References

- Blissett, A.H., 1962, One Mile Geol. Map Series -Zeehan; Explan. Rept. Geol. Surv. Tasm.
- Both, R.A. and Williams, K.L., 1968, J. Geol. Soc. Aust.,15(2), 217-243.
- Brown, A.V., 1982, Unpub. Rept. 1982/46; Geol. Surv. Tasm.
- Friedman, G.M., 1980, SEPM Spec. Publ.28, 69-80.
- Lutley, W.M., 1975, Unpubl. M.Sc. Thesis; Uni. of Adelaide.
- Waller, G.A., 1903, Geol. Sketch Plan Zeehan Mining Field; Govt. Printer, Hobart. .
- Walter, M.R., and Bauld, J., 1983, Precambrian Research,21, 129-148.



# THE GRANITOID ASSOCIATION OF SCHEELITE MINERALISATION IN THE ARDLETHAN-KIKOIRA DISTRICT, CENTRAL NEW SOUTH WALES

J.A. Anderson

Exploration Division, Aberfoyle Resources Limited

Large areas of subeconomic scheelite mineralisation were recently discovered 100 km N of the Ardlethan tin deposits, which provided the principal hardrock production (approx. 20,000 tonnes Sn) of the Mt. Wills-Tallebung tin province ('Wagga Tin Belt'). Regularly-spaced centres of scheelite mineralisation are associated with structurally controlled cupolas projecting from a narrow, 15 km long stock N of the Kikoira pluton of Kikoira Granite. The Siluro-Devonian granitoids intrude flysch-like psammo-pelites of Late Ordovician age.

As for most stockwork tin and tungsten deposits, a cupola association is recognised at Ardlethan where the 'Mine Granite' equivalent of the Kikoira Granite is brecciated and mineralised above an apophysis of slightly younger Ardlethan Granite (Paterson, 1976; Richards *et al.*, 1982). During 1979-83, additional cupola-related targets were sought in the district N of Ardlethan by using geochemistry to select mineralising plutons and magnetics to delineate blind appendages or cupolas at the margins of such plutons.

Three igneous suites with close temporal relationships are recognised for the Siluro-Devonian lithologies of the Ardlethan, Kikoira and Erimeran complexes. These are, with decreasing age:-

- 1) 'Bolero suite' - adamellite porphyries and rhyodacites characterised by hornblende relicts and fresh garnet;
- 2) 'Kikoira suite' - Kikoira Granite (biotite muscovite adamellite)
- 3) 'Ardlethan suite' - Ardlethan Granite and related rhyolites with an anomalous Sn Rb F U geochemistry similar to that of the Tertiary 'tin' (or 'topaz') rhyolites of North America (Burt *et al.*, 1982, Huspeni *et al.*, 1984).

All three suites have S-type geochemical characters.

The Ardlethan and Kikoira suites have different Rb/Sr versus Sn differentiation trends, however Sn Rb U K<sub>2</sub>O enrichments and Sr Ba Ce TiO<sub>2</sub> depletions in both suites enable the selection of plutons that are likely to be mineralising. The undifferentiated and unprospective Bolero porphyries may be predecessors of the Kikoira suite.

At least seven plutons of Kikoira Granite host varying degrees of minor Sn W Au Ag mineralisation and coincide with a linear gravity low trending N of Ardlethan. The plutons produce quieter and lower amplitude magnetic patterns in comparison with the intruded sediments (Webster, 1984). The longitudinal margins of the more mineralised plutons are bounded by positive magnetic linears representing NNW fracture control, whereas the elongate rhomboidal shapes and en-echelon distribution of the plutons reflect the sinistral control of the NW component of the Lachlan set of conjugate linears. The structural control on pluton emplacement contrasts with the concept of control by crustal thickness used by Rickard and Ward (1981) in the eastern Lachlan Belt.

Concentrations of the NW linears intersect the Wagga Tin Belt at approximate 100 km intervals, coinciding with strong NW-oriented pluton terminations and tin/tungsten fields (e.g. Pulletop, Ardlethan, Erimeran). A similar concentration of NW linears and strong terminations are evident for the Kikoira pluton, which also has the most prospective differentiation geochemistry of the Kikoira suite. However, although cassiterite- and wolframite-bearing quartz veins on the western margin of the pluton sourced the major Kikoira-Gibsovale alluvial deposits (7,000 tonnes Sn), the veins are small and have a recorded production of less than 3 tonnes Sn and WO<sub>3</sub> (Heugh, 1980).

A 15 km trend of magnetic lows and hornfelsed sediments was subsequently recognised beyond the northern termination of the Kikora pluton. At the south end of the trend, an outcropping 500 x 1500 m cupola of tourmaline biotite muscovite adamellite was characterised as a highly differentiated member of the Kikora suite. The cupola has a 50 m thick apogranite zone of tourmaline-enriched leuco-adamellite with evenly-disseminated pyrite and scheelite. There is a sharp transition to the underlying adamellite.

The hornfelsed sediments host fine networks of scheelite-bearing quartz carbonate pyrite arsenopyrite veinlets at prospects situated 4 and 8 km N of the leuco-adamellite. The central prospect is well defined by a 500 m diameter zone of muscovite-tourmaline alteration and W-As anomalies. Veining and geochemical anomalies at the northern prospect outline a broader but more erratic zone. Bulk assays of 0.1 - 0.3 %  $WO_3$  were obtained from the bottom intervals of several holes drilled below the oxidation limit. Associated Sn values are rarely anomalous. Scheelite is not preserved in the oxidation zone, however tungsten values are maintained in limonite and goethite, probably as tungstites indicative of humid Tertiary conditions (Varlamoff, 1970).

Although the cupola of scheelite-bearing leuco-adamellite was the only granitoid physically detected, the centres of sediment-hosted network veining are considered to be underlain by similar cupolas. The magnetic trend and the broader diffuse character of the northern mineralisation indicate the cupolas are connected at depth by a N-plunging, narrow stock of Kikora Granite. In parallel with the regional pattern, the magnetic and hornfelsed sediment trends are disrupted by NW sinistral displacements at regular intervals and in proximity to the tungsten prospects.

The model of a N-plunging stock with cupola and vein development at regularly-spaced linear intersections, is similar to the Xihuashan-Piaotang model described by various Chinese workers and summarised by Tanelli (1982). The model includes the 'five-storey' zoning concept which implies the 'net-vein' mineralisation such as described above, may overlie zones of higher grade 'thick-vein' mineralisation of up to 300 m vertical extent.

The S-type granitoid source and non-calcareous sediment host contrast with the usual I-type, skarn association for scheelite mineralisation.

Acknowledgement- the investigation was conducted by Aberfoyle Exploration Pty. Ltd. in joint ventures with The Shell Company of Australia Ltd., Electrolytic Zinc Company of Australasia Ltd. and Jennings Industries Ltd.

#### References

- Burt, D.M., Sheridan, M.F., Bikun, J.V. and Christiansen, E.H., 1982, *Econ. Geol.*, **77**, 1818-1836.
- Heugh, J.P., 1980, Cargelligo-Narrandera 1:25,000 Metallogenic Map - Mine Data Sheets and Metallogenic Study; *Geol. Surv. NSW*.
- Huspeni, J.R., Kesler, S.E., Ruiz, J., Tuta, Z., Sutter, J.F., Jones, L.M., 1984, *Econ. Geol.*, **79**, 87-105.
- Paterson, R., 1976, *Excurs. Guide No. 15C*, 36-43; 25th IGC.
- Richards, J.R., Compston, W. and Pateron, R., 1982, *Proc. Australas. Inst. Min. Metall.*, **284**, 11-16.
- Rickard, M.J., and Ward, P., 1981, *J. Geol. Soc. Aust.*, **28**, 19-32.
- Varlamoff, N., 1970, Abstract in *Int. Geochem. Explor. Symp. 3rd. Prog. and Abstracts*; *Canad. Inst. Min. Metall.*
- Webster, S.S., 1984, *Explor. Geophysics*, **15**, 15-31.

# CLOSED-SYSTEM BEHAVIOUR FOR THE TIN-TUNGSTEN SYSTEM AT ZAAIPLAATS, SOUTH AFRICA

A.S. Andrew<sup>1</sup>, P.J. Pollard<sup>2</sup>, R.G. Taylor<sup>2</sup> and D.I. Groves<sup>3</sup>

<sup>1</sup>CSIRO Division of Mineral Physics and Mineralogy, North Ryde  
<sup>2</sup>James Cook University of North Queensland, Townsville  
<sup>3</sup>University of Western Australia, Nedlands

Tin mineralization in the Potgietersrus tinfield (Strauss, 1954) is associated with granites which form part of the acid phase of the Bushveld Igneous Complex. Mineralization at the Zaaipplaats mine (Taylor and Pollard, 1986), occurs in the Bobbejaankop Granite and its fine-grained marginal phase (Lease Granite) as irregular, disseminated zones and as crosscutting, pipe-like orebodies. Within the Bobbejaankop Granite a major, low-grade, sheet-like horizon of cassiterite-scheelite mineralization occurs 100 metres below the roof of the pluton. The granite within this horizon contains 1-4% by volume of interstitial vugs which are filled by hydrothermal minerals including cassiterite and scheelite. In addition, larger vugs (up to 0.5x0.1m) infilled or partially infilled by similar hydrothermal minerals are present within the mineralized horizon, and these sometimes have an envelope of fine-grained, granophyric granite. The vug textures suggest that hydrothermal minerals were precipitated from fluids derived at a late stage in the crystallization history of the granite. The Zaaipplaats mineralization therefore provides a good example for study of the relationships between magmatic crystallization and hydrothermal fluid evolution in system apparently closed to externally-derived fluids.

Stable isotopes of oxygen and hydrogen in minerals are routinely used to recognize open-system behaviour and the influx of meteoric waters in alteration systems. So much so, that using oxygen and hydrogen isotopes, meteoric waters have been shown to be the major component of the aqueous fluid responsible for alteration in most granitoid suites and their associated mineral deposits. Closed-system behaviour in such suites therefore needs to be proven rather than assumed.

Oxygen isotope values have been determined on coexisting minerals from a suite of partially altered granites, vug-fillings and pipes and are summarized in the table. Fractionations between mineral pairs are used to demonstrate closed-system behaviour of fluid for much of the history of the tin-tungsten system at Zaaipplaats.

TABLE Summary of oxygen isotope data for mineral pairs. Analytical error  $\pm 0.1$  permil

Unit	$\delta^{18}\text{O}$ permil SMOW				
	quartz	K-feldspar	sericite	chlorite	cassiterite
Bobbejaankop Granite	7.7-8.5	9.7-10.6	6.2-7.7	0.5-6.8	
Lease Granite	8.0-9.4	9.5-10.1	6.8	7.6-7.7	
vugs in granites	7.8-11.7	9.6-10.1	7.6-9.3	0.4/11.7	-0.9--0.3
pipes in granites	7.3-13.3	8.9-11.4	7.0-9.1	0.6-3.5	-1.1--0.4

Bobbejaankop and Lease Granites: The fractionation factors,  $\Delta_{\text{quartz-K-feldspar}}$  are reversed and  $\Delta_{\text{quartz-sericite}}$  are generally less than 2, indicating reequilibration of K-feldspar and sericite with the magmatic fluid ( $\delta^{18}\text{O} = 7$ ) down to 400°C. Chlorite values suggest two generations one ( $\delta^{18}\text{O} > 6$ ) associated with the alteration involving magmatic fluid, and the other ( $\delta^{18}\text{O} < 1$ ; found only in the Bobbejaankop Granite) associated with late-stage influx of meteoric fluids.

Vugs and pipes: Fractionation factors are of similar magnitude to those in the granites.  $^{18}\text{O}$ -enriched values for quartz and sericite for some vugs and pipes suggests that these samples formed at lower temperatures (to 300°C) compared with quartz and sericite from other vugs and pipes and quartz from granite samples (which are assumed to have crystallized at magmatic temperatures). Except for one sample from a vug, chlorite values ( $\delta^{18}\text{O} < 3.5$ ) suggest a major meteoric component at either the waning stages of alteration, or possibly much later.

Cassiterite fractionation factors are poorly known but  $\Delta_{\text{quartz-cassiterite}}$  values of about 9 permil at 300-400°C have been measured from several natural occurrences. Using this value,  $\delta^{18}\text{O}$  values for cassiterite in the vugs and pipes appear to be in equilibrium with their coexisting quartz and/or feldspar and cannot be associated with the late-stage meteoric fluid, inferred to be in equilibrium with some chlorites from granites, vugs and pipes.

Oxygen isotope values show that except for a late-stage meteoric influx associated with some chlorite crystallization (or recrystallization), the Zaaipplaats system was closed, with quartz, K-feldspar, sericite, cassiterite and some chlorite crystallizing from and exchanging- $^{18}\text{O}$  with a cooling magmatic fluid at temperatures to 300-350°C.

#### References

- Strauss, C.A., 1954, Mem. Geol. Surv. South Africa 46, 241pp.  
Taylor, R.G., and Pollard, P.J., 1986, CIM Spec. Issue, in press.

# **Thermodynamic Analysis of Ore-Forming Conditions and the Sulfur Isotopic System in the Dachang Ore-Field, China**

Bai Zhenghua, Zhang Zheru, Zhang Zhenggen  
(Institute of Geochemistry, Academia Sinica)

Yan Rogxiu  
(215 Geological-Exploratory Team, Non-Ferrous Metal Company,  
Guangxi Province, China)

Isothermic  $\text{pH-fO}_2$  diagrams have been constructed on the basis of mineral assemblages of individual ore-forming periods and stages in the Dachang ore-field, Guangxi province, China. The ore-forming pH and  $\text{fO}_2$  conditions derived from these diagrams indicate that the pH decreases, the oxidation regime increases and the action of S intensifies progressively from the early stages to the later stages. By means of Ohmoto's model, the  $\delta^{34}\text{S}_{\text{ES}}$  have been calculated from the measured  $\Sigma^{34}\text{S}_{\text{min}}$ . Relative to  $\delta^{34}\text{S}_{\text{min}}$ , the calculations show that the frequency distribution of  $\delta^{34}\text{S}_{\text{ES}}$  is sharper, and the peak value is shifted in a negative sense by 2.5%.  $\Sigma\text{S}$  The sulfur in the whole ore-field comes from multiple sources, but each deposit has its own main S-source. However, the S-isotopic composition of each stage is nearly constant, suggesting that the ore-forming system is open to sulfur, and that the S-supply is sufficient. These conclusions are supported by the field geological relations.

GEOMETRY OF THE BAMFORD HILL GRANITE-HOSTED  
GREISEN SYSTEM, NORTH QUEENSLAND

P.L. Blevin

James Cook University of North Queensland, Townsville

W-Mo-Bi mineralised quartz-rich, pipe-like deposits are contained within the roof and flank zones of the high-level, high silica Permo-Carboniferous Bamford Stock. It forms part of a chain of stocks that have intruded along a major structural zone cutting in a north-north easterly direction through the central part of the Featherbed Cauldron Subsidence Area.

The unaltered granite is composed of subhedral, equigranular quartz (32%), pink K-feldspar comprising orthoclase and intermediate microcline (36%), sodic plagioclase (30%) and late biotite (2%). Plagioclase, K-feldspar and quartz lined miaroles, filled by quartz and biotite are common and reflect the order of crystallisation within the granite. Replacement perthites, rim albites and secondary biotites and K-feldspars are only present to a limited extent and are not as strongly developed as in the case of tin granites.

Along the roof and upper flanks of the stock's south-eastern contact is developed a carapace of texturally diverse and often miarole-rich (<15%) phases. The abundance and textural diversity of these phases diminishes into the stock over 50 to 100m. Pegmatitic, aplitic (both zoned and layered) and granophyric textures are all represented. Porphyritic microgranite sills within this zone have sharp upper contacts (usually with well developed biotite selvages) although downwards they are texturally gradational back into normal granite.

Pervasive greisen alteration (GRA) within the stock forms a zone up to 100m thick along the south-eastern roof and flank of the stock. The thickness of the alteration zone decreases both along strike and downdip. Petrographically, the GRA zone is characterised by the incipient replacement of the feldspars (now whitened) along microfractures, cleavages and twin boundaries by quartz and muscovite. Topaz is not present anywhere at Bamford Hill. Bodies of unaltered granite occur both within and above the GRA zone. Outside the granite in the adjacent volcanic wall rocks exogreisens are restricted to only four small patches. Quartz, andalusite, biotite and spinel have replaced the original dacitic ignimbrites.

A mineralised quartz-muscovite greisen (GRE) sheeted vein system with attendant quartz-rich pipe-like structures lies sub-parallel to the contact in the outer portion of the GRA zone. Sheeted greisens are best developed in the uppermost flank of the stock and give way at depth to more diffuse quartz-muscovite-feldspar greisen pods, which unlike the veins lack obvious structural control. In places, total silicification has resulted in the formation of ultragreisens. The "pipes" are complex structures up to 200m in length. In cross section they consist of a central zone of space-filling quartz with wolframite, molybdenite and bismuth surrounded by first one zone of silicified, then an outer zone of intensely greisenised, altered (GRA) granite. Downwards the pipes fade out within the GRA zone while upwards they commonly thin and branch out into flat lying poorly mineralised quartz veins which merge either into the sheeted greisens or into the quartz ultragreisens. The geometry of the pipes makes it unlikely that they have acted as conduits channelling fluids into the roof zone from deep inside the granite stock or from outside of it.

Based on physical observations a tentative model can be proposed for the evolution of the Bamford Hill mineralisation. The presence of vugs and miaroles among the texturally diverse rocks of the roof zone of the Bamford stock suggest episodic changes in the physical conditions of crystallization caused in part by the early evolution of a fluid phase. An evolving fluid phase pervasively greisenised the roof and flanks of the stock. Development of a fracture system sub-parallel to the contact of the stock acted to focus the fluid and enabled selective-intense greisenisation to take place. In some places this fluid was tapped by an externally directed fracture system allowing alteration of the volcanic wall rocks. Temperature quenching is the probable mechanism by which andalusite bearing assemblages were produced in these rocks. During the waning stages of hydrothermal activity chlorite-sulphide-fluorite-carbonate veining crosscut both the endo- and exo-greisen systems and locally brecciated the pipes.

It is concluded that the temporal and spatial interplay of the evolving fluid phase with internally generated, and externally imposed stress fields are critical in the formation and ultimate containment of "closed" granite-hosted mineral deposits.

BEHAVIOUR OF THE K-FELDSPARS IN THE BAMFORD HILL W-Mo-Bi GRANITE  
HOSTED MINERALISING SYSTEM, NORTH QUEENSLAND, AUSTRALIA

P.L. Blevin

Geology Department, James Cook University, Townsville

The Bamford Hill W-Mo-Bi deposit is contained within a high-level, silica rich Permian granite which intrudes the Permo-Carboniferous Featherbed Volcanics. The granite has within its roof zone several textural variants which pass downwards into more normal textured quartz-K feldspar-plagioclase-biotite granite. Stockwork at the contact give way to mixed pegmatoidal-aplitic phases which form sill like bodies within the pluton. Miaroles, lined with quartz, K-feldspar and albite and filled with muscovite or biotite are abundant.

Extensive, and locally intensive greisenisation with attendant pipe-like quartz-rich deposits of W-Mo-Bi is developed within the roof and upper flank zones of the pluton. Exocontact alteration zones in the surrounding volcanics occur at four locations along the mineralised zone. Late chlorite-carbonate-sulphide veining is also developed in both alteration zones.

K-feldspars occur in nearly all geological environments present in the mineralising system. These occurrences can be divided into "primary" feldspars of the unaltered granite and its textural variants, relict feldspars in the alteration zones, and hydrothermal feldspar present in the greisens, the late chlorite veins and in contact metasomatites. Those from the unaltered portions of the granite are strongly perthitic, commonly exhibit Carlsbad twinning and are characteristically microfractured. Perthitic albite occurs as films, veins and patches and where coarse enough, shows polysynthetic twinning. Albite overgrowths and swapped rims are common but are not as intensively developed as in the tin mineralised plutons of the adjacent region (Pollard et al. 1983). The K-rich component of the perthites shows cross-hatched twinning developed along fractures and adjacent to the perthitic albite. These twinned zones enclose islands of K-feldspar which may or may not be cross-hatched twinned. Some of these islands have been slightly rotated during microfracturing.

In the alteration zone K-feldspar is replaced by muscovite and quartz initially along microfractures and grain boundaries. Elsewhere, K-feldspars have also crystallised in muscovite ultragreisens and been produced as a result of bimetasomatic exchange reactions between the granite and an adjacent pyroxene bearing quartz-diorite.

Feldspars from all textural and alterational environments have been studied by X-ray diffraction and microprobe techniques to ascertain their strain, lattice parameters and degree of Al,Si ordering. Feldspars from the unaltered granite contain two structural states, one with low triclinicity approximating orthoclase and a less prominent state corresponding to intermediate microcline with triclinicities (as determined from the separation of 131) ranging up to 0.60. Ordering, such that it occurs, appears to be by an intermediate two step process. There is no correlation between either the abundance, or triclinicity of the microcline phase with increasing alteration. Feldspars precipitated by hydrothermal processes approximate orthoclase and show only partial ordering from T2 sites to T1 sites ( $2t1 = 0.80$ ) with no ordering within T1 being evident. In the adjacent tin granites the alkali feldspars are all intermediate microclines (Witt et al. 1984) with no feldspar approximating orthoclase having been described. In both the Bamford granite and the adjacent tin granites albite is invariably highly ordered low-albite regardless of geological origin.



The degree of ordering within alkali feldspars is usually ascribed to the presence and duration of fluid-feldspar interaction. At Bamford, the presence of miarole-bearing primary phases, the subsolidus textural re-adjustment of feldspars and biotite, and the presence of extensive greisen alteration documents a long history of fluid evolution and interaction within the granite. However, ordering in the K-rich feldspars has not only been retarded but by inference decreases with increasing alteration and fluid interaction at steadily lower temperatures (well within the stability field of microcline).

Chemical controls on the ordering of alkali feldspars include the presence and composition of a fluid/aqueous phase, and the composition of the host rock or precursor feldspar (Martin, 1972). It is clear from the above that the presence of an aqueous phase, while being a necessary condition for ordering, has not been sufficient in this instance. Fluid generated from the chemically more evolved tin granites should be more alkaline than that of the less evolved Bamford pluton with its extensive greisenous, rather than alkaline, alteration system. Its inferred lower  $a_{Na^+}/a_{H^+}$  and  $a_{K^+}/a_{H^+}$  ratios would prevent ongoing ordering of already existing K-rich feldspar and encourage the precipitation of partially ordered "monoclinic" feldspar phases. Thus it is suggested that the alkalinity of the fluid phase (the activity of K, and particularly Na) is an important control on K-feldspar ordering.

The use of K-feldspar triclinicity as a diagnostic tool in delineating barren and mineralised granites should be treated with caution, particularly in mineralised regions containing diverse granite associations (cf. Badejoko, 1986).

#### References

- Badejoko, T.A., 1986. Chem. Geol., 54, 43-51.
- Martin, R.F., in MacKenzie, W.S. and Zussman, J. (1972): "Feldspars", Manchester University Press, 313-336.
- Pollard, P.J., 1983. In "Permian Geology of Queensland", Geol. Soc. Aust., 413-429.

## TWO CONTRASTING TIN-TUNGSTEN METALLOGENIC PROVINCES IN TASMANIA

Peter L.F. Collins

Geological Survey, Department of Mines, Hobart, Tasmania

Primary tin and tungsten deposits in Tasmania are found in rocks ranging in age from Late Proterozoic to Late Devonian and are genetically and spatially associated with emplacement of Middle to Late Devonian granitoids. Although the tin/tungsten deposits and associated granitoids are widespread, most lie within two metallogenic provinces: NW Tasmania and NE Tasmania. Each province however, has a markedly different metallogenesis, reflecting a pronounced heterogeneity in the geologic and metallogenic development of western Tasmania compared to northeastern Tasmania, east of the Tamar River.

In western Tasmania, deformed and metamorphosed Precambrian sedimentary sequences form the basement for narrow trough accumulations of Eocambrian(?)–Cambrian and younger sedimentary and volcanic sequences. The Precambrian regions behaved as geanticlines during early trough deposition, and later acted as competent blocks during a period of major deformation of mid-Devonian age. Granitoid plutons were emplaced in the Late Proterozoic and Cambrian, and possibly also in the Ordovician. Several metallogenic episodes have resulted in formation of Late Proterozoic volcanogenic magnetite-pyrite deposits associated with mafic volcanism (e.g. Savage River); platinoids and Cu-Ni sulphides in tectonically emplaced Early Cambrian ultramafic bodies; several large volcanogenic massive sulphide deposits in the Middle-Late Cambrian Mt Read Volcanics (e.g. Mt Lyell, Rosebery, Que River, Hellyer); and probable syngenetic base-metal sulphides in Ordovician limestone.

In contrast, the sedimentary rocks of northeastern Tasmania are of Early Ordovician and Early Devonian age, and exhibit comparatively simple mid-Devonian deformation.

It is into these two markedly diverse regions that substantial granitoid masses were emplaced at high levels within the folded rocks throughout Tasmania during the Middle-Late Devonian (389–332 Ma). The relatively large batholiths in northeastern Tasmania contain several distinctive plutons composed mainly of I-type hornblende-biotite granodiorite and I- and S-type biotite granite/adamellite, with associated metallogenically specialised alkali feldspar granite. They are slightly older than the smaller I- and S-type biotite granite/adamellite and minor I-type hornblende-biotite granodiorite in western Tasmania. Most Devonian granites are equivalent to ilmenite series granitoids, but two major tungsten deposits are related to magnetite-series granitoids. The granite bodies in northwestern Tasmania are apparently linked at depth to form a major batholith that underlies all major tin and tungsten deposits.

The genetic types of tin and tungsten mineralisation associated with the Middle-Late Devonian granites have been greatly influenced by the pre-Early Devonian geology, particularly the prevalence of carbonate units in late-Late Proterozoic and early Palaeozoic sedimentary sequences of western Tasmania.

Tin and tungsten deposits in NE Tasmania are mainly cassiterite greisens (e.g., Anchor, Blue Tier) and quartz-wolframite-cassiterite vein deposits in Palaeozoic sediments above apophyses of altered alkali feldspar granite (e.g. Aberfoyle, Storeys Creek, Great Pyramid).

Small greisen and vein deposits are also found in western Tasmania (e.g. south Heemskirk, Interview River, Oakleigh Creek, Cleveland) but tin and tungsten mineralisation is dominated by skarn and carbonate-replacement deposits which formed at four stratigraphic horizons. Late-Late Proterozoic dolomite hosts cassiterite-pyrrhotite bodies that formed adjacent to cassiterite bearing topazised porphyry dykes at Mt Bischoff; and low grade skarn at St Dizier. Eocambrian(?) dolomites of the early trough deposits host the large cassiterite-bearing, strata-bound massive pyrrhotite deposits at Renison Bell. Limestone within Early Cambrian volcano-sedimentary sequences host cassiterite-stannite-chalcopryrite-pyrrhotite deposits at Cleveland; and scheelite bearing skarn at King Island. Ordovician limestone hosts several small scheelite-magnetite skarns at Kara; and low grade Sn-W-magnetite-fluorite skarn at Moina.

The total geological resource (production and reserves) of deposits in western Tasmania is of the order of 700 000 t Sn and 150 000 t  $WO_3$ , compared with about 50 000 t Sn and 20 000 t  $WO_3$  in northeastern Tasmania. This dramatic enrichment in western Tasmania reflects the origin of the two provinces and may be explained by high-level emplacement of major batholiths into a region that has been subjected to a protracted and complex geological evolution, with a multiplicity of tectonic events, and possibly coincident with locally anomalous Sn and W in the upper mantle.

## SILEXITE GEOLOGY AND MINERALISATION

M. Creech<sup>1</sup>, S. Sangameshwar<sup>2</sup>, B. Marshall<sup>2</sup>

1. Pacific Copper Limited 2. N.S.W. Institute of Technology

The rocks known as silexite occur at Torrington in Northern N.S.W. approximately 30 km northeast of Emmaville. Silexite is essentially a quartz rich rock with more than 5% topaz and significant tungsten and bismuth mineralisation. It can be compared to a classical greisen mineralogically, however, many field relationships display intrusive characteristics which are inconsistent with a simple metasomatic origin. Silexite intrudes and is proximal to a sedimentary roof pendant of Permian age outcropping within the Mole Granite. The Permo-Carboniferous Mole Granite is a late stage differentiate of the New England Batholith and displays many of the characteristics of a classical tin granite.

Pacific Copper has also been conducting research into the utilisation of topaz as a industrial mineral. Topaz is essentially a fluorine bearing aluminosilicate and upon calcination of 1300°C it converts to the refractory mineral mullite with excess silica and fluorine being driven off as the gases HF and SiF<sub>4</sub>. These gases will also be converted to commercial chemical compounds.

Therefore Pacific Copper Limited has attempted to understand silexite geology and to evaluate the associated metallic and topaz mineralisation employing drilling, mapping, geochemistry, petrography and observations made during a pilot mining operation in 1979-80. My work at the Institute has included more detailed petrography, geochemistry and fluid inclusion work. The results of this work has shown that silexite geology is complex and that wolframite and topaz grades vary considerably.

Silexite is divisible into two types based on textural and field relationships. They are a coarse, metasomatic silexite with an inhomogeneous, inequigranular texture, which is interpreted as a greisenized granite, and an intrusive silexite with a saccharoidal texture. The intrusive silexite is believed to be derived from partial melting of the earlier formed greisen.

Evidence for the metasomatic origin of silexite includes the appearance in both outcrop and microscopic scale of relict granite textures and also the occurrence of rocks which fall between granite and silexite mineralogically and chemically. However, characteristics such as sharp contacts between granite and silexite structures and the brecciation of metasediment within silexite indicates remobilisation. Fluid inclusion work by Eadington and Nashar (1978) and phase studies of the system 'Granite - H<sub>2</sub>O-HF' by Glyuk and Anilfiligov (1973) indicate temperatures of 600-750°C for silexite formation. This is consistent with partial melting of metasomatic silexite to yield intrusive silexite.

Tungsten mineralisation is believed to be independent of silexite intrusion, occurring in discrete quartz rich pegmatitic veining. Disseminated wolframite in intrusive silexite represents chemically remobilised tungsten. Larger irregular wolframite fragments are portions of pegmatitic veins that have been mechanically (physically) entrained in the partial melt. Mirolitic cavities also contain large tungsten crystals. Thus wolframite mineralisation and silexite formation are temporarily related. Bismuth mineralisation is variable but is consistently higher grade in intrusive silexite. Tin mineralisation is poor within silexite.

Based on field relationships between silexite, microgranite, pegmatitic mineralisation and metasomatism the following overlapping sequence of events can be recognised:-

1. Granite emplacement, cooling and formation of a carapace.
2. Alteration of outer granite carapace and formation of greisen and metasomatic silexite (greater than 5% topaz).
3. Tungsten, mineralisation associated with alteration fluids introduced as veining.
4. Continuing alteration of the granite with development of alkali rich fluids (and increased fluid pressures?) causes partial melting of silexite and dissolution of tungsten.
5. Intrusion of microgranites and fracturing of metasediment.
6. Intrusion into metasediment of partial melt together with mechanically and chemically remobilised tungsten.
7. Further pegmatitic veining within fractured silexite and metasediment.

The identification of intrusive and metasomatic silexite at Torrington has significant implications for tungsten mineralisation. Intrusive silexite includes mechanically and chemically remobilised tungsten with the latter process imparting a more consistent background grade. Metasomatic silexite includes only pegmatitic style of mineralisation within metasomatic silexite is far more erratic and generally poorer than grades within intrusive silexite.

#### References

Eadington and Nashar, 1978 - 'Evidence for the Magmatic Origin of Quartz - Topaz Rocks from the New England Batholith, Australia' - Contrib, Mineral. Petrol 67 433-438.

Glyuk and Anfiligov, 1973 - 'Phase Equilibria in the System Granite  $H_2O$ -HF at a Pressure of 1000 kg/cm<sup>2</sup>'. Geochemistry International Vol 10 pp 321-325.

# SOME HYDROTHERMAL REACTIONS THAT CONTRIBUTE TO THE MINERAL COMPOSITION OF TIN ORES IN GRANITES

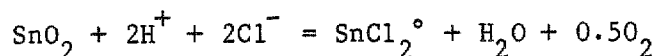
P.J. Eadington

CSIRO Division of Mineral Physics and Mineralogy, North Ryde.

The solubility of cassiterite under hydrothermal conditions defines its mobility, the conditions under which it precipitates, and indirectly, the minerals that are associated with cassiterite. Under reducing conditions the solubility of cassiterite may be approximated by the concentration of  $\text{SnCl}_2^\circ$  complex, for which

$$\log a_{\text{SnCl}_2^\circ} = \log K - 0.5 \log f_{\text{O}_2} - 2\text{pH} + 2 \log a_{\text{Cl}^-},$$

where  $a$  is the thermodynamic concentration in molality and  $K$  is the equilibrium constant for the reaction



Extrapolation from low temperature thermodynamic data by the method of like equal charges yields  $\log K = 15.7 - 17450/T(K)$ . The extrapolation uses experimental values for the dissociation of water measured in 3m NaCl solutions and has a linear relation with  $1/T$  at least to  $300^\circ\text{C}$ . Deviations probably occur near the critical temperature which for 3m NaCl solution is  $580^\circ\text{C}$ .

Since the temperature, pH and redox of hydrothermal fluids depend on equilibration with rocks, and  $a_{\text{Cl}^-}$  depends on properties of the granite magma that is the source of the hydrothermal fluid, the terms in the expression for the solubility of cassiterite ( $a_{\text{SnCl}_2^\circ}$ ) are dependent upon lithology, mineralogy and temperature distribution.

A valence change for tin occurs within the range of redox conditions that prevail in hydrothermal systems. This transition from tin IV to tin II complexes is marked by a change from low solubilities (ppb levels) of cassiterite to relatively higher solubilities (ppm levels). The redox corresponding to equal concentrations of tin II and tin IV hydroxy complexes is near the quartz fayalite magnetite (QFM) oxygen buffer, but for chloro complexes it is above the hematite magnetite (HM) buffer. This condition occurs at very low concentrations of tin since it is determined by the low solubility of cassiterite as tin IV complexes. Concentrations of chloro complexes of tin that are adequate for significant hydrothermal transport of cassiterite occur at much lower redox conditions, below the QFM buffer.

Lithological association. The ilmenite series granites have a mineralogy indicative of crystallization under relatively low redox conditions. A lithological association of cassiterite with ilmenite series or S-type granites is consistent with maximum cassiterite solubilities occurring at redox conditions below the QFM buffer.

Mineralogical associations. The occurrence of cassiterite ores with topaz or muscovite alteration results from hydrothermal reactions that affect pH and redox (Eadington and Gibling, 1979). Precipitation of cassiterite occurs through concurrent changes in the temperature (and equilibrium constant), pH, and redox across the zone of alteration. Topaz

has a higher density than muscovite, quartz, and K-feldspar and is observed in relatively closed hydrothermal systems such as granite cupolas where fluid pressures and  $a_{F^-}$  are likely to be high. Muscovite predominates in more open hydrothermal systems such as brecciated rocks where fluid pressures are likely to be low.

Boiling, mixing, and coupled reactions. Reactions originating within the fluid may also change the redox, pH or temperature in hydrothermal fluids and cause localised precipitation of cassiterite. These include boiling with partitioning of volatiles from the residual liquid, and mixing of hydrothermal fluids from different sources. If hydrothermal fluids are confined to fracture systems without fluid - rock equilibration, a coupled reaction between complexes of tin and arsenic, in which oxygen is conserved, may result in co-precipitation of cassiterite and arsenopyrite over a small cooling interval (Heinrich and Eadington, 1986). This may account for the correlation of high tin ore grades with high arsenopyrite abundance observed in some deposits.

In conclusion, the hydrothermal transport and precipitation of cassiterite is influenced by geological factors through terms in the expression for the solubility of cassiterite ( $a_{SnCl_2^0}$ ). These chemical relationships are consistent with some systematic features in the geologic occurrence of cassiterite mineralization in granites.

#### References

- Eadington, P.J. and Gibling., 1979, Alteration minerals and the precipitation of tin in granites, CSIRO Inst. Earth Res. Tech. Comm. 68.  
 Heinrich, C.A. and Eadington, P.J., 1986, Econ. Geol., v. 81, No. 3, in press.

# THE TAYLOR CREEK TIN DEPOSITS: PRODUCTS OF MAGMATIC PROCESSES

Ted Eggleston<sup>1</sup>, David Norman<sup>2</sup>

New Mexico Institute of Mining and Technology Socorro, NM 87801 USA

Tin deposits in southwestern New Mexico, USA are associated with Tertiary age high silica, "topaz" rhyolites. These tin deposits, commonly called Mexican type tin deposits, consist of hematite-cassiterite veinlets hosted by the rhyolite lava. Placer tin deposits are found in the streams that drain the rhyolite lavas. Production to date has been exclusively from the placer deposits. Though these deposits are not economic, they provide important insight into the magmatic processes that concentrate and deposit tin and have been studied by a combination of geological mapping, major, trace, and rare earth element geochemistry, O and Sr isotope geochemistry, and fluid inclusion studies.

The Taylor Creek Rhyolite which hosts the tin deposits is located at the top of the Mogollon-Datil volcanic field, a mid-Tertiary volcanic plateau consisting of more than a thousand metres of mafic to felsic lava flows and domes, felsic ignimbrites, and volcaniclastic sedimentary rocks. The Taylor Creek Rhyolite consists of a number of discrete rhyolite domes and flows scattered in an area of about 700 sq km. Each dome has minor associated tin. The rhyolite is moderately crystal-rich to crystal-rich with phenocrysts of quartz and sanidine in subequal proportions. Flow banding is pronounced in the domes that are as much as 250 m high.

The tin occurrences consist of hematite-cassiterite veinlets a few m long and high and a few cm wide. These veinlets are always found in lithophysal zones within 150 m of the carapace of the rhyolite dome, generally just below the carapace breccia that surrounds all the domes. The hematite and cassiterite occur as discrete crystals and as intimately intergrown masses. Wood tin, the botryoidal, cryptocrystalline form of cassiterite is the most common tin mineral in the placer deposits, but is rarely found in outcrop. Early magnetite was replaced by hematite.

Zones of intense vapor phase recrystallization (VPR) are found within a few tens of metres of the tin occurrences. Physical affects of VPR on the rhyolite lava are profound. VPR bleaches the rock and recrystallizes the groundmass. Groundmass crystal size is increased from about 0.1 mm to about 0.5 mm. Quartz is overgrown, frequently doubling in size. In zones of intense VPR, the normally dense rhyolite is converted to a punky rock resembling a poorly welded ignimbrite. Flow banding is probably responsible for concentrating the fluids necessary to produce the zones of intense VPR.

Two types of fluid inclusions have been identified in cassiterite and associated quartz and topaz. Large vapor inclusions are the most common inclusion. No condensate has been seen in these inclusions, so no homogenization information has been obtained. The second type of inclusion consists of glass, vapor, and 3 daughter minerals at room temperature. At about 350 deg. C. the glass melts to form a liquid-vapor inclusion that homogenizes to a liquid at about 680 deg. C. Two of the daughter salts dissolve at about 630 deg. C. The other daughter mineral is opaque and does not dissolve prior to homogenization. Fluid inclusions in late stage gangue minerals consisting of quartz, fluorite, and calcite homogenize at temperatures of 130 to 380 deg. C. and have salinities of about 1 eq. wt. % NaCl.



Quartz from the lithophysae associated with the tin veinlets has the same fluid inclusion homogenization temperature as the cassiterite and has a  $\delta^{18}\text{O}$  of 7.5 per mil (SMOW). Whole rock samples of intensely VPR rhyolite have the same oxygen isotopic composition as the fresh rock, about 7.5 to 8.5 per mil. Quartz from the late stage gangue assemblage has a  $\delta^{18}\text{O}$  of +6 to +11 per mil.

The host rhyolite is enriched in  $\text{SiO}_2$ , Cl, F, and the lithophile elements relative to "normal" rhyolites. Moderate depletions of  $\text{TiO}_2$ , CaO, and  $\text{Fe}_2\text{O}_3$  as well as extreme depletions of Ba, Sr, V, and Eu are likewise characteristic. Chondrite normalized rare earth element patterns are flat with large negative Eu anomalies. Initial  $^{87}\text{Sr}/^{86}\text{Sr}$  ratios of the rhyolite lavas cluster in two groups, one at 0.708, the other at 0.710 with no obvious pattern. Chemical effects of VPR include enrichment of Sr, and the rare elements and depletion of lithophile elements relative to fresh rhyolite.

The replacement of early magnetite by hematite indicates that the  $\log f_{\text{O}_2}$  of the solutions changed from below about -13 during deposition of the magnetite to above -13 during deposition of the tin mineralization.

The data above indicates that the tin mineralization was deposited from oxidizing magmatic fluids at magmatic temperatures. These same fluids are responsible for VPR of the host rhyolite. Late stage gangue minerals were deposited from lower temperature fluids with low salinities, possibly a short lived meteoric water dominated hydrothermal system.

Differentiation in a magma chamber, possibly at shallow depths, is necessary to produce the extreme depletions of Ba and Sr characteristic of these rhyolites. Sn was enriched in the fluid phase while the magma was differentiating. The Sr isotope data indicates the lower crust or upper mantle was the parent for the melts. Recycling of tin-rich Precambrian granites is not consistent with the Sr isotopic data.

The Taylor Creek Rhyolite was erupted at the beginning of rifting along this segment of the Rio Grande Rift.

**THE COMPOSITION OF ORE FLUIDS IN THE MOUNT PAYNTER  
TIN/TUNGSTEN DEPOSIT, N.S.W.**

H. Etminan<sup>1</sup> and N.C. Higgins<sup>2</sup>

Bureau of Mineral Resources, Geology and Geophysics  
Box 378, Canberra City, ACT 2601, Australia

Cassiterite and scheelite-bearing quartz veins at Mount Paynter occur in a shear zone within the Koetong granite and are associated with a number of late dykes and pegmatites. The hydrothermal alteration is dated at  $411 \pm 2$  Ma. The Koetong granite is one of a number of Silurian ( $417 \pm 3$  Ma) granites associated with tin mineralisation in the Wagga Metamorphic Belt (of the Lachlan Fold Belt). The age and geochemical signatures of the granites at Mount Paynter are identical to other S-type granites in the belt which are associated with tin deposits (e.g. Ardlethan). Geochemically they exhibit a high degree of fractionation (e.g. high Rb, low Sr) and high  $P_2O_5$ , U, and Nb, low V contents.

**Mineralisation:** Stage I consists of quartz veinlets containing feldspar with coarse tourmaline and muscovite on selvages. These appear gradational with pegmatites and aplites which occupy similar joint fractures in the granite. During Stage II mineralisation the major lode was formed within an east-west shear zone. The lode consists of many small veinlets which individually occupy dilatational fractures. It formed during a prolonged shearing episode which deformed and rotated early formed veinlets in the shear direction. Discontinuous pods of medium-grained to fine-grained granitic material occur within the lode and probably represent remnants of a pre-mineralisation aplitic dykes which provided the locus for later shearing. Quartz deposition is accompanied by cassiterite, arsenopyrite, tourmaline and sericite precipitation. Scheelite and minor sulphides occupy fractures opened during shearing of pre-existing quartz veinlets. Stage III mineralisation is marked by deposition of calcite veinlets containing minor fluorite and postdates all previous mineralising stages.

**Fluid inclusions:** Three types of fluid inclusions have been recognised in quartz and calcite from the Mount Paynter mineralisation. Type A inclusions contain aqueous solution, liquid  $CO_2$  and vapour  $CO_2$ , and are found in Stage I veins as isolated primary inclusions. The  $CO_2$  phases homogenise to liquid around  $22^\circ C$  and at this temperature the liquid  $CO_2$  occupies 25% by volume of the inclusion. Decrepitation of the inclusions occurred at  $220^\circ C$ , prior to complete homogenisation of water and  $CO_2$  phases, suggesting internal pressures greater than 1000 bars at this temperature. During freezing runs several irregular and rectangular birefringent daughter minerals were formed from the aqueous solution and these did not dissolve on heating until  $220^\circ C$ . The phase equilibria suggest that the daughter minerals are calcium sulphate and/or calcium carbonate. Based on microthermometric measurements the bulk composition of the type A inclusions is estimated to be:

$H_2O + \text{dissolved salts} = 92.5, CO_2 = 7.4, CH_4 = 0.1$  (mol %).

Type A inclusions have a bulk density of 1.08 g/cc. Primary type B are composed of a liquid phase and a vapour bubble with the latter occupying either 70 volume % (vapour-rich type B) or 40 volume % (liquid-rich type B) of the inclusion. Type B inclusions are found in stage II quartz associated with cassiterite deposition. Liquid-rich (type B) inclusions

homogenise between 310-350°C and exhibit Tm ice between -15°C and -17°C; gas-rich (type B) inclusions homogenise between 330 and 350°C with a Tm ice of -2.5°C. These data suggest that the liquid- and gas-rich type B inclusions were trapped from a boiling fluid at around 340°C. Combined microthermometric and laser raman microprobe measurements indicate a bulk composition for type B<sub>L</sub> inclusions of:

$H_2O = 92.37$ ,  $NaCl = 7.30$ ,  $CO_2 = 0.30$ ,  $CH_4 = 0.03$  (mol %).

and a bulk density of 0.80 gm/cc. Type C inclusions consist of aqueous solution and a vapour bubble with the latter occupying 7-20 volume % of the inclusion. Type C inclusions occur as secondary inclusions in Stage I and II quartz (type C1) but are primary inclusions in calcite of Stage III mineralisation (type C2). They contain no detectable  $CO_2$  but have high concentrations of dissolved salts (between 13 and 19 equiv wt% NaCl). Type C2 inclusions in calcite contain especially high concentrations of divalent cations and homogenise to liquid around 240°C. Secondary type C1 inclusions in quartz homogenise between 130 to 160°C.

**Stable isotopes:** Only preliminary isotopic data from calcite is available at this time. The  $\delta^{18}O_{SMOW}$  of calcite average 8.4 per mil and indicate an oxygen isotopic composition of the hydrothermal fluid (at 240°C) of <1 per mil during stage III mineralisation. These data suggest that meteoric waters were involved in the latter stage of the Mount Paynter mineralisation.

**Ore-forming conditions:** Fluids associated with stage I mineralisation, presumably of magmatic derivation, deposited feldspar bearing veins at temperatures >350°C and high fluid pressures (>1000 bars), contained moderate  $CO_2$  concentrations, and a high concentration of dissolved salts other than NaCl. Falling temperatures and pressures followed hydraulic fracturing during lode formation (stage II mineralisation) with cassiterite deposition occurring from a boiling fluid at 340°C and 150 bars. A twenty-five fold decrease in the concentration of  $CO_2$  and a three fold decrease in  $CH_4$  within the ore fluid occurred between mineralisation stage I and II, suggesting some change in pH (increase) of the ore fluid with time. However, decreasing temperature provides an adequate mechanism for cassiterite deposition in the Mount Paynter veins. Latter stages of mineralisation were deposited from fluids of dominantly meteoric derivation.

## ORIGIN OF ALBITE IN MINERALIZED GRANITES

Ilmari Haapala

Department of Geology, University of Helsinki, Helsinki,  
Finland

It is well known that the tin-bearing and related mineralized granites show geochemical, petrographic and mineralogical characteristics which separate them from normal barren granites. Different opinions exist about the origin of these properties, the main question being: magmatic or metasomatic.

The tin-bearing granites are typically leucocratic microcline-albite granites, the content of albite being commonly about 25 vol-%. An earlier generation of plagioclase (oligoclase) may also be present. Since Beus and Zalashkova (1964), numerous authors have emphasized the role of metasomatic albitization in the generation of the tin-bearing granites (e.g., Stempok 1971). The albite is interpreted to have formed mainly by albitization of K-feldspar (sodium metasomatism). This interpretation is without doubt correct in several instances, but often the term albitization is used too loosely, without considering other possible interpretations. There are several processes which may produce albite in a granitic rock:

- 1) exsolution from originally homogeneous alkali feldspar
- 2) metasomatic addition of albite
- 3) deanorthitization of plagioclase
- 4) direct crystallization from late-stage granite magma.

Exsolution of albite from alkali feldspar can produce, besides different types of perthite, also intergranular double albite rims or grain rows between two adjacent alkali feldspar grains, or albite overgrowths on plagioclase grains which are in contact with alkali feldspar (Fig. 1). The exsolution is catalyzed by postmagmatic fluids which also may cause marked autometamorphic recrystallization and mineral alterations. The intergranular albite grains are always oriented crystallographically according to the alkali feldspar or plagioclase grains on which they nucleated.

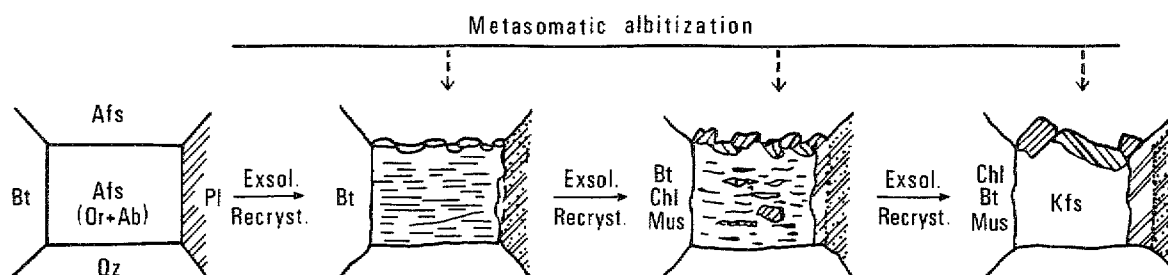


Fig. 1. A model of the development of intergranular albite in granite (simplified from Haapala 1977).

Metasomatic addition of albite is usually visible as albitization of K-feldspar. The albite thus formed possesses commonly a chess-board texture and contains patches of relict K-feldspar. Metasomatic albitization can also produce similar intergranular albite rims as exsolution (Fig. 1). Albitization is a common feature in tin-bearing pegmatites where albite occurs typically as fine-grained sugar albite or as platy cleavelandite.

Deanorthitization of plagioclase is caused by reactions between postmagmatic fluids and plagioclase. If the fluid contains fluorine, the anorthite component of plagioclase is used to form minerals like fluorite, topaz, muscovite and quartz in reactions such as  

$$\text{CaAl}_2\text{Si}_2\text{O}_8 + 4\text{HF} = \text{CaF}_2 + \text{Al}_2\text{F}_2\text{SiO}_4 + \text{SiO}_2 + 2\text{H}_2\text{O}.$$
The minerals formed occur as very small inclusions causing the turbidity of the host albite.

Direct crystallization of albite from a granite melt is not a common feature but takes possibly place in calcium-poor fluorine-rich magmas. Ongonites (topaz-bearing quartz keratophyres) are subvolcanic equivalent of albite granites (Kovalenko et al. 1971).

The topaz-bearing late-stage rapakivi granites of Finland offer good examples of albite formed by processes 1), 2) and 3); metasomatic albitization (2) is often present in lithium- and tin-bearing pegmatites. It is very difficult to distinguish between albite grains and rims formed by processes 1) and 2) in granites, but detailed petrographic work and chemical analyses (including microprobe analyses of feldspars) give valuable information of the origin of albite (Haapala 1977). The author is of the opinion that exsolution and recrystallization (adjustment to falling temperatures under subsolvus conditions) catalyzed by postmagmatic fluids is more important than generally has been considered.

#### References

- Beus, A.A. & Zalashkova, N.Ye., 1964, Internat. Geol. Review, 6, 668-681.  
 Haapala, I., 1977, Geol. Surv. Finland Bull., 286, 128 p.  
 Kovalenko, V.I., Kuzmin, M.I., Antipin, V.S. & Petrov, L.L., 1971, Dokl. Akad. Nauk SSSR, Earth Sci. Sect., 199, 132-135.  
 Stemprok, M., 1971, Soc. Mining Geol. Japan, Spec. Issue, 2, 112-118.

# EMPLACEMENT AND CHEMICAL EVOLUTION OF THE HEEMSKIRK GRANITE AND ITS ASSOCIATED TIN AND TUNGSTEN DEPOSITS

J. Hajitaheri<sup>1</sup> and M. Solomon<sup>2</sup>

Bureau of Mineral Resources, Box 378, Canberra City, ACT 2601, Australia

The mid Devonian Heemshirk Granite consists of the two major granite types, the red and the white granites, with the white granite intruding the red granite. The red granite consists of shallow dipping layers, each of which intruded and chilled against an upper pre-existing layer. Layering is only localised in the white granite and grain size gradually increases away from the contact with the red granite. The thickness of white granite is over 500 m, while the combined thickness of the red granite is about 300 m. It is postulated that the pluton grew by intrusion of sheets of granites into space created by subsidence within a roughly circular cauldron-type structure.

Chemically both granite types are similar. They show similar Harker variation trends and exhibit LREE enrichment and HREE depletion with a negative anomaly. Whole rock oxygen isotope data on the Heemskirk Granite and sediments indicates that assimilation of Precambrian sediments is not a significant process in causing chemical variation.

The Heemskirk Granite is extensively fractured. Some fractures are probably cooling joints and formed prior to the intrusion of the white granite. Volume expansion through the exsolution of fluid phase during the emplacement and crystallisation of the white granite caused the extension of these joints and initiation of new fractures in both the red and the white granites. The majority of microgranite dykes appear to be white granite melt intruded into joints within overlying red granite. In the southern part of the Heemshirk Granite the mechanical energy was sufficiently high to form breccias closely associated with greisenised dykes. Fractures in the red granite locally extended in to the country rocks. There is no evidence of penetration by ground water during this phase of alteration and mineralisation. However the fracture permeability remained sufficiently high in places to allow penetration by ground water at a later stage.

There are two major styles of mineral deposit in the Heemskirk Granite: 1) Cassiterite and wolframite associated with greisenized dykes, concentrated in the vicinity of the contact between the red and white granites, and deposited from a  $\text{CO}_2$ - $\text{NaCl}$ - $\text{H}_2\text{O}$  fluid at 300-520 °C<sup>0</sup> revolved from the white granite. 2) Polymetallic deposits associated with extensive sericitization and/or tourmalinization. This style of mineralization is hosted by the red granite and is located close to contacts with the country rocks. It was formed as a result of circulation of externally derived fluid through the granite and the country rocks.

25

# SKARN PARAGENESIS AND CASSITERITE PRECIPITATION AT MT BISCHOFF, TASMANIA

S.W. Halley<sup>1</sup>, J.L. Walshe<sup>1</sup>, and M. Solomon<sup>2</sup>

<sup>1</sup> Australian National University, Canberra

<sup>2</sup> Bureau of Mineral Resources, Canberra

At Mt Bischoff, in north western Tasmania, cassiterite, pyrrhotite and a variety of silicate phases have replaced dolomite in a distal skarn environment. The dolomite is part of a late Precambrian sequence of quartzites, siltstone and shales. This sequence has been intruded by numerous quartz feldspar porphyry dykes of Devonian age. All of the dykes show some degree of greisen style alteration. Feldspars within the dykes, show progressive replacement by sericite, then siderite, then sulphides with topaz followed by silicification with associated sulphides and topaz. Tin grades within these rocks increase with the intensity of alteration. Zonation of these alteration stages indicates that the dykes have been major conduits for the hydrothermal fluids.

Within the replaced dolomite a number of different assemblages can be defined based on the dominant gangue mineral. These include serpentine, chondrodite, talc, phlogopite, quartz and carbonate assemblages. Pyrrhotite occurs within all of these rock types. Replacement of the dolomite took place in two stages with the earliest formed assemblages containing serpentine and chondrodite. An outward zonation from serpentine to chondrodite to coarse grained magnesium carbonates reflected an increasing level of silica undersaturation moving away from the source of the fluids. This stage of dolomite replacement occurred at 420 to 450°C and cassiterite was undersaturated at this stage due to the high temperature.

The most extensive stage of dolomite replacement led to the development of the quartz, phlogopite, talc and carbonate assemblages which overprinted the earlier stage. As silicate minerals replaced dolomite, the activity of silica in the fluid was reduced and an outward zonation of quartz to talc to magnesium-iron carbonates developed. Precipitation of fluoride phases also lowered the hydrogen fluoride fugacity. Fluid inclusions indicate a temperature of around 350°C during this stage.

The highest tin grades are within the quartz and parts of the talc assemblage. Fluid inclusions provide abundant evidence of boiling during the formation of the quartz assemblage. Partitioning of volatile components, particularly H<sub>2</sub> and CH<sub>4</sub>, between the vapour and liquid phases during boiling increases the oxidation state of the liquid phase. This has probably been the major cause of cassiterite precipitation.

The fO<sub>2</sub> and fS<sub>2</sub> conditions during mineralization can be estimated from the mineralogy of the system, the non-stoichiometry of arsenopyrite and from CH<sub>4</sub>/CO<sub>2</sub> ratios in fluid inclusions. Log fO<sub>2</sub> values of -31.5 to -32.0 and log fS<sub>2</sub> values of -11.2 to -11.8 have been estimated for the main stage of dolomite replacement and cassiterite precipitation. The chemical conditions, mineralogy and paragenesis of this stage at Mt Bischoff is very similar to that at Renison Bell where there is also abundant evidence of boiling.

# SOME THERMODYNAMIC AND MASS-BALANCE CONSIDERATIONS ON THE HYDROTHERMAL PRECIPITATION OF CASSITERITE

C.A. Heinrich

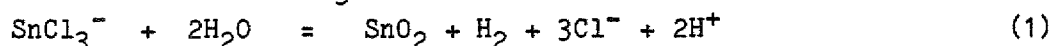
Bureau of Mineral Resources, Geology and Geophysics, Canberra

The stability of aqueous tin complexes and the solubility of cassiterite at high temperatures have recently been measured by Eugster and Wilson (1985) and Pabalan (1986). These studies have confirmed earlier predictions (see Eadington, this volume) that Sn(II) chloro complexes are likely to dominate tin transport at most conditions above 350°C, while Sn(IV) hydroxy-chloro complexes become important only at relatively low temperatures, acid, and/or oxidized conditions.

Cassiterite solubilities for typical granite-buffered conditions rapidly fall below concentrations that are realistically required to form an economic tin deposit (1-10 ppm) at temperatures below 400°C. Fluid inclusion indications for lower formation temperatures of many deposits have been interpreted by Eugster and Wilson (1985, p.99) to indicate tin transport under conditions of incomplete chemical buffering of the fluids by host rock minerals. This is indeed likely to occur where fluid are channelled into structures such as lode-veins that allow only limited wall-rock alteration (Heinrich and Eadington, 1986).

This paper presents some preliminary results from multicomponent mass transfer calculations that are being used to explore which processes are likely to dominate the chemical evolution of granite-derived fluids if they undergo cooling under conditions of incomplete rock-buffering. They aim at a better understanding of the efficiency, in terms of tin enrichment, of various possible ore precipitating mechanisms in order to judge which ones are most likely to form a deposit of economic ore grade. The simple model calculations probably represent important limiting cases to the complex natural processes.

The components H - O - Cl - Na - K - Si - Sn are at least required to model a tin ore-forming solution. It is assumed that a fluid in this system is equilibrated at high temperature with a relatively reduced granitic rock (an ilmenite-series granitoid buffering redox and pH conditions near Ni/NiO and K-feldspar+muscovite+quartz, respectively). At 500°C, a total NaCl concentration of 1m, and a total potassium concentration of 0.3m, the fluid can contain up to 10<sup>-3</sup>m tin as SnCl<sub>3</sub><sup>-</sup> (1000 ppm), as defined by the equilibrium



If a cassiterite-saturated fluid is cooled in contact with its source rock, 98% of its initial tin content will be precipitated above 400°C. However, if the same fluid cools in isolation from the host rock minerals, it will not precipitate any cassiterite at any temperature but will instead become increasingly cassiterite-undersaturated. This is due to two effects that counteract reaction (1), (a) the dissociation of HCl<sup>0</sup> (the dominant acid species at high temperature) according to

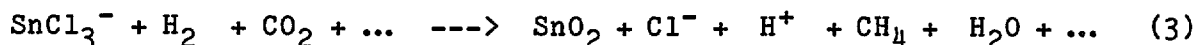


which causes a drop in pH from 5 at 500°C to 3.3 at 300°C, and (b) an effective drop in the redox level well below the initial Ni/NiO buffer due to the constant high content of H<sub>2</sub> in the solution.

Vapour separation will cause preferential loss of H<sub>2</sub> into the vapour phase and thus tend to counteract the effect (b) (above). However, combined mass and heat balance estimates indicate that this is unlikely to lead to cassiterite precipitation because, at least in a case of adiabatic vapour loss, the thermal effect of fluid cooling (promoting the pH drop), outweighs the chemical (oxidizing) effect of H<sub>2</sub> loss into the vapour.



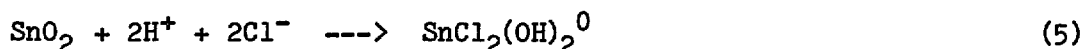
Carbon dioxide is present in many tin-ore forming fluids in concentrations of a few mole percent or more. Fluid-buffered cooling of a solution with  $x(\text{CO}_2)=0.1$  and otherwise identical composition as above first leads to partial precipitation of cassiterite, but below  $330^\circ\text{C}$  the solubility increases again to reach (in a closed system) the original Sn concentration near  $250^\circ$ . From  $500$  to  $330^\circ\text{C}$ , cassiterite precipitation from the dominant  $\text{Sn(II)}$  complex (eq. 1) occurs according to the following approximate bulk reaction (arrows = falling temperature):



This is driven to the right by the contribution from the reaction



which dominates the redox state of the fluid, and which outweighs the pH-decreasing effect of reaction (2), counteracting cassiterite precipitation. At temperatures below  $330^\circ\text{C}$ , however,  $\text{Sn(IV)}$  complexes become increasingly stable relative to  $\text{Sn(II)}$  species, thus diminishing the dominance of the redox effect (4) relative to the pH effect (2). This leads to the inversion of cassiterite solubility controlled by



Loss of  $\text{CO}_2$  by vapour separation has only a minor effect on the progress of reaction (3). In contrast to low-temperature, low-salinity systems, where the  $\text{CO}_2/\text{HCO}_3^-$  equilibrium is the dominant pH buffer in the fluid (e.g. Henley et al. 1984), the pH buffering capacity of equilibrium (2) dominates in high-temperature chloride-bearing solutions associated with tin deposition, even at high  $\text{CO}_2$ -contents. As a consequence preferential loss of  $\text{CO}_2$  into the vapour phase has a negligible pH effect and does not promote cassiterite precipitation.

The mass transfer calculations suggest a mechanism that could be crucial in the formation of an orebody of economic grade. This may involve a stepwise or two-stage enrichment process driven by a fluid that can initially be quite Sn-poor and cassiterite-undersaturated. Rock-buffered cooling of such a fluid will first lead to relatively low-grade cassiterite mineralization, because it requires consumption of a large amount of solid pH buffer (i.e. host rock) to neutralize  $\text{H}^+$  from reaction (2). However, once such a "protore" is extensively altered, cooling of subsequent batches of fluid of identical starting composition will, in the absence of  $\text{H}^+$ -consuming minerals such as feldspars, become increasingly acid and start to leach previously deposited cassiterite. This can result in 10-100 fold enrichment of the Sn-concentration in solution. Focussing of this enriched fluid and further cooling can then lead to re-precipitation of cassiterite without any wall rock alteration (e.g. in a lode-vein) provided the fluid contains some  $\text{CO}_2$ , and/or by local reaction with a suitable wall rock (e.g. in a breccia pipe) at any temperature. Compared with the fully rock-buffered "protore" stage, precipitation of a given amount of cassiterite at this "enrichment stage" will require (a) less fluid volume, (b) a fraction of the amount of reactive host rock or none at all, and will (c) be associated with less quartz precipitation. All of these factors will favour precipitation of a large amount of cassiterite in a small amount of host rock.

#### References

- Heinrich, C.A., Eadington, P.J. (1986) Econ. Geol., 81/3, in press.  
 Henley, R.W., Truesdell, A.H., Barton, Jr., P.B. (1984) Rev.Econ.Geol., 1.  
 Pabalan, R.T. (1986) Unpubl. Ph.D Thesis, Pennsylvania State University.  
 Eugster, H.P., Wilson, G.A. (1985). In High heat production granites, Inst.Min.Metallurg, 87.

**Paragenesis and Mineral Zoning in the Mt Carbine Tungsten  
Deposit, North Queensland**

N.C. Higgins<sup>1</sup> and D.L. Forsythe<sup>2</sup>

<sup>1</sup>Bureau of Mineral Resources, P.O. Box 378, Canberra, ACT, Australia,  
2601

<sup>2</sup>Queensland Wolfram Pty Ltd, PMB 13, Cairns, Qld, Australia, 4870

The Mt Carbine tungsten mine is one of the lowest grade producing tungsten mines in the western world operating at a head grade of 0.09% WO<sub>3</sub> through the utilisation of automatic ore sorters (photometric, X-ray fluorescence) to separate mineralised vein quartz from barren country rock. The ore minerals, wolframite and scheelite, are contained within quartz veins which cut metasediments (slates, cherts and basic volcanics) of the Siluro-Devonian Hodgkinson Formation. In the vicinity of the open pit the veins make up 10% of the rock volume.

Structural and mineral observations suggest that the ore mineralisation episode postdates the major deformational events in the country rocks and the sequence is as follows;

- 1) Development of a slaty cleavage (S<sub>1</sub>) during tight folding of sedimentary and volcanic units with partial to complete rotation of lithological layering towards parallelism with the slaty cleavage in zones of high strain. Tension gash quartz veinlets occur within cherty beds and are subparallel to S<sub>1</sub> planes. They contain minor sulphides but none of the common minerals (wolframite, apatite) of the ore stages. The rocks were folded under low greenschist facies conditions.
- 2) S<sub>1</sub> folded into open folds and kinks. In the open pit the axial planes of this deformation are rotated from 45° (on bench 345) to horizontal (Ruby Zone, bench 450).
- 3) Emplacement of undeformed andesite and dolerite dykes.
- 4) Porphyroblastic growth of andalusite due to the emplacement of the Permo-Carboniferous Mareeba granite and associated granite dykes.
- 5) Formation of near vertical wolframite-bearing quartz veins (stage I).
- 6) Dissection of stage I veins by sideways shear in subhorizontal faults.
- 7) Deposition of stage II mineralisation (chlorite ± fluorite ± albite ± scheelite etc) in these subhorizontal fracture planes and in vugs of stage I veins. Much of the scheelite is formed from replacement of wolframite.
- 8) Emplacement of felsite dykes.
- 9) Dismemberment of the mineralisation by steeply dipping sinistral faults (e.g. South Wall and Central faults).

Bell (1980) suggests the major deformations in the Hodgkinson Province occurred between 380-330 Ma. Out K-Ar age data of biotite from the mareeba granite yield an age of 278 ± 3 Ma which is identical to the age of hydrothermal muscovite from selvages of stage I veins.

The mineralisation may be divided into two stages. **Stage I** veins contain quartz + apatite ± wolframite ± K-feldspar ± biotite ± muscovite ± molybdenite ± bismuth and are surrounded by biotite + brown tourmaline alteration halos. Stage I veins are zonally arranged with a inner (higher temperature?) zone marked by the presence of K-feldspar-bearing, muscovite deficient veins. This zone coincides with the highest grade, both in individual vein and the grade of whole rock, and the most intense tourmalinisation of the country rock (>1000 ppm boron). Morphologically the veins are larger and more interconnected in this central zone than in other

zones. The K-feldspar bearing zone passes laterally into a zone of lower grade, parallel, thinner veins which contain muscovite, with a transition zone, of variable width, in which K-feldspar gangue and muscovite selvages coexist.

**Stage II** minerals fill open spaces within earlier quartz veins and occupy fractures which cut Stage I veins. These vugs and fractures may contain one or more of the following stage II minerals: fluorite  $\pm$  chlorite  $\pm$  schorl  $\pm$  albite  $\pm$  scheelite  $\pm$  cassiterite  $\pm$  pyrite  $\pm$  pyrrhotite  $\pm$  arsenopyrite  $\pm$  sphalerite  $\pm$  chalcopyrite  $\pm$  calcite. Scheelite replaces Stage I wolframite coating fractures and cleavage surfaces, but also occurs as coarser grains in stage II veinlets. The abundance of stage II minerals and veins is broadly concentric with the Stage I K-feldspar zone. Cassiterite, arsenopyrite, chalcopyrite and albite are more prevalent outside the K-feldspar zone and albite tends to replace primary K-feldspar in the transition zone. Replacive reactions associated with Stage II mineralisation (e.g. scheelite after wolframite, chlorite after K-feldspar) diminish towards the core of the K-feldspar zone.

We have no evidence for a major hiatus between stages I and II mineralisation episodes, but the mineralogic, structural and morphologic differences between each stage suggest that there is a fundamental change in style of mineralisation, perhaps from a prograde 'magmatic'-dominated system to a retrograde 'meteoric'-dominated system.

Bell, T.H., 1980, In, Henderson R.A. & Stephenson P.J. (Eds), The Geology and Geophysics of Northeastern Australia, Geol. Soc. of Aust., Queensland Div. Brisbane, 307-313.

# THE GENESIS OF THE CLAY DEPOSITS OF N.E. TASMANIA: A PRODUCT OF LOW TEMPERATURE HYDROTHERMAL ALTERATION?

N.C. Higgins<sup>1</sup> and M. Solomon<sup>2</sup>

Bureau of Mineral Resources, Box 378, Canberra, ACT 2601, Australia

The association of tin and clay deposits is one which occurs worldwide, the classic example being the Sn-W metallogenic province of S.W. England. The origin of such clay deposits is controversial, ranging from a hydrothermal process to weathering, or a combination of both. In N.E. Tasmania there is a clear association of clay deposits with alkali feldspar granite plutons which host tin-tungsten mineralisation. Most are redeposited clays associated with tin gravels, or Tertiary to recent river deposits (St Mount Cameron, St Helens, Pioneer). The Tonganah deposit, near Scottsdale, is a primary deposit and is mined from strongly kaolinised granite consisting 60% silica, 30% kaolin >12µm and 10% kaolin <12µm. The clay mined by APPM since 1975 produces a pure kaolin and is used as a paper filler. Tertiary weathering is postulated to have caused the formation of this and other clay deposits in Tasmania (Van Moort).

Recent mapping of the Tonganah deposit and the surrounding granites (Robinson, 1982), and company data, indicate that the kaolinisation occupies an elongate zone of 18 km<sup>2</sup> extent within coarse to medium grained biotite granite of the Scottsdale Batholith of Devonian age (K-Ar biotite 384 ± 3 Ma; unpublished data). At the clay mine the kaolinised host granite is a coarse grained and associated with a tin mineralisation. Tertiary sediments overlie unconformably the Ordovician-Devonian Mathinna Beds and kaolinised Devonian granite and consist of epiclastic sandstone and siltstone and cobble units. Several lateritic horizons occur within the Tertiary sediments. Drilling data in the area of the clay mine indicate that the kaolinisation has a funnel shape with a maximum depth of 70 m below the present day surface.

Geochemical and mineralogical data suggest that all phases of biotite granite present in the area are related by fractional crystallisation with the coarse and medium grained varieties representing the most fractionated phases. In particular, the medium grained variety (Mount Stronach granite) exhibits many of the mineralogical and geochemical characteristics typical of alkali feldspar granites of the Blue Tier and Eddystone batholiths (Higgins et al., 1985). These plutons are geochemically specialised (Sn, W, F, Li), and radiogenically enriched (high U, Th and K), and show evidence of substantial subsolidus alteration (Albitisation and sericitisation).

Drillcore from the Tonganah mine show a transition upward from sericitised coarse biotite granite through a smectite zone to kaolinised granite over several metres. K-feldspar and sericitised plagioclase are altered to kaolinite and halloysite; chloritised biotite to smectite and kaolinite; quartz remains unaltered. The clay beneath the Tertiary sediments is white but is generally discoloured (red-brown) below about 20 metres. This sequence is typical of a weathering profile through a granite body although the clay mineralogy is itself not unique to weathering situations.

The K-Ar biotite ages of unaltered granite samples average  $384 \pm 3$  Ma. K-Ar dating of clay size ( $-0.125+0.90$  mm) fractions (containing K-feldspar and mica contaminants) of three kaolinised granite samples from Tonganah indicate that with higher kaolin contents the K-Ar ages are significantly younger (Circa 360 Ma). Rb-Sr age data for the same fraction are consistent between 363-369 Ma assuming an initial ratio of 0.7100. Since kaolinite does not contain potassium the K-Ar data may be explained through argon loss from the remnant igneous primary feldspar contaminant either by weathering or a thermal effect at some later time. However, the Rb-Sr data suggest that the mica contaminant passed through its blocking temperature around 365 Ma indicating that there may have been a prolonged period of cooling and hydrothermal circulation within the granite after the initial granite emplacement.

Preliminary isotope data from Tonganah indicate significant variation in the  $\delta D$  within the Tonganah deposit. Near surface samples have  $\delta^{18}O_{SMOW}$  values between 19.4-20.5 per mil and  $\delta D$  between -60 and -75 per mil, and fall on the kaolinite weathering line. Deeper samples in the profile have significantly heavier  $\delta D$  (-40 to -50 per mil) and  $\delta^{18}O$  values between 18.5-20.0 per mil, and are displaced from the weathering line. The Pioneer and Sth Mount Cameron redeposited clays have  $\delta D$  values greater than -75 per mil. Our initial interpretation of these data is that the kaolinites with heavier  $\delta D$ 's represent hypogene clays formed at temperatures greater than  $30^{\circ}C$ . The isotopically lighter  $\delta D$  values could have formed by equilibration with recent surface fluids (associated with recent weathering). The hydrothermal fluid which formed these hypogene clays is isotopically different to that which is associated with fracture-fill kaolinite from late Devonian mineralisation at the Anchor mine, and present day meteoric waters, and represents a meteoric hydrothermal regime operating at some intermediate time.

Based on these preliminary isotope data, and the association of clay deposits with chemically specialised plutons in NE Tasmania, we suggest that these alkali feldspar granite plutons may have been the locus of prolonged hydrothermal convective circulation since granite emplacement, similar to the granites of SW England (Durrance et al., 1982). The limited geochemical data available suggest they contain sufficient concentrations of radioelements to have provided a long-lived heat source capable of driving a convective system, although alternative heat sources such as the emplacement of the Tasmanian Jurassic dolerites (180 Ma) may have provoked rejuvenation of hot groundwater circulation. In the latter case the alkali feldspar granite plutons would have provided ideal sites for subsequent kaolinisation, in preference to other granites, because of their low-iron nature and enhanced permeability resulting from their earlier metasomatic history. How much hydrothermal circulation models can produce the flat-lying geometry found at the Tonganah clay mine, remains unresolved.

- Durrance, E.M., Bromley, A.V., Bristow, C.M., Heath, M.J., & Penman, J.M., 1982, Proc. Ussher Soc., 5, 304-320.  
 Higgins, N.C., Solomon, M. & Varne, R. 1985, Lithos, 18, 129-149.  
 Robinson, P., 1982, Unpub. B.Sc. Hons thesis, University of Tasmania.  
 Van Moort, J., 1978, J. Aust. Ceramic Soc. 14, 13-19.

## INTERCONNECTED HYDROTHERMAL DRAINAGE OF THE PINE HILL INTRUSIVE SUITE

P.W.Holyland

Department of Geology & Mineralogy, University of Queensland, Brisbane, (Aust.)

The Upper Devonian Pine Hill Intrusive Suite underlies the Renison Bell tin district in western Tasmania. A number of separate intrusions formed a tapering ridge which outcrops at its narrowest, highest and most southerly point at Pine Hill. Subsurface limits are inferred from drilling, and outcropping quartz-porphyry dyke swarms which radiate from Pine Hill.

At least fifteen discharge points on the granite roof have acted as major escape channels for magmatic and meteoric fluids. At Pine Hill the discharge points are firstly; the ridge apex, where structurally weakened roof rocks have been extensively veined during greisenisation. Secondly, three calcareous horizons within the Crimson Creek formation in which contact skarns have been formed. Further to the north, along the granitoid ridge but away from the apex at Pine Hill, discharge points are all faults, or fault intersections, most of which have acted as the feeders for the main dolomite replacement deposits in the Renison Mine area.

Deposit types formed by the fluids have been subdivided into 13 mineral paragenetic stages (thermal metamorphism, early-stage 1-5 and late-stage 1-7), with styles typical of thermal metamorphism, prograde skarn (early-stage 1), retrograde skarn (early-stages 2-5), greisen (early-stage 5, late-stage 1), sulphide replacement (late-stage 1-3), and late meteoric water dominated stages (late-stage 4-7).

Fluid discharge through each point during early-stages 1-4 has been estimated from the product of total mass transfer and ore fluid solute concentrations. Calcareous horizons of the Crimson Creek formation acted as the major sinks during these stages. For late-stages 1-4, sulphur mass transfer, obtained from ore reserve estimates, has been used to estimate discharge. Sulphur concentrations in the fluid obtained by Patterson (1981) are  $10^{-2.4}$  molal for late stages 1-3, and between  $10^{-1.5}$  and  $10^{-2}$  molal for late stage 4.

Results of these measurements indicate that the largest discharge during skarn formation came from the Pine Hill apex zone, with subordinate amounts at three faults to the north. During late stages 1-3 the main discharge had shifted to the main Renison Mine area 2-3 kms to the north of Pine Hill, with a maximum from fault intersections on the eastern margin of the mineralised area, where the mine sequence R.L. is lowest. During late-stage 4, discharge from intersections at the west and south of the mine area became dominant, while concomitantly, descending meteoric fluids moved downdip in the dolomite horizons, leaching and pyritising the pyrrhotitic orebodies (late-stage 2) above 2250m R.L.

Fluid pressure at each discharge point for each paragenetic stage has been estimated using measured values of rock mass tensile strength, estimated values of regional stress, and observed rock failure mechanisms. Strength testing of all mine sequence lithologies indicates that the major strength controls were firstly, thermal metamorphism, which increased rock strength by a factor of 2-3, and secondly, fracturing, which decreased rock strength by a factor of up to 5 and locally higher. Failure mode changed from 'pervasive micro-tensile' fracturing, through vertical sheeted tension veins accompanied by horizontal bedding-plane veins, followed by tensile failure in faults, extensional shear failure, and finally

compressive shear failure. These failure modes indicate that fluid pressure declined from a peak equalling the maximum principal compressive lithostatic stress plus the rock tensile strength, to values approaching hydrostatic. By combining the strength values, with the failure mode observations, for a depth estimate of 2.5 kms, total fluid pressures can be calculated. These are about 70 Mpa (early-stage 1-5), >62 MPa (late-stage 1-3), >50MPa (late-stage 4), >45MPa (late-stage 5), >25MPa (late stage 6-7).

The above estimates of temporal and spatial variations in fluid pressure and discharge were combined in a pressure transient analysis of the discharging system, in which major features of water movement were duplicated using a simple 2D finite difference model.

The overall discharge history from the Pine Hill intrusive suite can be summarised as follows. Initial fluid production was at a maximum below the apex zone, probably due to the pressure dependance of volatile solubility in the magma. Subsequent patterns of migrating discharge and decreasing fluid pressure can be explained by the evolution of an interconnected drainage network. During late-stage 1-3, differences in flow between discharging points were probably related to their distance from each other, and to the nature of the sinks. Later, during late-stage 4-7, influx of meteoric water was controlled by the relative magnitude of previous discharges and by the elevation of the granite ridge above the main intrusive mass, which restricted the volume of high pressure fluid, and hence allowed greater influx from the surrounding country rocks.

#### References

Patterson, D.J., Ohmoto, H., & Solomon, M., 1981, Econ. Geol., 76, 393-438.

## Some Geologic Constraints on Genetic Concepts for Tin and Tungsten Deposits

I.N. Kigai

Institute of geology of ore deposits, petrography, mineralogy, and  
geochemistry (IGEM), Acad. Sci., Moscow, the USSR

In connection with the complexity of geological objects, narrow specialization of scientists, and involvement of physicists, chemists and mathematicians in solving genetic problems of ore deposits, the geologists have to be very careful in disclosure of principal regularities and bringing our theories abreast of the most reliable geologic data.

A very important problem is temporal relationship between a wall-rock alteration and ore deposition during an uninterrupted mineralization, i.e. in the course of a single stage. From theoretical geologic analysis and experimental data it is known (Korzzhinskii, 1969; Zharikov & Zharaiskii, 1973) that different zones of a monochronous metasomatic column initially appear almost simultaneously (on a microscopic level) and subsequently just grow thick like an accordion pleats. Any ore assemblage is always seen as superimposed on the alteration zones, and a vein filled with the same ore minerals is often bordered by zones of either advanced, moderate alteration or practically unaltered country rock. Therefore the vein can not be treated as a regular rear zone of the metasomatic column. These data lead to a conclusion that ore deposition took place substantially later than the wall-rock alteration of the same stage. From experimental data this time lag is estimated to be about  $10^4 - 10^5$  years for typical thicknesses of metasomatic zones (Kigai, 1979).

Taking all these points into consideration we may guess that (1) abrupt decrease of a rising fluid pressure, i.e. the throttling of fluids (cf. Barton & Toulmin, 1961; Ivanov et al., 1973) could not be a principal cause of ore deposition, and (2) when making any physico-chemical calculations or simulations of mineral equilibria, like those ingeniously performed by H. Helgeson (1979), it is necessary to consider that the fluids involved respectively in wall-rock alteration and ore deposition were not identical by composition, salinity, pH values and sometimes by the phase state.

Another important question is hydrological conditions of ore formation. In several vein-type tin and tungsten deposits silica leached from country rocks at the middle levels during greisenization or tourmalinization have been redeposited at lower horizons rather than above ore bodies as might be expected in the case of a running-water conditions. Extensive fluid inclusion studies of tin and tungsten deposits have revealed fluid pressures substantially higher than geostatic ones, which also evidences the stagnant conditions. It seems to be most probable that mineralization in hydrodynamically closed conditions with the temperature dependent natural convection of fluids is typical of endogenic ore deposits (Kigai, 1977).

Based on the above listed and many other geologic and experimental data, a model for endogenic hydrothermal mineralization implicating a suggestion of a heterophase fluids have been developed (Kigai, 1977).



References

- Barton, P.B., Jr, & Toulmin, P., 3d, 1961, U.S. Geol. Surv. Prof. Paper 424-D, 348-352.
- Helgeson, H.C., 1979, Geochemistry of hydrothermal ore deposits, 2nd ed., H.L. Barnes, ed. (Russ. transl. - 1982, pp 451-480).
- Ivanov, S.N., Ksenofontova, L.N. & Anfilogov, V.N., 1973, Doklady (Proc.) Acad. Sci., USSR, 211, 3, 694-696 (in Russ.).
- Kigai, I.N., 1970, Problems of hydrothermal ore deposition. Schweizerbart, Stuttgart, 261-264.
- Kigai, I.N., 1977, MAWAM Proc., v. 3, Prague, 343-348.
- Kigai, I.N., 1979, The main parameters of natural processes of endogenic ore formation. Novosibirsk, Nauka, 2, 7-34
- Korzhinskii, D.S., 1969, The theory of metasomatic zoning. Moscow, Nauka, 112 pp.
- Zharikov, V.A. & Zaraiskii, G.P., 1973, Geology of ore deposits, No 4, 3-19 (in Russ.).

## Tin and Tungsten Deposits of the Soviet Far East and their relationship to Granitoids

I.N. Kigai & V.A. Baskina

Institute of geology of ore deposits, petrography, mineralogy, and  
geochemistry (IGEM), Acad. Sci., Moscow, the USSR

Cassiterite-sulfide deposits of tourmaline and chlorite related types, minor or rare tin/tungsten greisen-related and sheelite-sulfide scarn deposits occur within the Soviet segment of the Circum-Pacific ore belt. The deposits are post-orogenic, their ages vary from middle Cretaceous to Eocene with the general tendency of being younger southward and eastward.

The deposits are associated with mixed volcano-plutonic complexes comprising stocks and dykes of gabbro, monzonite, granodiorite, normal and leucocratic granite, as well as dykes and flows of basalt, trachybasalt and shoshonite, andesite and trachyandesite, dacite, rhyolite and trachyrhyolite. From petrochemical and mineralogical composition of the rocks, high chromium content of granite and greisen up to 1000 ppm),  $^{87}\text{Sr}/^{86}\text{Sr}$  ratio 0.704 to 0.708, those magmatic series are partially of mantle origin, but formed under great influence of assimilation and paligenetic melting of sialic crustal rocks.

Important tin deposits are practically absent at the Pacific coastal region and appear only where the continental crust is thicker than 30 km (Lishnevskii & Beskin, 1986). The deposits are located in dome structures, above the core consisting of granite cupola surrounded by quartz-biotite hornfels. In typical multi-stage tin deposits, early quartz-tourmaline-cassiterite assemblage has been formed just after emplacement and partial crystallization of leucogranitic melt, whereas the sulfide-dominated mineralization of later stages was preceded by, and has been alternating with, injections of basaltic and andesitic dykes (Dubrovskii & Kigai, 1974). These data and similar relationships for some other tin producing regions (England, East Europe) suggest that without thick sialic crust and leucocratic granites there are no tin deposits. This holds also for tungsten. Basic mantle magmas may have been a major source of sulfur and base metals for later stages of mineralization.

Tin/tungsten granitoids belong to calc-alkaline and peraluminous types, according to L. Tauson's (1977) classification. They are enriched in K, have high K/Na ratio, larger Sn content in later phases of a magmatic suite and can be distinguished from barren granites only by wider dispersion of tin and tungsten contents. This makes the use of the granites in search for ore rather difficult.

V.A. Baskina (1982) has found in Marytime province that basic, intermediate and acid igneous rocks, either pre-ore, intra-ore or post-ore, reveal, in comparison to background values, a marked primary enrichment in K, Li, Rb, F, B, Cr, Zn, Pb, and Ba along with the wide dispersion of their content. The places of such enrichment are located along some meridional and latitudinal zones of deep-seated faults and perhaps they correspond to ore-concentrating knots of long endogenic activity. The use of these local haloes of indicative elements is assumed to be more promising.

References

- Baskina, V.A., 1982, Magmatism of ore-concentrating structures in the Prymor'e. Moscow, "Nauka", 260 pp (in Russ.).
- Dubrovskii, V.N. & Kigai, I.N., 1974, Zoning of hydrothermal ore deposits, v. 2. Moscow, "Nauka", 19-88 (in Russ.).
- Lishnevskii, E.N. & Beskin, S.M., 1986, Depth environment of endogenic ore formation. Moscow, "Nauka", 60-75 (in Russ.).
- Tauson, L.V., 1977, Geochemical types and potential ore capacity of granitoids. Moscow, "Nauka", 280 pp (in Russ.).

## GRANITES ASSOCIATED WITH W-Sn SKARNS

Teunis Kwak

c/- Department of Geology  
La Trobe University, Bundoora, Vic.

Tungsten- and -tin-bearing skarn can be separated into two categories namely (1) W-skarns with varying amounts of Mo, Cu and Zn, with no or only trace Sn values and (2) Sn-skarns with varying amounts of W, Zn, Li, Be, F, Cu, Mo, etc. Some of (2) may have W greater than Sn. The former are related to magnetite-series, I-type granites while the latter, to ilmenite-series S-type. Such I-type intrusions characteristically occur near plate margins (e.g. Cordilleran of North America) while S-types occur in more continental areas above thick prisms of continental crust. Globally, S-types and associates Sn-skarns may be almost absent in some areas (e.g. North America).

Both W- and Sn(-W) skarns may be subdivided into oxidized and reduced types depending upon the bulk chemical  $\text{Fe}^{+3}/\text{Fe}^{+3}+\text{Fe}^{+2}$  ratios of primary, not retrograde, assemblages. The following W-skarns occur based on their dominant minerals: magnetite + andradite + molybdscheelite  $\pm$  diopside and andradite - grossularite + diopside - hedenbergite + molybdscheelite (oxidized types) or grossularite - andradite + hedenbergite - diopside + scheelite or grossularite - almandine - spessartine + hedenbergite + scheelite + pyrrhotite  $\pm$  plagioclase reduced types). Nearly all these are proximal (< 300 m from pluton's contact) and calcic (e.g. Costabonne, France is partly magnesian).

Proximal Sn-skarns can be divided into andradite + wollastonite, magnetite, magnetite + fluorite  $\pm$  vesuvianite and forsterite + hedenbergite + magnetite  $\pm$  spinel  $\pm$  vesuvianite types. These can be greisenized ("exogreisen") nearest the pluton or "greisen" skarns (also called exogreisens) can occur where carbonate is replaced directly by greisen solutions. Distal Sn-skarns or "cassiterite-sulphide replacement" deposits are pyrite-, pyrrhotite- or, rarely, magnetite-dominant with talc (magnesian) or chlorite (calcic) and cassiterite.

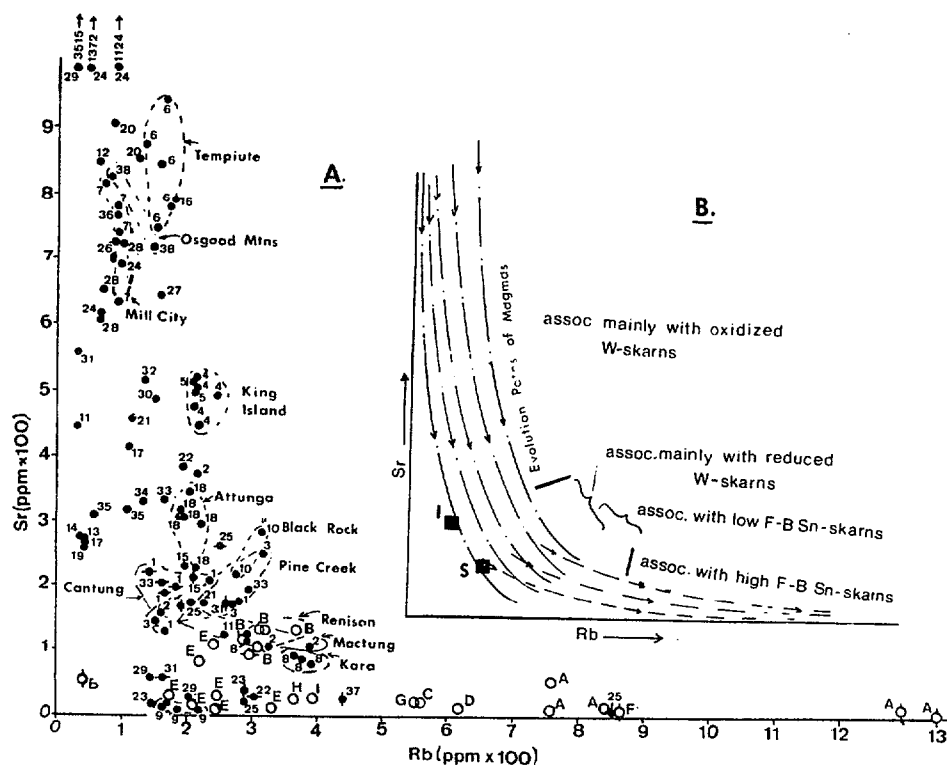
The following is based upon a compilation of the chemical analyses of granites from 70 W-Sn skarn deposit areas. Granitic plutons associated with W-skarns have the following characteristics: (a)  $\text{Na}_2\text{O}/\text{K}_2\text{O}$  ratios vary from 2.0 to 0.25, (b)  $\text{Fe}_2\text{O}_3/\text{FeO}$  ratios are mainly greater than 0.3 and up to 0.6;  $\text{Fe}_{\text{Total}}$  values are high (3)  $\text{Fe}_{\text{Total}}/\text{CaO}$  ratios are just under 1.0, and, importantly (d)  $\text{Rb}/\text{Sr}$  ratios vary from 4.0 to almost 0.0. In contrast, granites associated with Sn(-W) skarns have the following characteristics: (e)  $\text{Na}_2\text{O}/\text{K}_2\text{O}$  values are nearly always less than 1.0 and may be as low as 0.4; "apogranites" having high  $\text{Na}_2\text{O}/\text{K}_2\text{O}$  values are not found (f)  $\text{Fe}_2\text{O}_3/\text{FeO}$  values are generally low ( $\leq 1.0$ ) and commonly near 0.5;  $\text{Fe}_{\text{Total}}$  values are low, (g)  $\text{Fe}_{\text{Total}}/\text{CaO}$  values are high and (h)  $\text{Rb}/\text{Sr}$  values are always high varying from 2.0 up to 85.0 with most in the range of 5.0 to 10.0.

Using the  $\text{Rb}/\text{Sr}$  ratios (Figure 1) as indications of the degree of evolution or differentiation of the parent magma, it is apparent that

the largest W-skarns (e.g. Mactung and Cantung, Yukon, Canada; Pine Creek, Calif., USA) are associated with highly evolved I-type granites ( $Rb/Sr$  values  $\approx 1.0$ ). They may even exhibit mild greisenization (muscovite - quartz - fluorite  $\pm$  tourmaline). Most large oxidized W-skarns such as Mill City, Utah, USA, Tempiute, Nev., USA and King Island, Tas., Australia are related to less evolved granites ( $Rb/Sr$  values  $\approx 0.4$ ) although some may be evolved (Kara, Tas., Australia). Evolved I-types are often associated with skarns having minor Sn-values (up to 0.6 wt%  $SnO_2$ ). These granites also often occur as small stocks.

High F- Sn skarns are invariably related to small, highly greisenized granite cupolas (Moina and Mt. Garnet skarns, Qld., Australia) having very high  $Rb/Sr$  values ( $> 10.0$ ). Large oxidized Sn skarns are often related to less evolved granites but some of the largest distal Sn skarns (Renison, Tas., Australia) are probably related to such granites as well ( $Rb/Sr \approx 2.0 - 4.0$ ).

Generally, evolved I-type granites are associated with the largest W-skarns and evolved S-type granites with the largest Sn-W skarns. Some large Sn-W skarns appear to be associated with less evolved S-type granites. Compared to the I-type granites of the eastern Australia (point I in Figure 1B) the granites associated with W-skarns are higher in Rb and  $K_2O$  as well as some having much higher Sr values. The granites are quartz monzonitic and the differences to those in eastern Australia may be the reason W-skarns are so small in eastern Australia (except for King Island which is also quartz monzonitic) as compared to those in the western USA and Canada.



The variation of Sr with Rb for granites associated with W-skarns (solid dots) and Sn-skarns (circles). Symbols with vertical lines through them represent dykes and those with horizontal lines represent aplite dykes. The numbers in Figure 1A refer to individual analyses from a specific deposit. In Figure 1B the interpreted paths of the evolution of both I-type (---) and S-type (—) magmas are given. I = average I-type and S = average granite for eastern Australia after Chappell and White, 1983.

# **INTEGRATION OF GEOLOGY AND GEOPHYSICS IN THE DEVELOPMENT OF EXPLORATION MODELS FOR MASSIVE SULPHIDE TIN DEPOSITS IN WESTERN TASMANIA**

Ross R. Large

University of Tasmania, Hobart.

Massive sulphide tin deposits in Western Tasmania (Renison Bell, Cleveland, Mt. Bischoff and Severn) have above average tonnage-grade characteristics compared to other styles of tin mineralisation throughout the world. The sulphide deposits consist of stratabound lenses of massive pyrrhotite-cassiterite within a sedimentary carbonate host horizon of either dolomite or limestone. The orebodies are spatially related to the emplacement of ilmenite series granites (plus related quartz-porphyry dykes), and a spectrum of mineral assemblages and tin grades are developed according to distance of carbonate replacement from the source granites. The tin deposits are restricted to three separate carbonate bearing stratigraphic levels within the Precambrian-Cambrian Dundas Trough sequences; the Upper Oonah Formation, Success Creek Group and the Crimson Creek Group. Local cycles of sedimentation appear to control the deposition of the favourable carbonate host rocks at each of the three stratigraphic levels. Structural preparation of the ore solution plumbing system by early faulting is considered to be a necessary prerequisite for fluid access from the granites to the host carbonates.

Recent studies of the aeromagnetism and regional gravity of the Dundas Trough have led to a new interpretation of the regional geology and consequent controls on tin mineralisation. The regional aeromagnetic pattern accentuates the importance of the Huskisson Synclinorium as a major NNW trending fold structure which can be traced for over 45 km and is refolded about NNE trending axes. The Heemskirk and Meredith granites, outlined by magnetic low areas, are interpreted to be intruding major synclinorial structures separated by the Renison anticlinorium. The favourable host stratigraphies for tin mineralisation can be traced, using aeromagnetic data, on either side of the synclinorial structures. Superimposed on this magnetic pattern is a gravity trough structure extending along a north easterly trend between gravity lows over the Heemskirk granite and Granite Tor. This feature is very pronounced on the residual gravity map, and is interpreted to relate to a flat topped granite ridge extending north easterly under the Dundas Trough and adjacent Mt. Read Volcanics. The major tin deposits are aligned along the northern and southern margin of this structure, where the edges of the granite ridge cut the favourable stratigraphy in the synclinorial structure.

The exploration model developed by this approach concentrates on the definition of discrete magnetic (or geochemical) anomalies that occur in a favourable local stratigraphic and structural setting, within high priority areas as defined by the regional aeromagnetism and gravity.

# LANCANG RIVER GRANITOID BELT AND ITS TIN MINERALIZATION, WESTERN YUNNAN, CHINA

Liu Chanshi<sup>1</sup>, Zhu Jinchu<sup>2</sup> and Cai Dekun<sup>3</sup>

Geology Department, Nanjing University, Nanjing, China

Lancang River Granitoid Belt (LRGB) is located in the western part of Yunnan Province, China. It is distributed along the Lancang River Deep Fault (LRDF) of nearly NS trend and exposed on an area of about 10000 km<sup>2</sup>, extending southwards through Burma to link with the tin-mineralized belt of central Thailand and central Malaysia.

After the middle Palaeozoic Era, the Qiantang-Tangla-Baoshan block rifted from the Gondwanaland was carried by Palaeotethyan oceanic crust to drift northeastwards. Finally, it was coalesced to the southeast China platform by collision between these two blocks during the late Triassic.

The LRDF belt 800 km long is a suture zone and the LRGB granitoids are the products of colliding actions between two continents. This has been confirmed by the following evidences: 1) The floral groups of early to middle Palaeozoic strata on both sides of the suture are significantly different. One belongs to Cathaysian affinity while another to Gondwanaland. 2) Island arc type andesites of middle Palaeozoic age occur widely along this zone. 3) The paired metamorphic zones represented by high-pressure mineral assemblage and high-temperature mineral assemblages respectively have been clearly detected. 4) Hercynian mafic to ultramafic rocks, as the remains of early oceanic crust have been found in the zone. 5) The Hercynian-Indosinian granitoids are linearly arranged in the zone.

According to the relationship between ages of granitoid emplacement and collision activity, the LRGB granitoids can be divided into three types.

A. Pre-collision granitoids. They are spatially restricted in the Precambrian-Cambrian regional metamorphic rocks with gneissic structure and generally are small in scale, mainly including Shiganghe granite (585 Ma, Rb-Sr) and Tiechang granite (472 Ma, Rb-Sr).

B. Syn-collision granitoids. They make up more than 90% of granitoids in LRGB, linearly extend in nearly NS direction and consist of many multiple-cyclic composite granitic batholiths. Based on the isotopic data, their ages of emplacement began in the Carboniferous Period (Pinhejie granite, 210-264 Ma, Rb-Sr: 244-190 Ma, K-Ar).

C. Post-collision granitoids. They occur scatteredly within the early granitic bodies and the surrounding rocks (Lalitoushan granite, 64 Ma, K-Ar).

The granitoids of syn-collision type are mainly biotite monzonitic granites and usually have porphyritic textures with phenocrysts of K-feldspar up to 4-5 cm long, some of which are partially Al-Si ordered microcline, the other is completely Al-Si ordered maximum microcline. The biotite contained is Mg-biotite with the occupancies of Mg ions in octahedral sites more than 37%. The chemical characteristics of this granite type are: 1) moderate SiO<sub>2</sub> contents (69%±); 2) greater ANKC values (mostly >1.1; 3) lower alkalinities (K<sub>2</sub>O + Na<sub>2</sub>O <7%); 4) greater Sn, W contents (3 times of crust's average); 5) moderate REE contents ( $\Sigma\text{Ce}/\Sigma\text{Y}=3-4$ , and slight Eu negative anomalies ( $\text{Eu}/\text{Eu}^*=0.95-0.67$ ); 6) high initial Sr ratios (Lancang granite 0.7176-0.7227; Pinhejie granite, 0.7153-0.7205);

7) rich in  $^{18}\text{O}$  (Pinhejie granite with  $\delta^{18}\text{O}$   $10^{\circ}/\text{oo}$ ).

Above-mentioned characteristics suggest that the granitoids formed by colliding activity between two continental blocks have some similar features to S-type granitoids derived from the continental crust.

The main tin-mineralizations of this area are spatially closely associated with multiple cyclic granitoids and in time related to Indosinian, Yanshannian and Himalayan granitoids.



# **MAGMATIC EVOLUTION OF THE POIMENA GRANITE AND ASSOCIATED TIN-BEARING ALKALI-FELDSPAR GRANITES, NORTHEASTERN TASMANIA.**

D. E. Mackenzie, Bureau of Mineral Resources, Australia.

A major component of the Middle Devonian Blue Tier Batholith of northeastern Tasmania, at the southern end of the Lachlan Fold Belt, is the Poimena Granite. It consists largely of coarse, porphyritic (megacrystic) biotite granite, interleaved with, or overlain by, in its upper parts, medium and fine-grained variants which have been emplaced into the roof zone during cooling and contraction of the main body. The finer-grained granites tend to be more differentiated than the main mass, and there is some evidence of quenching in the finest-grained granites, which tend to be highest in the pluton. Sericitic and greisen alteration are concentrated in these fine-grained rocks in the southern part of the pluton.

The Poimena Granite is intruded by several small bodies, probably also 'sheet'-like in form, of biotite-oligoclase-bearing phyrlic alkali-feldspar granite and aphyric Li-mica-topaz-albite alkali-feldspar granite (AFG). Contacts are sharp, and thermal effects, such as recrystallisation of biotite, are present in the Poimena Granite up to 1km from the contacts. Alteration of Poimena Granite by fluids from the AFGs appears to be very limited, and concentrated in the southern end of the Poimena pluton, notably around the Anchor mine.

Major and trace-element data from almost 200 samples, including 69 new analyses, show that as the Poimena Granite evolved towards slightly more felsic compositions ( $\text{SiO}_2$  increases from 70.2 to 75.3%),  $\text{Fe}_{\text{total}}$ ,  $\text{MgO}$ ,  $\text{CaO}$ ,  $\text{Na}_2\text{O}$ ,  $\text{P}_2\text{O}_5$ ,  $\text{K/Rb}$ ,  $\text{Ba}$ ,  $\text{Li}$ ,  $\text{Sr}$ ,  $\text{Zr}$ , and  $\text{Sn}$  decrease, while  $\text{K}_2\text{O}$ ,  $\text{Rb}$ , and  $\text{LREE}$  increase and the rocks become more peraluminous. Trends on variation diagrams are generally rectilinear, but are not tightly constrained, suggesting that crystal fractionation was perhaps complicated by injections of 'fresh' magma. The AFGs are geochemically distinct from the Poimena Granite, and show systematic, generally linear, trends on most variation diagrams. These trends are at large angles, or even directly opposite to those of the Poimena Granite:  $\text{Fe}_{\text{total}}$ ,  $\text{MgO}$ ,  $\text{CaO}$ ,  $\text{K}_2\text{O}$ ,  $\text{K/Rb}$ ,  $\text{Ba}$ ,  $\text{Pb}$ ,  $\text{Zr}$ ,  $\text{Y}$ , and  $\text{LREE}$  decrease,  $\text{Na}_2\text{O}$ ,  $\text{P}_2\text{O}_5$ ,  $\text{Li}$ ,  $\text{Rb}$ ,  $\text{Sr}$ ,  $\text{Nb}$ ,  $\text{Sn}$ ,  $\text{W}$ ,  $\text{Ga}$ , and  $\text{F}$  increase, and the rocks become more peraluminous as  $\text{SiO}_2$  decreases from the less evolved biotite and oligoclase-bearing phyrlic AFGs to the most evolved aphyric AFGs.

The AFG data are consistent with fractionation of a peraluminous magma, probably unrelated to the Poimena Granite magma, towards more albite-rich compositions under the influence of its high fluorine content, which displaces the 'granite minimum' towards the albite corner. The source of this magma could have been a refractory one, relatively enriched in high melting-point phases such as biotite and sphene (which may be rich in  $\text{Sn}$ ). This model is in accord with isotopic abundance and age data on the Blue Tier Batholith presented elsewhere in this Conference by Sun et al., and with models proposed for evolution of similar  $\text{Sn}$ -mineralising granites, for example, elsewhere in the Lachlan Fold Belt, and in Cornwall.

The dramatic enrichments (in Rb, Li, Sn, F, etc.) and abrupt changes, even reversals, in chemical trends of the AFGs relative to the Poimena Granite have been interpreted as the result of intense hydrothermal alteration, by fluids rich in Na, Rb, Li, Sn, F, etc., of extreme fractionates of the Poimena Granite. However, it is difficult to account by this mechanism for (1) the apparent normal intrusive nature of the AFGs and the general lack of alteration adjacent to them, (2) the consistent, regular, linear chemical variation in the AFGs, (3) the large angles, or reversals, and, in some cases, gaps, between the Poimena Granite trends and the AFG trends, (4) the lack of evidence of significant concentration of Sn, Li, and F with differentiation in the Poimena Granite, and (5) the consistent, higher values of Nd from the AFGs relative to those from the Poimena Granite (as shown by Sun et al., this conference).

# THE SOURCES OF ORE-FORMING ELEMENTS IN THE DACHANG TIN FIELD, CHINA

Minlu Fu

Department of Geology, La Trobe University, Bundoora, Vic, 3083.

The Dachang ore field is one of the most important tin, zinc, lead, antimony, silver, indium and cadmium provinces in China and contains many large hydrothermal cassiterite-sulphide deposits. These include the Changpo, Bali, Longtoushan, Lamo, Dafulou and Kangma deposits. They are hosted in both early Devonian sandstones and siltstones as well as in middle Devonian limestones, marls, and interbedded cherts and siltstone. The NNW-trending Longxianggei anticline is the most important structural system in the Dachang ore field and parallel to it there are a series of subsidiary folds and faults. The cassiterite-sulphide deposits are mainly located in its NW limb and controlled by subsidiary fold called the Changpo anticline. The Longxianggei granite is intruded along a fault, near and parallel to, the axis of the Longxianggei anticline. It is responsible for the tin mineralization, is characterised by abundant tourmaline, and is dated by K-Ar methods to have been intruded between 97-107 Ma. Although several deposits in the Dachang field have been studied, emphasis is here placed on the Changpo deposit, the largest of the cassiterite sulphide replacement deposits.

Paragenesis of sulphides. In the Changpo deposit the mineral zonation of pyrite at the top and pyrrhotite in the bottom of the deposit was apparently explained by temperature,  $fO_2$ , and  $fS_2$  variation. The pyrrhotite is assumed to have precipitated under a more sulphur-poor, reducing environment than the pyrite. However, more detailed examination of the Changpo, Bali, Longtoushan deposits has shown that the sulphide zonation pattern is more complex than previously described. For example, the pyrite-bearing No 92 orebody is located at the bottom of the Changpo deposit, whereas the pyrrhotite-bearing No 91 orebody in which magnetite is also found is located in the middle of the deposit. Detailed investigation of the No 92 orebody shows that the type of sulphide species present depends on the composition of the wall rock. Adjacent to siltstone pyrite predominates; near limestone pyrrhotite is concentrated. Analyses of wall rock indicate the Fe/S ratio of the wall rock is the main control of mineral paragenesis. Where the Fe/S ratio exceeds 100, pyrrhotite is the predominant sulphide. If the Fe/S ratio is less than 5, pyrite is the predominant sulphide. Between these limits both pyrrhotite and pyrite occur together in the same orebody. These data suggest that the iron and sulphur in the ore horizons are mainly derived from the wall rocks during the mineralisation episode.

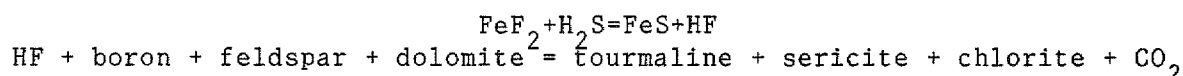
Co/Ni ratios of pyrite. Co/Ni ratios have been used to differentiate between hydrothermal (Co/Ni ratio ~1-5) and sedimentary (Co/Ni ratio <1) pyrites. With few exceptions, the pyrites of the Changpo deposit have Co/Ni ratios <1 similar to pyrite from wall rock, both proximal and distal to the deposit. This may imply a common sedimentary source for Fe and S in the Changpo deposit. Pyrites from the Longtoushan deposit have Co/Ni ratios <1 suggesting a mixed source for the Fe and S. The wall rocks in this deposit are limestone with low concentrations of Fe and S.

Sulphur isotopes. The  $\delta^{34}S$  of pyrite from the Changpo orebodies average -41 per mil (9 samples); pyrite from proximal wall rocks average -3.7 per mil (5); pyrite from distal wall rocks average -4.30 per mil (4).  $\delta^{34}S$  of 66 samples of sphalerite can be divided into three groups, based on their different paragenesis, which have average values of -1.3, -4.3, -6.4 per mil respectively. These data support the premise that Fe and S are mainly

derived from one source (wall rock) whereas Zn may be derived from several sources.

Lead isotopes. Without exception 12 samples from 4 deposits in the field have  $\mu$  values ( $^{238}\text{U}/^{204}\text{Pb}$ ) of 8 and show anomalous lead. Calculations show that the anomalous lead separated from a source  $2 \times 10^9$  years ago and mixed with common lead of the granite during mineralisation. It can be concluded that the lead was derived from several isotopically distinct sources.

Leaching experiments. A mixed sample representing the proportions of different wall rock in the Dachang field was leached for 7 days in a titanium autoclave. The temperature, pressure and composition of the fluid used was determined from fluid inclusion data. The experiments indicated that tin, zinc, lead and copper may be mobilised from both wall rocks and granite. Tin mobilisation was found to be related to  $[\text{F}^-]$  and not  $[\text{Cl}^-]$ . Copper, lead and zinc were mobilised easily in  $\text{Cl}^-$  bearing fluids but  $\text{F}^-$  is the more powerful mobilizer of Fe. As Fe-F complexes would have flowed through sulphur-enriched wall rocks the following reactions might have occurred.



This explains why cassiterite is usually accompanied by sulphides and tourmalinization, chloritization and sericitisation.

In conclusion, the Fe, S, and Pb in the Dachang cassiterite-sulphide deposits appear to be dominantly derived from wall rock sources. Sn and F, and in part Zn, are contributed by magmatic sources. The sulphide species precipitated with cassiterite is strongly controlled by wall rock.

## TUNGSTEN MINERALIZATION IN SOUTH KOREA

Kun Joo Moon

Korea Institute of Energy &amp; Resources, Seoul, Korea

Tungsten ore deposits in South Korea are mainly W-Mo type and a few are W-Cu, W-Fe types. Mode of occurrence of W minerals classifies these deposits as pegmatite, beccia pipe, quartz vein, and skarn types. Ssangjeon and Ogbang are pegmatite type W deposits. Dalsung and Ilkwang are breccia type W-Cu deposits. Quartz vein types include cheongyang, Daehwa, Donsan, Wolak,, Dongbo, Sannae, and Bonguje. These deposits except for the last (free of molybdenite) are W-Mo type ore deposits. Sangdong, Buam, Chilbo, Ulsan, and Seoseok are skarn type W ore deposits. The W skarn orebodies contains scheelite only, but scheelite usually contains small amounts of molybdenum (1-4% Mo), and the skarn is generally associated with quartz veins which bear scheelite and/or wolframite associated with molybdenite.

Molybdenite-bearing-quartz vein with no tungsten minerals are reported in many places. Annual production of tungsten and molybdenum amounts to about 4,500 M/T( $\text{WO}_3$  70%) and 600 T/M( $\text{MoS}_2$ ) respectively. Among them, 99% of total W and a half of Mo products are recovered or the Sangdong mine. Sangdong is the most significant tungsten ore deposit in the country and it displays almost the same types of mode of occurrence of tungsten minerals as other W ore deposits such as the skarn, quartz vein and stockwork types.

Exploration drilling, which discovered a hidden granite apophysis at about 500 meters below the present orebody at the Sangdong mine, indicates clearly that the tungsten mineralization is related to a granitoid as a source rock. The age of the granite (sericite) is more or less equivalent to the age of the skarn (biotite) formation (81 to 85 Ma). Limited numbers of ore deposits are age-dated as follows: Ogbang (26 Ma), Bonguje (168 Ma), Daehwa (89 Ma), Ilkwang (69 Ma), Sannae (65 Ma). Although limited, these data indicate that tungsten mineralization take place in several cycles of granitic activities from Permian to Cretaceous periods.

Tungsten mineralization associated with molybdenum appears to follow the tungsten mineralization and seems to be important at the later stage of Cretaceous plutonism. The W-Mo mineralization is followed by Mo mineralization Molybdenite-bearing quartz veins without association of tungsten minerals occur in several deposits such as Jangsu and Samdong Mo ore deposits. More age dating are required to confirm this model of early W to late Mo mineralization.

Through studying the Sangdong ore deposits, the cycles of tungsten (in Korea) mineralization may be easily understood. The Sangdong orebody is composed of skarn and quartz veins. As the distribution of Mo-rich scheelite tends to increase in the central zone (quartz-mica) skarn, so the content of Mo in the core of scheelite crystals is generally higher than that of crystal rims in the skarn orebody. Quartz veins in or near the skarn contain generally more molybdenite than scheelite, like other W-Mo vein type ore deposits. Locally scheelite occurs in the Sangdong skarn closely associated with magnetite like the Ulsan W-Fe skarn ore deposit. Wolframite-bearing quartz veins in the Sangdong correspond to the W-Cu orebody like Dalsung in terms of mineralogy. Recently discovered are molybdenite-bearing quartz veinlets in the Jangsan Quartzite, which is overlain by the Myobong Slate which encloses the present ore deposit. This

localized occurrence of molybdenite veins indicates that molybdenum mineralization without association of tungsten took place much later than W-Mo type mineralisation. Sulfur isotope composition of molybdenite from Sangdong (quartz vein, skarn, Jangsan Quartzsite) and Sannae (quartz vein) is almost the same ( $\delta^{34}\text{S}$ , 4.9-6.3 permil, 5.2-6.0 permil, respectively) indicating a genetic relation between the two deposits.

Since the studied W-Mo deposits display similarities in their temperatures of mineralization, mineralogy and isotopic composition, it may be concluded that tungsten deposits in South Korea mainly formed in several cycles of plutonism ranging from Permian to Cretaceous periods, they are genetically related and their ore fluids were originated from source similar to the Sangdong Granite.

Cretaceous granites which are related to major tungsten mineralization are reported as I-types and magnetite series granites. This may explain the characteristic Sn-free feature of the tungsten deposits.

## GEOCHEMISTRY OF MICAS FROM PORTUGUESE TIN AND TUNGSTEN DEPOSITS

Ana M.R. Neiva

Department Mineralogy and Geology, University of Coimbra, Portugal

In the tungsten-tin deposit from Panasqueira there is magmatic muscovite of S-type granite, muscovite as product of greisenization and muscovite of tungsten-tin quartz veins in selvages along the quartz veins and schist contact or precipitated within the quartz vein. The muscovite of greisenized granite has more W, Sn, Nb, Ta, Zn, Ba, Cs and less Ti,  $\text{Fe}^{2+} + \text{Mg}$ , F, V, Li, Ni, Zr, Sc, Y, Ce, Rb than the muscovite of parental granite and crystallized at lower temperature and under greater  $f_{\text{H}_2\text{O}}/f_{\text{HF}}$ . The muscovites of quartz veins have more W, Sn, Zn, Cu, Pb, Ba, Cs and less Ti, Nb, Ta, Li, Ni, Zr, Sc than the muscovite of granite and crystallized at lower temperature and under greater  $f_{\text{H}_2\text{O}}/f_{\text{HF}}$ . They also have more Mg, Cu, Ba, similar or more W and less Nb, Ta than the muscovite of greisenized granite.

In the tin deposit from Montezinho, tin-tungsten deposits from Argoselo and Vinheiros and tungsten deposit from Borralha, muscovite also mainly occurs in quartz veins particularly in selvages along the quartz veins and schist contact. Generally the analysed muscovite have more Sn and W.

The muscovite of tin-tungsten quartz veins has more W, Ni, Y, Ce, Rb and less Na,  $\text{Na}/(\text{Na}+\text{K})$ , V than the muscovite of tin quartz veins. The muscovite of tungsten-tin quartz veins has more  $\text{Fe}^{2+} + \text{Fe}^{3+}$ , F, Li, similar or more Mg and less Nb, Ta, Sn, Cs than the muscovite of tin-tungsten quartz veins. The muscovite of tungsten quartz veins has more Al, V and less  $\text{Fe}^{2+} + \text{Fe}^{3+}$ ,  $\text{Fe}^{2+} + \text{Fe}^{3+} + \text{Mg}$ , F,  $\text{F}/(\text{F}+\text{OH})$ , Zn, Ni, Li, Y, Rb, Cs and crystallized under greater  $f_{\text{H}_2\text{O}}/f_{\text{HF}}$  than the muscovite of tungsten-tin quartz veins. The muscovite of tungsten quartz veins has more W, V, and less Na,  $\text{Na}/(\text{Na}+\text{K})$ , F,  $\text{F}/(\text{F}+\text{OH})$ , Nb, Ta, Zn, Sn, Li, Rb, Cs and crystallized under greater  $f_{\text{H}_2\text{O}}/f_{\text{HF}}$  than the muscovite of tin quartz veins.

The Sn - ( $\text{MgFe}^{2+} + \text{Fe}^{3+}$ ), Sn - F, Sn - Cs, F - ( $\text{Mg} + \text{Fe}^{2+} + \text{Fe}^{3+}$ ), F - Cs positive correlations were found for the muscovites of quartz veins from each deposit. The Ta - Nb, Sn - Li and Li - F positive correlations were only found within the muscovites of tin quartz veins and also within the muscovites of tin-tungsten quartz veins.

In all the deposits there is metasomatic schist rich in muscovite bordering the quartz veins. Tourmalinite with rare muscovite was also found in Panasqueira in contact with quartz veins. Muscovite of those rocks has more Mg and F and crystallized under lower temperature and great  $f_{\text{H}_2\text{O}}/f_{\text{HF}}$  than the muscovite of selvage in contact. In Panasqueira the muscovite of metasomatic schist and tourmalinite has more K, F and less  $\text{Fe}^t$ , Mg, Na,  $\text{Na}/(\text{Na}+\text{K})$  and crystallized under lower temperature and  $f_{\text{H}_2\text{O}}/f_{\text{HF}}^t$  than the white mica of country phyllite.

At the tungsten deposit from Borralha the country rock schist was contact metamorphosed and metasomatically altered into a muscovite-ripidolite schist with rare biotite and also into a muscovite schist with almandine-spessartine through interaction by fluids associated with the tungsten quartz veins. The muscovite of contact metamorphosed and metasomatically altered schists has more  $\text{Na}/(\text{Na}+\text{K})$ , F, W, Nb, Ta, Zn, Sn, Li, Rb, Cs, and less Cr, V, Ni, Cu, Sc, Y, Nd, Ce, La, Sr and crystallized under lower temperature and  $f_{\text{H}_2\text{O}}/f_{\text{HF}}$  of more metasomatically altered schists.

Tin and tungsten have origin in granite magma originated by partial melting of sedimentary source materials and were concentrated in the hydrothermal fluids with decreasing temperature. Fluorine seems to have transported tin, but did not transport tungsten. As water and chlorine concentrate in fluids they also probably transported tin. Tungsten enters muscovite structure with more difficulty than tin and was probably transported by water as tungstic acid or  $WO_4^{2-}$ .

The metasomatic effects caused by the quartz veins fluids on the country rock suggest that the reactions with the country rock favour concentration of tin and tungsten.



## GENESIS OF THE MAYO-DARLE SN DEPOSIT, CAMEROON

David I. Norman<sup>1</sup> and Eaun Mearns<sup>2</sup>

New Mexico Institute of Mining and Technology, Socorro NM 87801, USA and  
Mineralogisk-Geologisk Museum, Sars Gate 1, Oslo, Norway

The Mayo-Darle complex consists of syenite, granite, rhyolite with benmorite clasts, and granite porphyry. The deposit is lode veins and geater than 100 mT of stockworks which are mineralized with cassiterite, quartz, topaz, and zinnwaldite. Fluid inclusion studies on igneous and vein quartz indicate an ore fluid or a temperature of 600°C and a salinity of 50 eq. wt. % NaCl was present throughout the granite. The Rb-Sr and Sm-Nd isotopic composition of fluid inclusion waters in igneous quartz from granite and from vein minerals was analyzed as well as the isotopic composition of rocks. These data indicate that the granite which hosts the mineralization was intruded at 59 Ma from a mantle derived melt with some crustal component; major element modelling suggests differentiation from an alkaline basalt parent. The Rb-Sr isotopic compositions of fluid inclusion waters indicate that the ore fluids could not have been derived from the granite at the time of crystallization. Rather an age of mineralization of 45 Ma is indicated, which is about the age of the porphyry. Sm-Nd isotopic analysis of inclusion fluids (analytic methods for this type of analysis were developed by us and are being reported) are in progress and will indicate the amount of crustal material in the ore fluids and whether the crustal component in the granite could have resulted from interaction with hydrothermal fluids. Splits of the inclusion-liquid samples isotopically studied will be analyzed for trace elements by neutron activation methods this spring and the results will be reported.

## ASYMMETRY OF CENTERED PLUTONS IN JAPAN

Tamotsu Nozawa

Geology Dept., Shimane Univ., Matsue, Japan

A lot of centered plutons are found in Japan. They are mostly of diapiric intrusion and have nearly common size of around 10 km in diameter. They are usually of Cretaceous and early Tertiary age and a few exceptions of Jurassic. They are composed of two or more concentric zones of different composition, mafic in border and felsic in core, changing gradually zone to zone. In most predominant case, they have quartzdiorite- or tonalite-border and granite porphyry core, changing through granodiorite and granite successively.

Comprehensive study reveals that some of them have a distinct tendency of asymmetry or de-centering. Among 72 centered plutons which I and my colleagues have collected from all through Japan, 42 plutons have regular zoning structure, that is, mafic border and felsic core, excluding centered complex of cauldron type. Because of irregularity in outline and in zoning structure and of coverage of younger rocks, asymmetrical structure could be studied on around 20 plutons. As a result, more than half of these 20 plutons have distinct tendency to have felsic core deviated southwards, southeastwards or rarely eastwards. Only two or three have deviation northward or westward. The rests are apparently well concentrated, not deviated, or deviated too weakly to determine the direction of deviation.

The reason for the asymmetry of centered plutons is not yet sure. One possibility would be found in tectonic effect caused by subduction of plate from Pacific Ocean during Mesozoic and early Tertiary. During these times, when most of the centered plutons in Japan were emplaced, Kula Plate was moving northwards in the northwestern Pacific and the Japanese Islands was located further northwest than the present position close to the eastern margin of the Eurasia Continent. After Kula Plate moved away to the north, Pacific Plate replaced the Kula Plate and moved westwards, probably in late Cretaceous age. Around Miocene age, the Japan Sea opened and the Japanese Islands was shifted southeastwards accompanying anti-clockwise rotation to get the present position. The asymmetry of centered plutons is considered to retain the direction of subduction of Kula Plate of Mesozoic age.

Detailed mechanism of asymmetric emplacement is a further problem. A number of instances of similar asymmetry of centered plutons are wanted to make a comprehensive study, especially from island arcs and continental margins in and around the Pacific Ocean.

# THE TECTONIC CONTROLS ON THE INTRUSION OF SPECIALIZED PEGMATITES IN THE GREENBUSHES PEGMATITE DISTRICT, WESTERN AUSTRALIA

Partington, G.A.<sup>1</sup>

<sup>1</sup> University of Western Australia Perth

**Introduction.** The Greenbushes Pegmatite District is situated 250 km. south of Perth in the Archaean Western Gneiss Terrain subdivision of the Yilgarn Block (Fig. 1). The district has been the main centre of production of alluvial tin in Western Australia since the beginning of this century and more recently for the production of tin, tantalum and lithium from one of the largest rare-metal pegmatite deposits in the world. The Greenbushes Pegmatite Group and related granitoid intrusives have been emplaced in what appears to be the root zone of a major tectonic structure. The pegmatites and granitoids have been metamorphosed, deformed and possibly remelted by tectonic reactivation along this structure.

**Tectonic Environment.** The intrusive rocks in the Greenbushes Pegmatite District have all been emplaced along a major sinistral transcurrent shear structure (Fig. 2), analogous to the present San Andreas Fault system. The zone has been active from the late Archaean to the end of the Proterozoic, with three major movements and associated medium grade metamorphism along this zone accompanied by syntectonic pegmatite and granitoid emplacement (Partington et al, 1986). The Donnybrook-Bridgetown shear zone (Fig. 2) is characterized by having a steeply dipping planar fabric with a

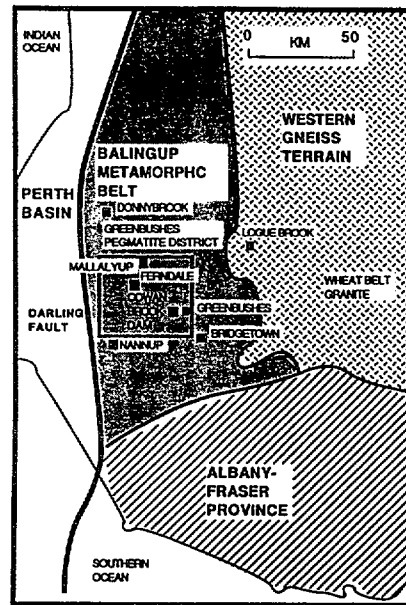


Fig. 1. Geological And Location Map Of The Greenbushes Pegmatite District

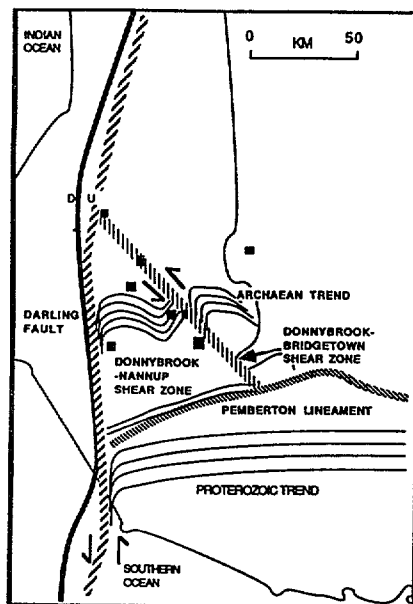


Fig. 2. Greenbushes Pegmatite District Structural And Tectonic Map

horizontal stretching lineation; the lineation was caused by transcurrent movement and these structures are similar to structures recognized in other transcurrent shear zones (Nicolas et al, 1977). A model of viscous heating (Nicolas et al, 1977) combined with heat derived from the associated tectonism concentrates plastic flow along the axis of the shear zone and is responsible for a high grade core complex and associated anatexis at the centre of the shear zone with zonal isograds reflecting decreasing metamorphic conditions symmetrically away from the core. The partially melted rocks tend to rise building arched structures at shallower depths corresponding to areas of dip slip lineation development as seen in the Greenbushes Pegmatite District. This type of process will restrict melts to the shear zones, and within the Greenbushes District, three distinct movement events are recognized and associated with shear deformation, metamorphism, anatexis and pegmatite and granitoid intrusion.

**Controls on Pegmatite Intrusion.** Shear zones have long been recognized as fluid channelways for hydrothermal and metamorphic fluids (e.g. gold; Philips & Groves, 1983). At deeper levels and at P-T conditions compatible with anatexis, however, the same shear zones are ideal structures for localizing and concentrating anatectic melts. In the case of the Greenbushes Pegmatite, it was intruded during major ductile

movements into the root zone of the Donnybrook-Bridgetown Shear Zone. The Greenbushes mine area shows little evidence for early brittle deformation (Bettenay et al, 1985). However experimental studies suggest tensional openings can develop during ductile transcurrent shearing due to the presence of shear bands (Harris & Cobbold, 1985) and shear hardening (White et al, 1980). The initiation of voids would cause large pressure gradients to develop such that fluids or melts in the region would rapidly migrate into the zone of shearing. Once intrusion of the fluid or melt has begun it will become a self propagating process as the heat from intrusion drives the shear which in turn attracts more fluid or melt. This process with extension of a more ductile medium in a less ductile one will cause intrusion generally parallel to the c-planes in the main shear zone (Fig. 3). Further continuous deformation in what would now be areas of contrasting ductility will produce folds, kinks and more voids so facilitating differentiation of the pegmatite magma. The longevity of the tectonism (Partington et al, 1986) and the presence of large amounts of lithium in the pegmatite melt, which would have significantly lowered

the solidus of the pegmatite, could account for its highly specialized nature.

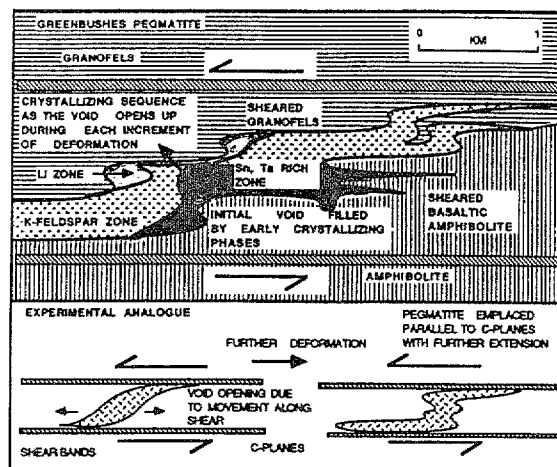


Fig. 3 Deformational Processes Controlling The Emplacement Of The Greenbushes Pegmatite Group.

**Summary.** There is a strong structural control on pegmatite and granitoid emplacement in the Greenbushes Pegmatite District. This is due to the presence of a major Archaean shear zone now evident on remote sensing imagery. The zone displays sinistral strike slip movement with various episodes of reactivation occurring throughout its history. Late structures, metamorphism and localized igneous and sedimentary events have been controlled by these movements along the shear zone. Tectonically, the Greenbushes Pegmatite District is very similar in form to other major transcurrent shear structures past and present. Such zones appear to be concentrators and collectors of fluids - magmatic, metamorphic, and hydrothermal. They act as ideal channelways, and with favourable chemical environments, for later associated ore deposition either as pegmatites low within the crust in ductile structures or higher in the crust within brittle structures as vein deposits.

**Acknowledgements.** I would like to thank Dr. L.F. Bettenay for all his help and encouragement in the initial stages of the project and Greenbushes Tin NL. for providing financial and logistical support. Finally to my fellow students and staff, especially Dr. L. B. Harris and D.I. Groves for suggestions and ideas. The author was in receipt of a Commonwealth Postgraduate Award throughout the project.

#### References

- Bettenay, L.F., Groves, D. I., & Partington, G.A., 1985, final report on WAMPRI project number 4.  
 Harris, L. B., & Cobbold, P.R. 1984, *J. Struct. Geol.*, **2**, 37-44.  
 Nicolas, A., Bouchez, J.L., Blaise, J., & Poirier, J.P., 1977, *Tectonophysics*, **42**, 55-73.  
 Partington, G. A., McNaughton, N.J., Kepert, D.A., Compston, W., & Williams, I.S., 1986, *Abstr. of the Conference on Correlation and Resource evaluation of Tin/Tungsten Granites in the SE Asia and the Western Pacific Region*, in press.  
 Phillips, G.N., & Groves, D.I., 1983, *J. Geol. Soc. Aust.*, **30**, 25-39.  
 White, S.H., Burrows, S.E., Carreras, J., Shaw, D., & Humphreys, F.J., 1980, *J. Struct. Geol.*, **2**, 175-187.

<sup>1</sup> University of Western Australia, Perth

2 Australian National University, Canberra

**Introduction.** Detailed geochronological isotope studies were undertaken to complement the structural, metamorphic and petrological study of the Greenbushes Pegmatite District (Partington, 1986a). Samples of granitoid and pegmatitic phases were selected for their known structural relationships and analysed to elucidate the chronological framework of the region and the source area of the mineralised pegmatites. SHRIMP and conventional U-Pb analyses of zircons constrained the age of the older events whereas whole rock and K-feldspar Pb-Pb analyses together with published data allowed the age of the younger events to be reassessed.

Age Constraints. Determination of the absolute ages of the Pegmatite Groups contained within the Greenbushes Pegmatite District are critical to the understanding of the tectonic history of the area as a whole. Because the Pegmatite Groups and associated granitoids are confined to major shear zones, dating of these bodies can help define the duration and spatial extent of a given shearing event (Partington, 1986b). Dating of syntectonic bodies will also place chronological constraints on metamorphic events that either produced or overprinted the intrusion. Four major tectonic events can be recognized in the district. These are outlined in Table 1. An early crust forming event has been recognized at ca 3.1 Ga (Fletcher et al, 1983) and is confined to the tonalitic gneiss of the Bridgetown sequence (Partington, 1986a). These rocks were affected by D1 dextral shearing and represent early crust on which the mafic volcanics and sedimentary sequences of the Greenbushes Pegmatite District were evolved. Major D2 sinistral shearing, metamorphism and granitoid intrusion was initiated at ca 2.61 Ga (Compston et al, 1984) with intrusion of the Greenbushes Pegmatite Group at 2.53 Ga in association with peak metamorphism and deformation. The longevity of this major tectonic event has

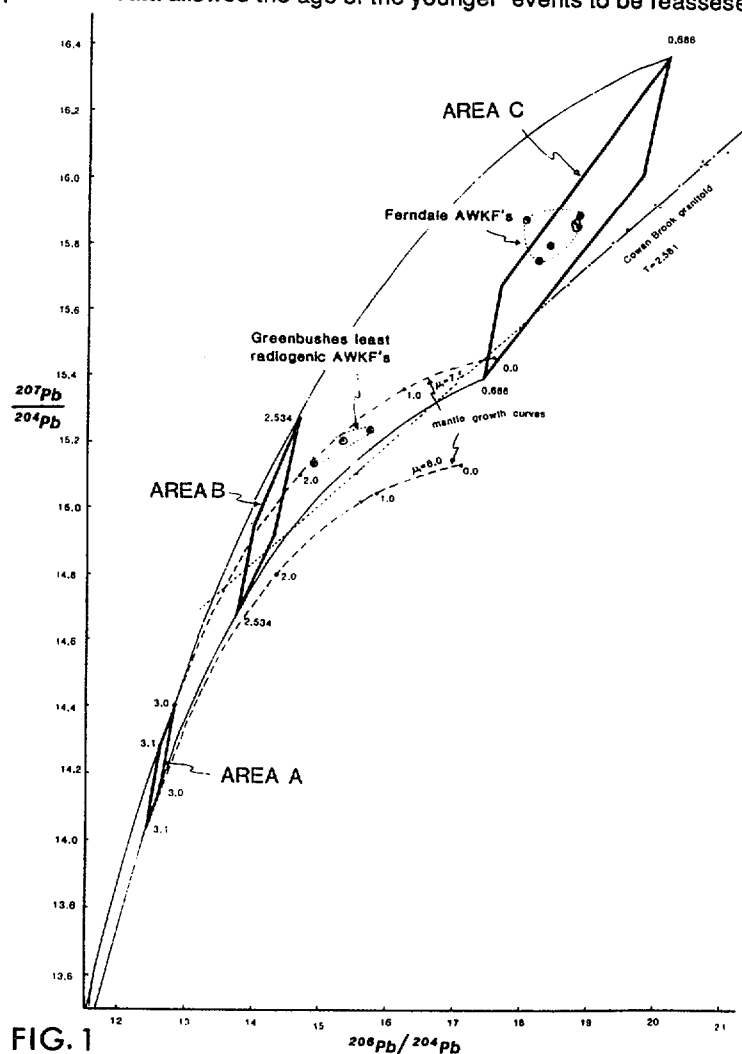


FIG. 1

had important consequences to the differentiation and eventual crystallization of the rare-metal pegmatites of the Greenbushes Pegmatite Group. Further deformation, metamorphism and pegmatite intrusion occurred at ca 1.1 Ga (Table 1.) due to reactivation along the major structure encompassing the Greenbushes Pegmatite District (Partington, 1986b). The last recognized metamorphic event in the district occurred ca 0.7-0.5 Ga ago (Table 1.) and is marked by reactivation of sinistral shearing, metamorphism and intrusion of the Ferndale Pegmatite Group (Kepert, 1985).

**Isotopic Constraints on Pegmatite Source.** Initial Pb isotope ratios from K-feldspars from the Greenbushes Pegmatite Group and Ferndale Pegmatite Group were used to constrain the possible source areas for these pegmatites. The initial assumptions used were that prior to formation of the terrain at 3.1-3.0 Ga, the Pb isotopes evolved along a mantle growth curve with a  $\mu_1$  of 7.5-8.0 which are typical values for the Archaean mantle (Moorbath & Taylor, 1981). At the time of crustal formation the Pb isotopic composition of the district is predicted to lie in the field defined by area A in Fig. 1. Values for  $\mu_2$  which successfully model the Pb isotope evolution of the pegmatites in the district are 10-15 which implicates either a dominantly basaltic or metamorphically depleted sialic crust as the pegmatite source. At the time of the intrusion of the Greenbushes Pegmatite Group (2.53 Ga),

area A will have evolved to area B and at the time of intrusion of the Ferndale Pegmatite Group (0.69 Ga), area A will have evolved to area C (Fig. 1). As K-feldspars preserve their initial Pb isotope ratios, K-feldspar from each pegmatite group should lie within the predicted fields (Fig. 1). Ratios from the Ferndale Pegmatite generally lie within the predicted field whereas the K-feldspars from the Greenbushes Pegmatite Group approach the predicted field and lie towards the least radiogenic end of a secondary isochron for the pegmatite. These and other K-feldspars were partly or completely recrystallized during M3 and do not preserve their Pb isotopic composition at 2.53 Ga. They are thus not conformable with area B. However the least radiogenic feldspar analyses approach the modelled range and therefore, it may be expected that unaffected K-feldspars would fall within the area B (Fig. 1). This suggests that both Pegmatite Groups were derived from sources which were indistinguishable on the basis of their U/Pb ratios and were normal compared to typical Archaean lower to middle crust. Whole rock Pb isotope analyses of granitoid pods from the Cowan Brook outcrop, which are structurally contemporaneous with the Greenbushes Pegmatite Group define a whole rock isochron of age 2.58 Ga, which is within error of the age of the Greenbushes Pegmatite Group (Table 1.). This isochron may be extrapolated to intersect area B and therefore is compatible with having the same source as the Greenbushes and Ferndale Pegmatite Groups at its time of formation.

**Summary.** Tectonic structures, which define the the Greenbushes Pegmatite District have been activate episodically from the early Archaean to the end of the Proterozoic. These events represent reactivations along a major transcurrent shear zone (Partington, 1986a) with associated deformation, metamorphism, anatexis and eventual granitoid and pegmatite intrusion.

Isotope modelling suggests that the pegmatite fields, although having different ages were derived from indistinguishable

source regions. Consequently other processes must be invoked to explain the differences in scale of mineralisation present within the three pegmatite groups.

**Acknowledgements.** I would like to thank Greenbushes Tin NL. for finance and logistical support, and Roger Thompson, Mike Hatcher and John Davis for much helpful discussion. Also staff and students at the University of W.A. for ideas and suggestions. Finally thanks to Niels Dahl for sample analysis. The author was in receipt of a Commonwealth Postgraduate Award throughout the duration of the project.

#### References

- Arriens, P.A., 1971, Geol. Soc. Aust., Spec. Publ., 3, 11-23.  
 Compston, W., & Arriens, P.A., 1968, Can. J. Earth Sci., 5, 561-583.  
 Compston, W., Williams, I.S., & McCulloch, M. T., 1984, Ann. Rept. Research School of Earth Sciences, A.N.U., 96-97.  
 Fletcher, I. R., Wilde, S. A., Libby, W.G., & Rosman, K.J.R., 1983, J. Geol. Soc. Aust., 30, 330-340.  
 Moorbath, S.M., & Taylor, P.N., 1981, In Kröner A. ed., Precambrian Plate Tectonics: Developments in Precambrian Geology 4, Elsevier.  
 Partington, G.A., 1986a, Abstr. of the Conference on Correlation and Resource evaluation of Tin/Tungsten Granites in the SE Asia and the Western Pacific Region, in press.  
 Partington, G.A., 1986b, University of Western Australia Ph.D. Thesis, (in prep).  
 Wilson, A. F., Compston, W., Jeffery, P.M., & Riley, G.H., 1960, J. Geol. Soc. Aust., 6, 179-195.

AGE(Ga)	SYSTEM	ROCK TYPE	LOCATION	REFERENCE
3.11	Sm/Nd MODEL	GNEISS	5 KM SE BRIDGETOWN	FLETCHER ET AL, 1983
3.07	Sm/Nd MODEL	GNEISS	15 KM SSE BRIDGETOWN	FLETCHER ET AL, 1983
2.66	Rb/Sr WR	GRANITE	WHEATBELT GRANITE	ARRIENS, 1971
2.61	U/Pb ZIRCON	GRANITE	LOGUE BROOK GRANITE	COMPSTON ET AL, 1984
2.58	Pb/Pb WR	GRANITE	COWAN BROOK DAM	PARTINGTON, 1986 THIS STUDY
2.53	U/Pb ZIRCON	PEGMATITE	GREENBUSHES	PARTINGTON, 1986 THIS STUDY
ca 1.1	U/Pb ZIRCON	PEGMATITE	GREENBUSHES	PARTINGTON, 1986 THIS STUDY
ca 1.1	Pb/Sr MUSC	PEGMATITE	MALLALYUP	WILSON ET AL, 1960
0.68	Pb/Pb K-FELD	PEGMATITE	FERNDALE	KEPERT, 1985 THIS STUDY
0.66	Rb/Sr K-FELD	PEGMATITE	DONNYBROOK	COMPSTON & ARRIENS, 1968

TABLE 1. Summary of the Available Geochronology from The Greenbushes Pegmatite District.

# TECTONIC ENVIRONMENT AND FEATURES OF GRANITE EMPLACEMENT AND RELATED MINERALIZATION IN SOUTH CHINA

Pei Rongfu, Wu Liangshi, Zhao Yu

Institute of Mineral Deposits, CAGS  
Beijing, China

To begin with, the authors describe, in detailed, the structural layers in South China and divide them into five categories: (1) Pre-Sinian structural layer, (2) Sinian-Early paleozoic structural layer, (3) Devonian-Middle and Lower Triassic structural layer, (4) Late triassic-cretaceous structural layer, and (5) Cenozoic structural layer. At the same time, it is indicated that the above mentioned five structural layers belong to turbulent to stable, unstable, relatively steady, mobilization, and uplift and subsidence, respectively, from which the evolution of tectonic environment as a sequence of geosyncline-platform-mobilized platform can be recognized.

According to the features of different structural layers and their distribution in South China, the authors have delimited four areas of tectonic environment of granite emplacement: (1) Hunan-Guangxi stable area, (2) Jiangxi-Guangdong transitional area, (3) Coastal mobile area, and (4) Zhejiang-Jiangxi-Hunan-Guangxi old land area. The magma activities in stable area are controlled by fold and fold-fracture and magmatite are mostly a nature in shallow source. In transitional area, the activities of magma are both migmatite granite and biotite granite and epigranite-subvolcanic rock. All them lie between stable and mobile and show a transitional nature as well. Mobile area is a position that is developed in regional fracture-fault block, with which structural activities and strength of magma activity are rather strong and gradually getting weaker, the composition of them is from lime-alkali to alkali. In old land area, the activities of granite are controlled by deep fracture of basement.

On the basis of tectonic environment of granite and taking further step to study the state of magmatism, this paper divides tentatively the type of emplaced body of granite into six kinds: (1) permeation type, (2) stoping type, (3) injection type, (4) filling type, (5) pulse type, and (6) eruptive type. Actually, the above mentioned emplaced bodies can completely reflect whether the process is kinetic or static state of magmatism. For instance, the former three kinds of bodies emplaced under closed and semi-closed condition were emplaced from permeation of "rock juice" to stoping replacement and to injection along bedding. It can be recognized that the condition of emplacement of those bodies transforms from static state gradually to kinetic; while latter three kinds are formed in a condition of fairly open space, by magmatic filling to eruption, and show a mechanism of kinetic state which is from kinetic to strongly explosive.

Additionally, the mineralization of each type of emplaced body is mentioned. On the basis of the associated pattern of six kinds of emplaced bodies, there are three patterns in space: (1) juxtaposed associated, (2) cluster associated, and (3) cutting associated.

The various emplaced bodies and its associated patterns in South China are closely related to the evolution of geohistory and tectonic environment. The emplaced bodies of the Pre-Yanshanian (the Pre-Mesozoic) were relatively simple, taking the permeation and injection as the most common type; the Yanshanian were relatively varied, besides the stoping type in dominant, the eruptive type and pulse type occupy an important place. In addition, in coastal mobile area, the eruptive type is the most important and the types of stoping and filling are secondary; and the emplaced bodies often show a cutting associated pattern. In the stable area of Hunan-Guangxi, pulse type is secondary, the associated pattern of which mostly occurred in cluster. In the transitional area, all types of emplaced bodies and its associated patterns occurred

#### References

- Ren Jishun, Jiang Chunfa, Zhang Zhengkun, Qin Deyu, 1980, The Geotectonic Evolution of China, Geological Publishing House, China.
- Mo Zhusun, Ye Bodan, 1979, Geology Granite of Nanling, China, Geological Publishing House, China.
- Pither, W.S., Berger, A.R., The Geology of Donegal: a Study of Granite Emplacement and Unroofing, New York, Wiley-Interscience.



**MINERAL DISTRIBUTION STUDY FOR CASSITERITE  
AND ASSOCIATED HEAVY MINERALS IN PHUKET, THAILAND**

by

Jaturong Praditwan  
SEATRAD Centre  
Ipoh  
Malaysia

**ABSTRACT**

A detailed study has been undertaken of the palong and/or jig concentrates produced by the 24 tin mines operating on Phuket Island, Thailand (see Fig. 1) in February 1984. This involved collection of representative samples, removal of the light fraction by flotation with tetrabromoethane (sp gr 2.96) and microscopic examination of six different size fractions with respect to mineral abundances, their mineralogical characteristics, presence of intergrowths, grain shape, sorting and liberation.

Results showed that, after cassiterite, columbite-tantalite, wolframite, monazite and ilmenite are potentially the most abundant by-product minerals from tin mining. The general characteristics of those heavy minerals are as follows:

Cassiterite from the primary deposits is typically angular-subangular whereas, subangular-subrounded grains are associated with secondary deposits. Grain sizes varies from 212 $\mu$  to 3.35 mm with the coarser size predominating in the central part (Amphoe Kathu), corresponding to the primary deposits, whereas the finer size predominate in the alluvial deposits to the south and east. Cassiterite content of concentrates varies from 15.2 to 89.2%. There are no obvious trends or systematic differences between primary and secondary deposits.

Columbite-tantalite grains from both primary and secondary deposits are subangular and range from 212 $\mu$  to 1.7 mm. Coarsest grains are principally associated with primary deposits. Columbite-tantalite concentrations varies from 0.1 to 6.9% and its ratio to cassiterite are significantly higher in the primary deposits with greatest abundances in the central part of the island in contrast to the low values associated with the placer deposits on the east coast.

Nb-Ta rutile from both primary and secondary deposits is subangular and, compared to other heavy minerals, relatively fine grained (212 to 850 $\mu$ ). Concentrations of Nb-Ta rutile, which varies from trace to >6.0%, and the Nb-Ta rutile:cassiterite ratio are both lowest in the primary deposits around Amphoe Kathu. The highest concentrations and ratios to cassiterite are found in the placer deposits on the east coast.

Wolframite was only identified in concentrates from ten mines with the value varies from trace to 18.0%. The highest value are found in primary deposits around Amphoe Kathu. Wolframite grain present as angular to subangular grains with size range of 212 $\mu$  to 1.7 mm.

Monazite concentrations vary from less than 0.5% to maximum of 4.2%; concentrations from primary deposits are lower than in the alluvial deposits. Grain size ranges from 212 $\mu$  to 1.7 mm the coarser sizes being associated with primary deposits around Amphoe Kathu.

Ilmenite concentrations, which vary from less than 1% to more than 20%, and the ilmenite:cassiterite ratio are notably lower in concentrates from the primary deposits around Amphoe Kathu. Ilmenite grains from primary deposits are subangular to subrounded whereas those in secondary deposits are subrounded. Grain size varies between  $212\mu$  to 1.7 mm with the coarser size predominating in the primary deposits in the central part of the island.

Comparing primary and secondary deposits on Phuket Island, several distinct mineralogical and physical trends are apparent as follows:

Primary deposits have a greater abundance of columbite-tantalite and wolframite. In contrast, ilmenite and Nb-Ta rutile are most abundant in the secondary deposits. Their grain size typically decreases, whereas sorting and liberation increase in going from primary to secondary (placer) deposits. Heavy mineral:cassiterite ratios clearly demonstrate that potential production of columbite-tantalite and wolframite is principally associated with a few of the primary deposits. In contrast, ilmenite and Nb-Ta rutile are largely associated with placer deposits.

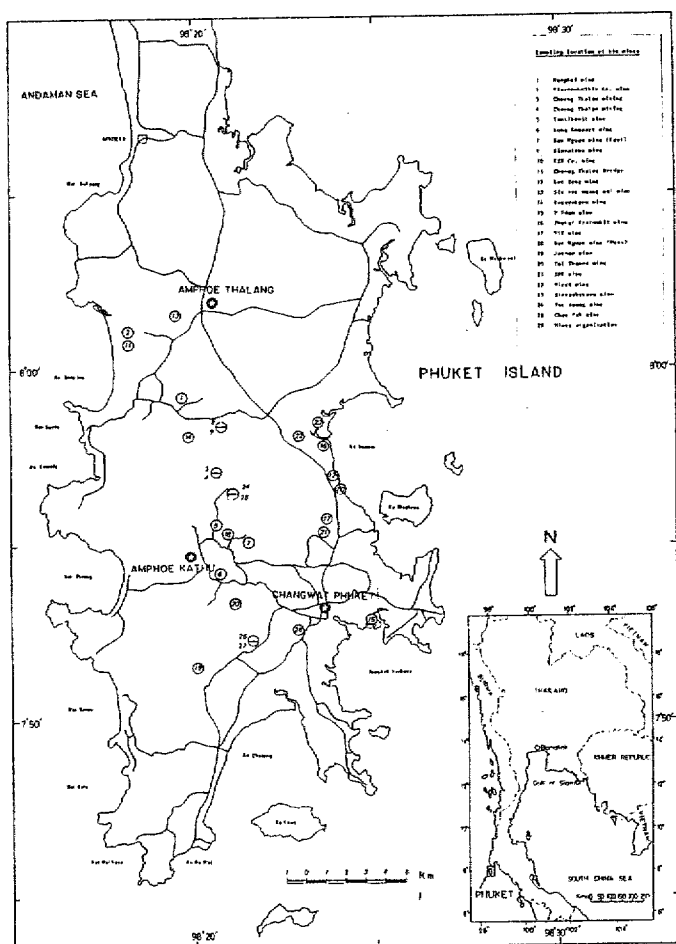


Figure 1 : Phuket Island and Sampling location

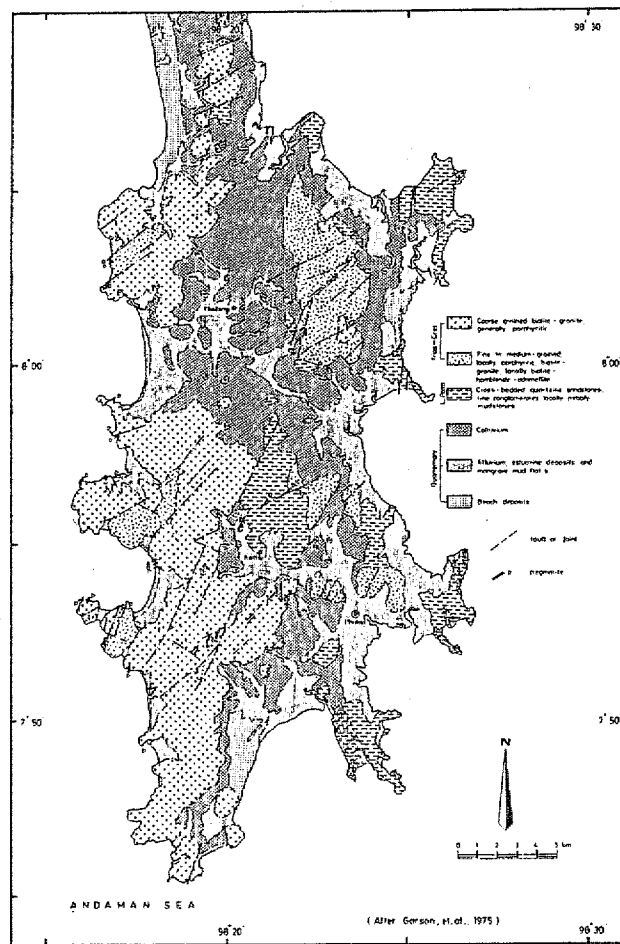


Figure 2 : Geologic map of Phuket Island

# THE POSSIBLE AGE OF THE MAXIMUM TIN/TUNGSTEN MINERALIZATION AT PHUKET ISLAND, SOUTHERN THAILAND

P. Putthapiban<sup>1</sup>, P. Jackson<sup>2</sup> and C.M. Gray<sup>2</sup>

<sup>1</sup>Geol. Surv. Div., Dept. of Min. Res., Rama VI Rd., Bangkok, Thailand

<sup>2</sup>Geology Department, La Trobe Univ., Bundoora, Victoria, Australia 3083

The results on the studies of Phuket tin granite suite (Khao Tosae, G-4) using Rb/Sr isochron method, mineral isotopic age determinations (Rb/Sr, K/Ar and Fission Track) and a fluid inclusion approach are presented. The emplacement age of the granite suite is  $78 \pm 4$  m.y. with an exceptionally high initial  $^{87}\text{Sr}/^{86}\text{Sr}$  ratio of  $0.7428 \pm 18$ . The Rb/Sr muscovite and biotite (as well as one lepidolite) ages are  $70 \pm 1$  m.y. and  $55 \pm 1$  m.y. respectively, whereas the K/Ar ages of both muscovite and biotite are  $55 \pm 1$  m.y.. The fission track age of apatite is  $43 \pm 3$  m.y. (see details in Table 1). These results clearly show the systematic decrease in ages from the emplacement of G-4 granite (with blocking temperature of  $750^\circ\text{C}$ ) to Rb/Sr muscovite age (with blocking temperature of  $500^\circ\text{C}$ ) to Rb/Sr biotite, K/Ar muscovite and biotite ages (with similar blocking temperatures of  $250^\circ\text{C}$ ) to fission track age of apatite (with blocking temperature of  $100 \pm 20^\circ\text{C}$ ).

Plots of the observed granite and mineral ages against the known blocking temperatures reveal an exponential cooling history of the granite terrain after the granite emplacement (Fig. 1).

The presence of tin/tungsten minerals in the Khao Tosae granite and the related dykes suggest that the mineralization should have taken place as early as  $78 \pm 4$  m.y. (the age of the granite emplacement) and this could have persisted until  $55 \pm$  m.y. ago (the age of lepidolite from the tin greisen).

The possible age of the maximum tin/tungsten mineralization is further delineated through fluid inclusion studies. Assuming the granite emplacement occurred at 1 kb, the average temperature of the fluid inclusions in the tin pegmatite should be  $386^\circ\text{C}$  and  $540^\circ\text{C}$  whereas that of tin greisen should be  $443^\circ\text{C}$ . If this assumption on the depth of the G-4 granite emplacement and the preliminary study on the fluid inclusion are acceptable, it is quite likely that the possible ages of the maximum tin/tungsten mineralization for the pegmatite are  $65 \pm$  m.y. ( $386^\circ\text{C}$ ) and  $72 \pm$  m.y. ( $540^\circ\text{C}$ ) and that of the greisen is  $69 \pm$  m.y. ( $443^\circ\text{C}$ ).

Table 1 The mineral Rb/Sr, K/Ar and Fission Track ages in m.y. of granites from the Khao Tosae Suite (G-4)

Sample No.	Location	Rb/Sr ages			Fission Track Age		K/Ar ages	
		Musc	Biot	Lepidolite	Apatite		Musc	Biot
KP15	N of Karon Beach	$55.8 \pm 0.6$			$42.7 \pm 2$			
KP49	Ban Kho En	$70.9 \pm 1$						
KP47/2	Ko Tha	$68.2 \pm 1$						
KP/3	N of Karon Beach	$71.9 \pm 1$						
KP39	Kathu tin mining area			$55.9 \pm 0.6$				
KP*	Khao Tosae						$57.4 \pm 1.5$	$55.4 \pm$

Note - \*Bignell, 1972 and Garson et al., 1975 - The K/Ar ages are recalculated using decay constants of Steiger and Jager (1977)

### References

Bignell J.D. 1972 Ph.D thesis. Oxford Univ.

Garson M.S, Young B., Mitchell A.H.G and Tait B.A.R. 1975. Overseas Mem. No 1 IGS London, 112.

Steiger R.H. and Jager E. 1977. Earth Planet. Sci. Lett. 36, 359-362

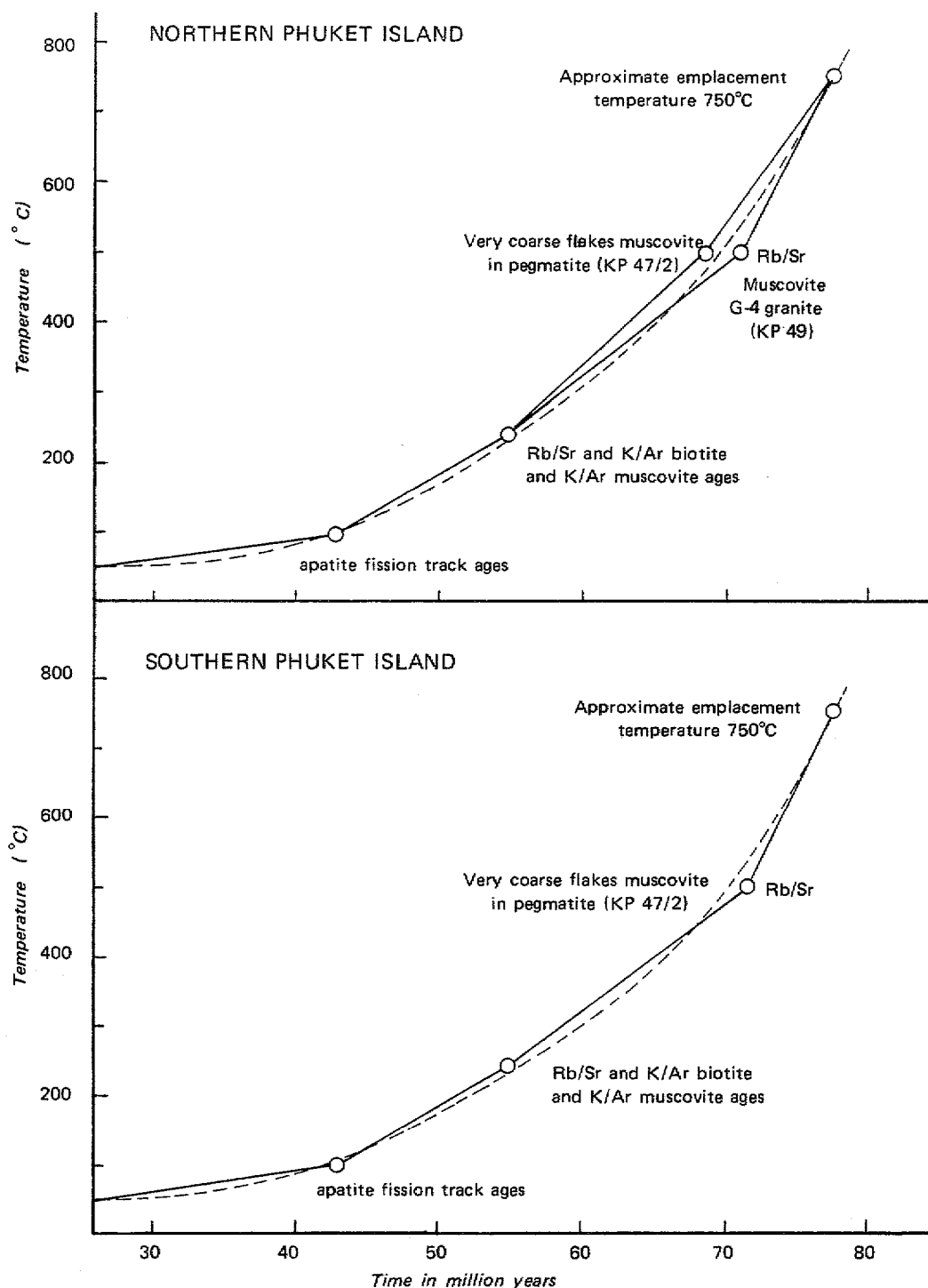


Fig. 1 Cooling history of the Khao Tosae Granite Suite (○), Phuket Island, southern peninsular Thailand derived by a combination of different dating methods.

## GEOLOGY, BRECCIATION AND PARAGENESIS OF THE ARDLETHAN TIN FIELD

Ren, S. K. &amp; Walshe, J. L.

Australian National University, Canberra, ACT

The Ardlethan Tin Field is located in central NSW, at the western extremity of the Lachlan Fold Belt. Disseminated cassiterite and sulphide mineralization is hosted in two breccia pipes in the mine granite which intruded the Ordovician sediments in the late Silurian (417 ± 2.5 MA) and was followed closely by a series of differentiated granitic intrusives: a garnetiferous quartz-feldspar porphyry, the Ardlethan granite, microgranite dyke and the mine porphyry dykes. The Ardlethan granite appears to be the source of the hydrothermal fluids.

The mine granite is a biotite rich S-type granite, grey coloured, containing about 35% K-feldspar, 25% plagioclase, 25% quartz, 15% biotite and accessories of ilmenite, zircon, apatite and cordierite. Its contact with the Ordovician sediments is flat with weak alteration. Sedimentary inclusions are common along the contact zone in the mine granite and digested to biotite - plagioclase patches.

The Ardlethan granite is pink to white, medium to extremely coarse grained, contains 40% quartz, 30% K-feldspar, 20% plagioclase, 3-5% biotite, 0-2% muscovite, about 3% tourmaline and accessories of zircon, apatite, ilmenite, topaz, fluorite, cassiterite and pyrite. A large number of quartz and tourmaline nodules occur along the eastern margin. It contacts the Ordovician sediments sharply and probably the mine granite at depth. Greisenization occurs along its eastern margin as numerous small pipes with or without mineralization.

The microgranite is finely even grained and white in colour. It intrudes the Ardlethan granite, the Ordovician sediments and the Mine granite. The light coloured mine porphyry dykes intruded the major WACS (Wildcherry-Ardwest-Carpathia-Stackpool) breccia pipe succeeding the onset of the brecciation. Both the microgranite and Mine porphyry are biotite free.

The WACS breccia pipe contains several strongly brecciated zones which focussed the hydrothermal alteration and mineralization. The Wildcherry, Ardwest and Wildcherry South deposits were contained in the mine granite breccia zone, the Carpathia and Blackreef deposits were spatially associated with one sedimentary breccia zone and the Stackpool and the Godfrey deposits another. The mine granite fragments occur in all the zones with varying size and angularity. The microgranite fragments occur in the sedimentary breccia zones. The mine porphyry fragments occur in the Wildcherry, Ardwest and Wildcherry South zone near the major mine porphyry dyke and the Carpathia-Stackpool sedimentary breccia zone which was intruded by two small mine porphyry dykes.

Cassiterite mineralization was associated with sericite alteration and tourmaline alteration with large amounts of quartz formation. In the Wildcherry, Ardwest and the Wildcherry South deposits cassiterite was associated with sericite, tourmaline and quartz. Pyrite, chalcopyrite, sphalerite and galena postdated the cassiterite and were overprinted by chlorite alteration. The Perseverance deposit, the depth extension of the Wildcherry South deposit, was associated with tourmaline alteration and sericite alteration. The Carpathia and Stackpool deposits were also associated with very strong tourmaline alteration and sericite alteration. Vertical

tourmaline pipes are very common in association with these mineralizations. The high grade Blackreef and Godfrey deposits at depth are associated with extremely strong tourmaline alteration and sericite + siderite alteration which formed halos surrounding the deposits. Arsenopyrite occurs in association with cassiterite in most of the deposits and is rich in the high grade Blackreef deposit. Varying amounts of fluorite and cookeite occur in the Perseverance, Blackreef, Godfrey and the Godfrey South deposits as vug infill with toothy quartz.

Biotite alteration occurs at depth of the breccia pipe below the orebodies. Massive fine grained secondary biotite occurs in fractures or as a feldspar alteration product. Chlorite altered secondary biotite occurs below the Perseverance deposit indicating that biotite alteration occurred at higher levels at earlier times.

The White Crystal deposit is hosted in a separated smaller breccia pipe, the White Crystal breccia pipe. It is characterised by large angular fragments, strong topaz alteration, large vugs and toothy quartz, fluorite and cookeite. Cassiterite was associated with topaz, sericite, quartz, tourmaline and small amounts of wolframite and arsenopyrite. Sulphide mineralization overprinted the cassiterite mineralization. Toothy quartz, cookeite and fluorite occur as vug infill at late stage.

Fluid inclusion study suggests that the temperatures of the cassiterite mineralization are between 330 to 360°C for the deposits in the WACS breccia pipe and 320 to 350°C for the White Crystal deposit, sulphide mineralization occurred between 220 to 270°C, and the toothy quartz, fluorite and cookeite infilled vugs at 150 to 190°C. Fluid inclusions of two phase (Liquid H<sub>2</sub>O + Vapor CO<sub>2</sub>) and three phase (Liquid H<sub>2</sub>O, Vapor CO<sub>2</sub> and Liquid CO<sub>2</sub>) occur throughout the temperature range and homogenize to vapor phase or liquid phase depending on the initial fluid/vapor volume ratios, allowing a pressure estimate of 400-450 bars for cassiterite stage and suggesting that the fluids continued to boil as temperature declined which can only happen if the pressure declined which probably reflects the shift from lithostatic pressure to hydrostatic pressure in the breccia pipes.

Mineralization is interpreted as part of a dynamical process in which focussed fluid flow, rock-fluid reaction, energy release, and volatile loss resulted in physico-chemical gradients in the breccia pipe. Biotite alteration, sericite and tourmaline alteration with cassiterite mineralization, sulphide mineralization, and chlorite alteration formed sequentially in the breccia pipe from depth to surface. Decreasing temperature and fluid flux with time resulted in the retreat of that zonation and chlorite overprinting the earlier mineralized deposits. The high grade cassiterite-sulphide-tourmaline mineralization of the Blackreef, Godfrey and the Godfrey South deposits represents another stage of fluid input along highly permeable zones and marks a partial return to high temperature in the breccia pipe.

The close association of cookeite and fluorite suggests that the fluids were late stage, Li and F rich magmatic fluids. Together with other geology, mineralogy and geochemistry characteristics it is clear that the hydrothermal fluids were from the Ardlethan granite. The cookeite contents vary systematically from none in the Wildcherry, Ardwest and Wildcherry South deposits, small amounts (0.5-1.0%) in the Perseverance, Blackreef and Godfrey deposits, a relatively large amount (1-2%) in the Godfrey South deposit to the richest (3-5%) White Crystal deposit, reflecting a continue evolution of fluid chemistry and suggesting that the White Crystal brecciation and mineralization was a reactivation of the magmatic - hydrothermal system.

## OXIDIZED AND REDUCED GRANITOIDS FROM THE KOFU COMPLEX, CENTRAL JAPAN

SATO Kohei and SHIBATA Ken

Geological Survey of Japan, Tsukuba, Ibaraki 305, Japan

Granitic rocks show a wide range variation of magnetic susceptibility in proportion to the content of accessory magnetite. The magnetic susceptibility data for Japanese granitoids show regional variations conformable to the metallogenic provinces, for example, Sn, F and major W deposits are distributed in the low magnetic granitoid terrains (e.g., Ishihara, 1977; Sato, 1980). The susceptibility also varies within a terrain or a pluton, suggesting that "the properties of a granitoid magma reflect the source region, but may also change significantly during the history of a given magma" (Wones, 1981). In the present study the Kofu complex having a large intrabody variation of magnetic susceptibility was examined on the basis of the major element chemistry, ilmenite composition and Sr, S and O isotope data.

The Kofu complex, the largest Neogene granitoid mass in the Japanese islands, is emplaced in Cretaceous sedimentary strata (Shimanto group) and Neogene volcanic piles (Nishiyatsushiro and Okubo groups) (Fig. 1). The plutons emplaced in the sedimentary strata are composed of or accompanied by low magnetic rocks ( $< 2 \times 10^{-3} \text{SI}$ ), whereas the plutons emplaced in the volcanic piles are always rich in magnetite ( $10\text{--}60 \times 10^{-3} \text{SI}$ ). It is remarkable that the Tokuwa granodiorite consists mainly of the high magnetic H-facies with lesser occurrences of the low magnetic L-facies along the contact with the sedimentary rocks. The L-facies contains metasedimentary xenoliths and is widely exposed in the area where surrounding sediments are dominated by pelitic rocks bearing graphite.

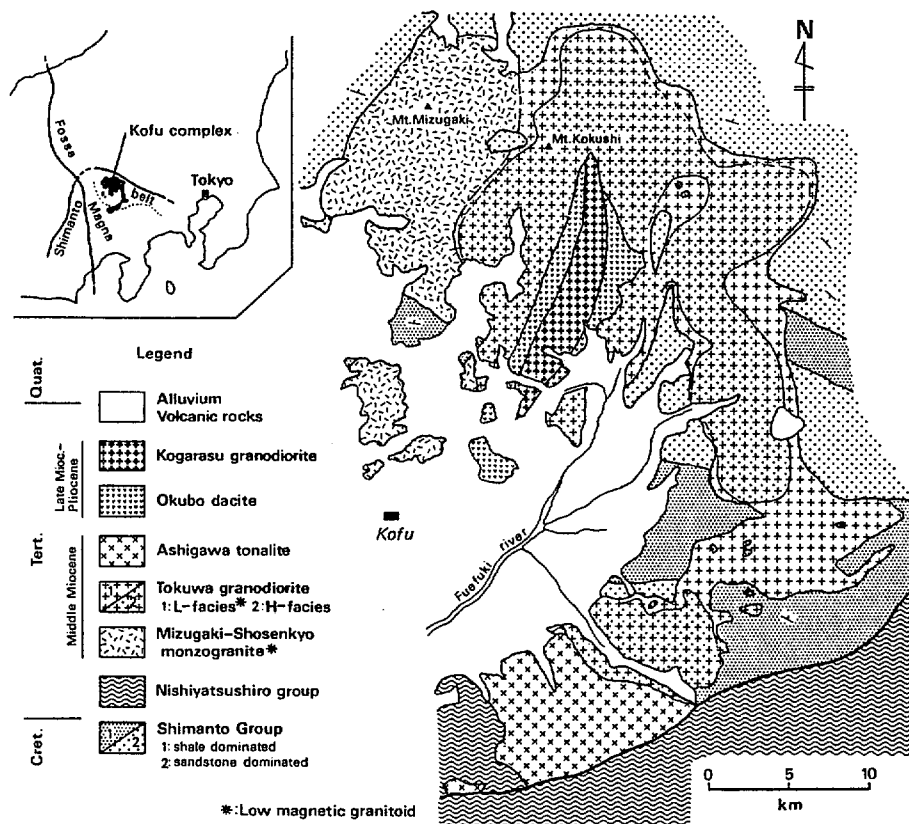


Fig. 1: Geologic map of the Kofu complex, showing the distribution of high and low magnetic granitoids.

The  $\text{Fe}_2\text{O}_3/(\text{Fe}_2\text{O}_3+\text{FeTiO}_3)$  ratio of accessory ilmenites correlates well with the magnetic susceptibility of the host rocks (Fig.2). This correlation implies that reduced conditions favored precipitation of iron as mafic silicates instead of magnetite, giving rise to low magnetic susceptibilities and low  $\text{Fe}^{3+}/\text{Fe}^{2+}$  ratios of the rocks. The low magnetic rocks have higher  $^{87}\text{Sr}/^{86}\text{Sr}$  ratios than the high magnetic rocks (Fig.3) and are characterized by high  $\delta^{18}\text{O}$  (+8~+11‰) and low  $\delta^{34}\text{S}$  (-11~-3‰) values (Sato et al., 1982). The field relation corroborated with the isotope data suggests that the low magnetic rocks involved sedimentary materials and formed in reduced conditions presumably through the gain of carbon, although the bulk chemistry still remains within the I-type field (Sato & Ishihara, 1983). The Tokuwa granodiorite magma was locally reduced by wall sedimentary rocks at the site of intrusion, probably before significant plagioclase crystallization. Such a reduction would not have taken place in the plutons emplaced in the volcanic piles.

### References

- Ishihara, S., 1977, *Mining Geol.*, 27, 293-305.  
 Sato, K., 1980, *Mineral. Deposita*, 15, 327-334.  
 Sato, K., Matsuhisa, Y. & Ishihara, S., 1982, *Abstr. Ann. Joint Mtg., Mining Geol. Japan, Japan. Assoc. Miner. Petrol. Econ. Geol. and Miner. Soc. Japan*, 96.  
 Sato, K. & Ishihara, S., 1983, *Bull. Geol. Surv. Japan*, 34, 413-427.  
 Wones, D. R., 1981, *Mining Geol.*, 31, 191-212.

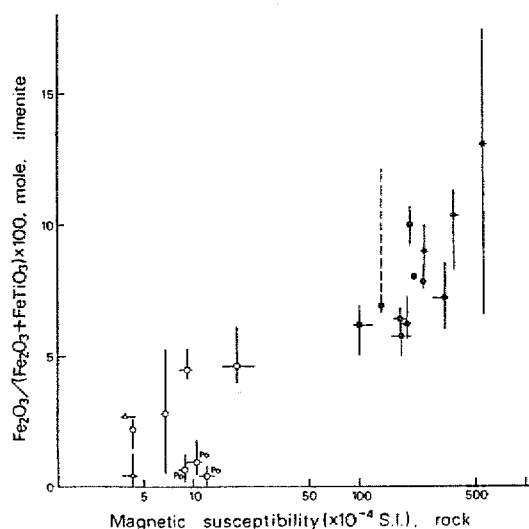


Fig.2: Relation between  $\text{Fe}_2\text{O}_3/(\text{Fe}_2\text{O}_3+\text{FeTiO}_3)$  ratio for ilmenite and magnetic susceptibility of the Kofu granitoids. Symbols are the same as those in Figure 3. Subscript Po indicates pyrrhotite-rich specimens.

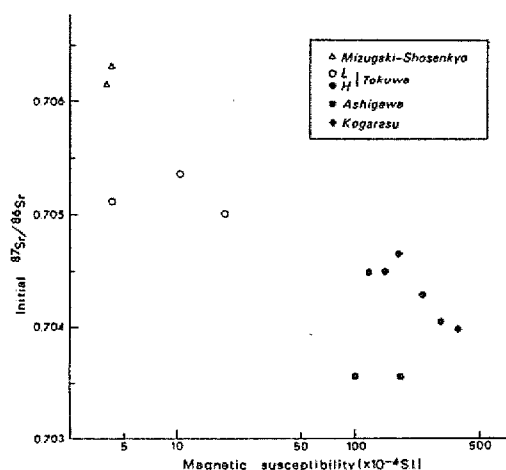


Fig.3: Initial  $^{87}\text{Sr}/^{86}\text{Sr}$  ratio vs. magnetic susceptibility plot for the Kofu granitoids.



# Geochemistry of the Nam Salu Horizon, Kelapa Kampit, Belitung, Indonesia

M.O. Schwartz\* and Surjono\*\*

\*Bundesanstalt für Geowissenschaften und Rohstoffe,  
Hannover, Fed. Rep. of Germany

\*\*Directorate of Mineral Resources, Bandung, Indonesia

The Nam Salu horizon belongs to a sequence of Carboniferous-Permian metasediments and metatuffs which have been intruded by granitoids of Triassic age. It is a steeply dipping, 20-45 m thick layer of stilpnomelane-chlorite-biotite schist, which is exposed over a length of 3 km. Occasionally, the schist has preserved an eutaxitic texture, which characterize it as being derived from tuffs or tuffaceous sediments. Some layers contain laminas with abundant magnetite and ilmenite. Discordantly or parallel to the banding, occur pyrite and pyrrhotine. Marcasite, arsenopyrite, sphalerite, chalcopryrite, galena, siderite, rutile, sphene and hematite, which are subordinate, rarely exhibit parallelism and often are randomly or discordantly distributed. Minute grains of cassiterite of 5-200  $\mu\text{m}$  grain size are concentrated in some sulphide or magnetite-rich bands, but more often their distribution bears no relation to the lamination of the rock. Locally, the cassiterite concentrations reach ore grade, as e.g. over a length of 90 m in the Nam Salu open pit.

59 rock samples which have been collected from the Nam Salu horizon and its country rock over an area of 1 x 4 km have been analysed for 37 elements.

The chemical composition of the Nam Salu horizon which is exposed in the open pit has little in common with the presumed premetamorphic protolith (tuffaceous sediments or shale). The rock, which has 1-2 % Sn, is characterized by very high concentrations of Rb, Cs, Be, Bi, W, F and Fe (Table 1). The hanging/foot wall of the Nam Salu horizon, which is much richer in quartz, does not show such high values.

Sn is significantly negatively correlated with Si, Zr and Sc and positively correlated with W, Nb, F, Y, Cu, Rb, Li, La, K, Cs, Fe and U (arranged in the order of decreasing values). With the possible exception of Y and La, the positively correlated elements indicate the influence of post-despositional changes to which the rock has been exposed. In particular, the very high concentrations of Cs (325 ppm), Rb (1380 ppm) and Be (26 ppm) can only be explained by metasomatism from hydrothermal solutions derived from a crystallizing granite magma. Though there are no granites exposed which may be considered as source *senso stricto*, there is further evidence of magmatic activity in the Kelapa Kampit area (dacite porphyry in the mine and hornblende granite to granodiorite 7 km SE of Kelapa Kampit). The stratabound character of the Sn mineralization can easily be explained by the fact that the rock was more reactive to hydrothermal solutions than its quartz-rich hanging/foot wall.

TABLE 1: Averaged abundances of major and minor elements at Kelapa Kampit, Belitung, Indonesia

Beritung, Indonesia							
	Nam Salu horizon (stilpnomelane- chlorite-biotite schist)		Country rock of the Nam Salu horizon (open pit and drill core)				Dacite porphyry (hydro- thermally altered)  (drill core)
	Open Pit	Drill core	Chlorite schist	Quartz- ite, meta- sdst./ silt- stone	Chert	Calc- sili- cate fels	
I. Major elements (%)							
SiO <sub>2</sub>	34.23	32.49	53.68	82.19	90.33	46.03	67.68
TiO <sub>2</sub>	1.08	1.46	1.21	0.35	0.14	0.72	0.42
Al <sub>2</sub> O <sub>3</sub>	9.62	11.61	12.80	6.36	3.25	6.36	13.19
Fe <sub>2</sub> O <sub>3</sub> (total Fe)	39.87	40.72	19.42	5.26	2.66	27.12	11.73
MnO	0.38	2.14	0.37	0.15	0.10	0.66	0.32
MgO	3.64	3.20	3.36	1.16	0.81	3.28	0.58
CaO	0.13	0.43	1.00	0.02	0.01	11.62	0.01
Na <sub>2</sub> O	0.07	0.09	0.57	0.16	0.13	0.28	0.05
K <sub>2</sub> O	4.16	2.33	2.28	1.37	0.79	0.31	2.40
P <sub>2</sub> O <sub>5</sub>	0.10	0.09	0.12	0.03	0.02	0.10	0.02
L.O.I.	3.77	3.83	3.46	2.10	1.18	2.34	2.76
Total	97.05	98.38	98.28	99.16	99.40	98.81	99.17
II. Minor elements (ppm)							
Ba	403	370	114	178	123	152	226
Be	26	n.a.	n.a.	n.a.	n.a.	n.a.	n.a.
Bi	163	<6	6	<6	<6	<6	<6
Ce	69	80	81	62	37	37	83
Co	28	n.a.	n.a.	n.a.	n.a.	n.a.	n.a.
Cr	116	115	86	43	76	46	<1
Cs	325	n.a.	n.a.	n.a.	n.a.	n.a.	n.a.
Cu	169	17	31	32	36	198	5
F (HCl-soluble)	603	n.a.	n.a.	n.a.	n.a.	n.a.	n.a.
La	155	133	70	34	13	37	45
Li	22	n.a.	n.a.	n.a.	n.a.	n.a.	n.a.
Mo	5	6	8	4	5	7	<3
Nb	52	13	12	7	5	11	6
Ni	41	41	41	17	13	91	<5
Pb	216	4960	3000	1200	447	4	66
Rb	1380	577	317	129	81	39	261
Sc	13	22	19	5	4	16	10
Sn	16400	90	42	127	135	434	17
Sr	13	20	54	8	4	100	11
Ta	<5	<5	5	5	6	<5	<5
Th	30	26	24	24	21	16	31
U	13	6	4	3	<3	6	4
V	152	215	151	83	26	116	30
W	115	12	21	9	<5	<5	<5
Y	89	33	33	18	7	24	46
Zn	354	3630	5030	1050	293	788	540
Zr	78	106	132	152	30	63	183
No. of analyses	23	7	5	19	2	3	1

# PHYLLOSILICATE AND RUTILE CHEMISTRY AS INDICATORS OF THE Sn-POTENTIAL OF SE AUSTRALIAN GRANITOIDS

K.M. Scott

CSIRO, Division of Mineral Physics and Mineralogy, North Ryde, NSW 2113

In southeastern Australia Sn-specialized granitoids are distinguished from barren granitoids by their ferroan and stanniferous biotites and chlorites and the presence of Nb-, Ta-, Sn- and W-rich rutile. Use of these parameters allows an accurate appraisal of the Sn-potential of granitoids to be made.

In granitoids chlorites have  $\text{Fe}/(\text{Fe}+\text{Mg}+\text{Mn})$  ratios that are similar to those for coexisting biotites but muscovites generally have much lower ratios than the biotites, especially where compositions are more magnesian (Fig. 1). These features occur because chlorite, as a breakdown product of igneous biotite, inherits its mafic signature. However igneous muscovite formed subsequent to biotite when the proportions of the mafic cations available to muscovite were different to the proportions at the time of biotite formation. Thus, whereas the  $\text{Fe}/(\text{Fe}+\text{Mg}+\text{Mn})$  ratio of chlorite approximates to that of biotite and can be used where biotite is altered to chlorite, the  $\text{Fe}/(\text{Fe}+\text{Mg}+\text{Mn})$  ratio of muscovite only provides a minimum for biotite's ratio.

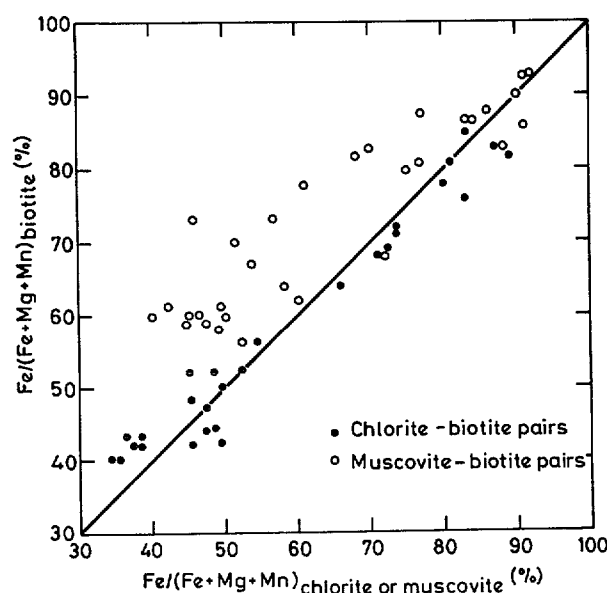


FIG.1  $\text{Fe}/(\text{Fe}+\text{Mg}+\text{Mn})$  RATIOS FOR PHYLLOSILICATES

The biotites and chlorites in Sn granitoids are particularly ferroan  $\text{Fe}/(\text{Fe}+\text{Mg}+\text{Mn}) \geq 0.80$ , and contain  $> 200$  ppm Sn whereas barren granitoids are more magnesian, often  $\text{Fe}/(\text{Fe}+\text{Mg}+\text{Mn}) \sim 0.55$ , and contain  $< 100$  ppm Sn. In the Walwa area of NE Victoria where the mineralization occurs in pegmatitic and aplitic dykes, biotite/chlorite from the Pine Mountain Granite has  $\text{Fe}/(\text{Fe}+\text{Mg}+\text{Mn})$  ratios =  $0.92 - 0.94$  and Sn = 250 ppm which identify it as a Sn granitoid rather than the Koetong Granite where these parameters are  $0.57 - 0.78$  and  $< 100$  ppm Sn respectively.

At Ardlethan the major mineralization occurs in a non-Sn granitoid, the Mine Granite. Emplacement of the mineralization is accompanied by introduction of Fe and loss of Mg (Scott, 1981) and alteration of biotite to chlorite. With alteration the  $\text{Fe}/(\text{Fe}+\text{Mg}+\text{Mn})$  ratio of the mafic phyllosilicates increases from 0.57 to 0.85 and up to 830 ppm Sn is recorded in chlorite. Thus the association of Fe-rich phyllosilicates and high Sn content is developed with Sn mineralization, even in an originally barren granitoid.

Figure 1 shows that in Sn granitoids with very ferroan biotite compositions, muscovites may have similar  $\text{Fe}/(\text{Fe}+\text{Mg}+\text{Mn})$  ratios e.g. the Ardlethan Granite. There the relative proportions of Fe, Mg and Mn must have been maintained in the period from biotite to muscovite crystallization. Furthermore muscovite from altered Ardlethan Granite also has the same ratio, implying either that the fluid responsible for alteration was not significantly different from the magmatic fluids at the time of crystallization of the igneous micas or that no Fe, Mg or Mn was introduced during the alteration process. As bulk changes in these elements do occur with alteration (Scott and Rampe, 1984), there is obviously a very close association between magmatic and hydrothermal processes in this area.

Chalcophile and Sn-associated elements, Be, Bi, Cs, Cu, F, Li, Rb, Sn, Tl and Zn, are all higher and Ba and Sr lower in the biotites of Sn granitoids relative to non-Sn granitoids. Muscovites also shown these differences but generally at lower levels than biotites.

Inclusions of rutile (up to  $20 \times 8 \mu\text{m}$ ) occur along the cleavages of biotite and chlorite. Those in Sn granitoids have greater Nb, Ta, Sn and W content than those in less differentiated rocks from the same district. In an extreme case where tantalite/columbite forms e.g. in the dykes at Walwa, Sn and W contents of the Nb-Ta bearing phases are low due to the formation of separate Sn and W phases. Tantalum is subsidiary to Nb in the rutiles of granitoids giving rise to disseminated Sn deposits e.g. Ardlethan. However in pegmatitic deposits, e.g. Lode Hill (Scott, 1981), Ta is more abundant in the rutiles.

Therefore, once the phyllosilicate geochemistry has identified a Sn granitoid, rutile compositions may indicate whether associated mineralization is likely to be of pegmatitic or disseminated (greisen) form.

#### References

- Scott, K.M., 1981, Proc. Australas. Inst. Min. Metall., No. 280, 17-28.  
 Scott, K.M. and Rampe, M., 1984, J. Geochem. Expl., 20, 337-354.

**Nd and Sr isotope study of granitoids of the Blue Tier and  
Eddystone Batholiths, N.E. Tasmania, and associated Sn-W  
mineralisation**

S-S Sun<sup>1</sup>, N.C. Higgins<sup>1</sup>, M.T. McCulloch<sup>2</sup>

1. Bureau of Mineral Resources, Geology and Geophysics, Canberra
2. Research School of Earth Sciences, Australian National University

The middle to late Devonian plutons of the Blue Tier and Eddystone Batholith intrude quartzwacke and mudstone of the Ordovician-Devonian Mathinna Beds. Four granitoid types are recognized: hornblende-biotite granodiorite, biotite, biotite-cordierite-garnet granite and alkali feldspar granite (AFG). Minor diorite bodies and dolerite dykes are also present. Sn and W mineralisation is genetically associated with the AFG.

On the basis of geochemical data,  $^{87}\text{Sr}/^{86}\text{Sr}$  initial ratios (0.707-0.714), oxygen isotope data ( $\delta^{18}\text{O}_{\text{SMOW}} = +9$  to  $+13$ ), and radiometric age dates (367 to 388 m.y.), it has been established that the major plutons of the Blue Tier and Eddystone Batholiths were generated from heterogeneous crustal sources during a relatively short interval of granite magmatism (11 m.y.). Geochemical variation within each major granitoid type, except the AFG, is due to crystal fractionation possibly accompanied by some country rock assimilation (Cocker, 1982; Higgins et al., 1985; 1986; McClenaghan, 1985). According to Higgins et al. (1986) restite unmixing exerts little control on the chemical variation in these granitoids. The highly fractionated AFG appear to be derived by fractional crystallisation from spatially and temporally associated biotite and biotite-cordierite-garnet granite plutons, but are modified chemically by sub-solidus metasomatism involving albitisation, and locally, greisenisation (Higgins et al., 1985). Two petrographic types of AFG occur, namely, fine grained phyrlic AFG and fine to medium grained equigranular AFG. The former are texturally and chemically partially affected by sub-solidus albitisation, the latter represent completely recrystallised and metasomatised rocks. The two AFG plutons discussed in detail here, the Mt Paris and Anchor plutons, are spatially and temporally associated with the Poimena biotite granite pluton.

Major granitoid types (other than AFG) of the Blue Tier and Eddystone batholiths all have similar  $^{143}\text{Nd}/^{144}\text{Nd}$  initial ratios ( $\Sigma\text{Nd} = -4.9$  to  $-6.5$ ) at 370 m.y. More fractionated samples within individual plutons have lower  $\Sigma\text{Nd}$  values suggesting progressive involvement (up to 20%) of the sedimentary country rocks which have  $\Sigma\text{Nd}$  about  $-11$ . Alternatively, this variation may be partly related to source heterogeneity. The source model age for all granitoids (except AFG) based on a depleted mantle evolution model ( $T_{\text{DM}}$ ) is calculated to be about 1.5 b.y.

$\Sigma\text{Nd}$  initial ratios for mildly metasomatised phyrlic AFG from the Mt Paris and Anchor mine areas range from  $-6.9$  to  $-2.0$  (mostly  $-2$  to  $-4$ ) and do not follow the isotopic trend related to fractionation within the Poimena pluton (except  $\Sigma\text{Nd} < -6.5$ ), suggesting involvement of a component with higher  $\Sigma\text{Nd}$  value ( $\sim -2$ ) during their generation. This component could either represent the magmatic character of these AFG (the variation in  $\Sigma\text{Nd}$  due to source heterogeneity) or a metasomatic fluid which modified them. If the  $\Sigma\text{Nd}$  value of  $-2$  indeed represents the magmatic character of the AFG, then they cannot be directly related to the Poimena biotite granite pluton by simple fractional crystallisation. Furthermore the range in  $\Sigma\text{Nd}$  of  $-2$  to  $-6$  cannot be achieved by selective metasomatic leaching of the most

fractionated Poimena granite samples even if the poimena pluton is several million years older than the AFG.

Dolerite dikes and diorite bodies of similar age to the Blue Tier and Eddystone batholiths have positive  $\epsilon_{\text{Nd}}$  (+0.5 to +6) at 370 m.y. They have a chemistry similar to world-wide occurrences of post-orogenic alkali basalt dykes and may represent the surface expression of basic magmas involved in an underplating event which triggered melting of the lower crust to produce the granitoids (Higgins et al., 1986). The more positive  $\epsilon_{\text{Nd}}$  values of the AFG might be explained if these mafic magmas were somehow involved in their generation.

Nd and Sr isotope data from hydrothermal minerals (apatite, fluorite and siderite) deposited after the higher temperature albitisation and greisen alteration (and accompanying cassiterite deposition) suggest mixing of fluids of magmatic and meteoric (?) origins.  $^{87}\text{Sr}/^{86}\text{Sr}$  initial ratios of these minerals (0.721-0.723) are half way between magmatic (0.710) and country rock Mathinna Beds values (average 0.729 at 370 m.y.), except for one apatite sample (0.713); whereas  $\epsilon_{\text{Nd}}$  values of these minerals (-4.0 to -5.5, except one fluorite = -9.2) are closer to the magmatic (?) values of the AFG ( $\sim -3$ ) than values for Mathinna Beds ( $\sim -11$ ).  $^{87}\text{Sr}/^{86}\text{Sr}$  values of the hydrothermal minerals appear to respond to the influence of the country rock Mathinna Beds much faster than their corresponding  $\epsilon_{\text{Nd}}$  values, implying that Sr is more mobile than Nd during leaching of the Mathinna Beds. The Nd and Sr isotope data may suggest that meteoric (?) convective circulation in the country rocks entered the AFG soon after fractures developed in the granite during mineralisation.

#### References

- Cocker, J.D. 1982. J. Geological Society of Australia, 29: 139-158.
- Higgins, N.C., Solomon, M & Varne R. 1985. Lithos, 18: 129-149.
- Higgins, N.C., Turner, N.J. & Black, L.P. 1986. Contrib. Mineral. Petrol., 92: 248-259.
- McClenaghan, M.P. 1985. BMR Journal of Geology and Geophysics, 9: 303-312.

**THE FELBERTAL (MITTERSILL) SCHEELITE DEPOSIT, AUSTRIA:  
A W-Mo-Be VEIN SYSTEM RELATED TO FELSIC PLUTONISM,  
NOT A SUBMARINE-EXHALATIVE DEPOSIT**

Alfonso G. Trudu<sup>1</sup> & Alan H. Clark

Dept. of Geological Sciences, Queen's University, Kingston, Ont. Canada

<sup>1</sup>Now at Dept. of Earth Sciences, Monash University, Clayton, Vic. Australia

The Felbertal deposit near Mittersill, Austria, has been interpreted as the type example of submarine-exhalative scheelite mineralization (Höll, 1975). Höll describes the mineralization as comprising a sequence of scheelite-bearing quartzite horizons, genetically related to ultramafic to felsic volcanism, with minor quartz-scheelite veins, produced by a younger remobilization of uncertain origin. Our detailed studies of the K-1, K-5, K-6 and K-7 orebodies of the Western Sector mine of the Felbertal scheelite deposit, integrated within the regional geologic framework, lead us to reject this interpretation and to propose the following geological history:

1. calc-alkalic volcanism, periodically interrupted by pelitic to psammitic sedimentation, produced the Ordovician Habach Formation;
2. emplacement of an Ordovician mafic magma which crystallized into a rock (now coarse-grained amphibolite) displaying a gabbroic texture and a petrochemistry different from that of the calc-alkalic basalts; the gabbro is accompanied by small bodies of hornblendite;
3. Hercynian (Permo-Carboniferous) metamorphism of amphibolite grade, as shown by relict clinopyroxene in the coarse-grained amphibolite, and also documented at a regional scale;
4. post-metamorphic intrusion of the Permian Zentralgneis batholith which, we infer, is represented, at Felbertal, as sills and dykes of a highly differentiated, aplitic phase (now albite gneiss) containing country rock xenoliths and K-feldspar megacrysts, the latter feature common to the batholith. Scheelite ore is spatially and temporarily related to the aplite: it occurs largely as a stockwork of petrographically-distinct quartz veins and veinlets containing megacrystic scheelite  $\pm$  beryl (with Pb-Bi sulphosalts, calcite and magnetite) and also as fine-grained scheelite disseminations throughout the country rocks. The scheelite is Mo-rich, thus typical of an oxidizing environment; this is also indicated by relict magnetite associated with megacrystic scheelite. The reaction between country rocks and ore fluids is recorded by the formation of micaceous haloes around the wider veins and by alkali (K-Na-Rb) enrichment mostly in the gabbroic and aplitic rocks;
5. Cretaceous Alpine thrusting leading to isoclinal folding of veins and country rocks. Fracturing of megacrysts of Ca-amphibole in the coarse-grained amphibolite, K-feldspar in the aplite and scheelite and beryl in the quartz veins is inferred to have occurred during this event. Although the regional geology indicates blueschist facies metamorphism associated with the Alpine thrusting, no features indicative of such metamorphic grade are recognized at Felbertal, except, possibly, for albitic cores in plagioclase.
6. Main, Paleogene Alpine greenschist-amphibolite facies metamorphism and deformation producing penetrative foliation (best observed in the country rocks); open refolding (best seen in the veins); growth of pyrite and pyrrhotite in host rocks and veins; replacement of the rims of Mo-rich scheelite megacrysts by Mo-poor scheelite and molybdenite-tungstenite s.s. under reducing conditions. Scheelite was locally remobilized and reprecipitated as restricted Mo-poor disseminations parallel to the foliation in adjacent country rocks.

7. Retrograde lower greenschist facies metamorphism, coeval with uplift and formation of Alpine fissures during late Paleogene to Neogene times, when chloritic replacement of biotite occurred.

The bulk of the mineralization is inferred to be linked in space and time to an aplitic phase of the Zentralgneis itself and occurs in veins associated with alkali (K-Na-Rb) metasomatism. We interpret the scheelite mineralization of the K-1, K-5, K-6 and K-7 orebodies of the Western Sector mine of the Felbertal scheelite deposit to be genetically related to the Zentralgneis batholith. Scheelite precipitation resulted from the reaction between hydrothermal fluids and calcium-rich host rocks, and not by interaction between sea water and supposedly ore-bearing solutions venting out on a seafloor during calc-alkalic volcanism, as suggested by Höll (1975). Present data show that this ultramafic volcanic rocks are a gabbro and a hornblendite, and this quartz-keratophyre, inferred to be a unit of the Ordovician calc-alkalic volcanism, is an aplite related to the Zentralgneis plutonic complex. Although extensively deformed, the scheelite mineralization was remobilized only at a mesoscopic scale during the Alpine orogeny. Veins show polyphase deformation and cataclastic textures in scheelite and beryl megacrysts: this supports a pre-Alpine origin for the ore. This point is strengthened by the very large Mo-rich cores in megacrystic scheelite which could only have crystallized under oxidizing conditions, whereas a reducing environment prevailed during the Alpine orogeny when Mo-poor scheelite formed. The "scheelite-bearing quartzite", a crucial ore type in Höll's (1975) submarine-exhalative model, is absent in the Western Sector mine. The supposedly syngenetic banding characteristic of this ore type is interpreted as a secondary feature caused by deformation; thus the "scheelite-bearing quartzite" can be considered to be a deformed quartz vein. The close relationship between scheelite mineralization and the Zentralgneis on both a deposit and regional scale suggest that the genetic interpretation presented here applies to the entire Felbertal deposit, which should be considered as an example of W-Mo-Be hydrothermal vein deposit related to a felsic pluton.

#### Reference

- Höll, R. (1975) Bayer. Akad. Wiss., Math.-naturw. Kl., Abh., N.F., 157A, 114 p.



## TIN-TUNGSTEN MINERALISED GRANITES IN NEW ZEALAND

A.J. Tulloch<sup>1</sup>, I.F. Mackenzie<sup>2</sup><sup>1</sup>New Zealand Geological Survey, PO Box 30368, Lower Hutt<sup>2</sup>Canyon Resources, Sydney

Granitoid rocks of the New Zealand foreland are composed principally of 2 distinct ages with subequal volumes in each: the mid Paleozoic S-type Karamea Suite is overprinted by mid-Mesozoic I and intermediate I-S type suites (Tulloch 1983, Tulloch & Brathwaite 1986). The Karamea Suite hosts some scheelite occurrences while the I-type granites are associated with low-grade Mo (-Cu) mineralisation. Scheelite mineralisation is restricted to that area which the Karamea Suite shares with the I-S suite and the L. Paleozoic greywackes and argillites of the Greenland Group. Away from mineralised areas the latter contains av 3 ppm W and < 5 ppm Sn (Price 1984).

New Zealand granite-related Sn-W occurrences can be classified into 3 groups:

a) Scheelite dominated systems associated with small bodies of fine-grained (muscovite) red-brown biotite granite, intrusive into Greenland Group. High K/Na, low Sr,  $Fe^{3+}/2+$  etc. (Table 2) indicate affinity with the Karamea Suite, supported by a single Rb-Sr model age of 376 Ma at Barrytown (Adams 1974). At least 5 occurrences known; those at Barrytown, Doctors Hill and Batemans are documented in Tulloch (1985), McKenzie (1983) and Pirajno and Bentley (1985) and salient characteristics are summarised below and in Table 1. At Doctors Hill biotite content of the granite averages 13.3%, and at Barrytown it ranges from 8.9-18.6%. In all 3 areas scheelite is found in quartz-tourmaline veins, or quartz-muscovite (tourmaline) greisenised granite or greywacke-argillite of the Greenland Group. Weak propylitic (chlorite, clinozoisite, sphene, sericite) and intermediate argillic (kaolinite) alterations are also described at Barrytown. Abundant sericitic alteration, tourmalinisation (and argillisation at Barrytown), and general scarcity of fluorine minerals and low whole rock, biotite F suggest these systems lie on the Boron-Greisen join of Taylor's (1979) Boron-Greisen-Alkali classification of granite-hosted tin systems, probably towards the Boron apex. Scheelite dominates the ore mineralogy of all 3 deposits. Traces of cassiterite, chalcopyrite and molybdenite are common to all deposits, in addition to wolframite at Barrytown and sphalerite at Batemans. All 3 have associated pyrite, arsenopyrite, tourmaline and minor calcite and topaz(?). Rutile, hematite, pyrrhotite, marcasite, magnetite, graphite, loellingite, fluorite, and bismuth occur in some deposits. At Barrytown and Doctors Hill topaz is specifically associated with wolframite and cassiterite respectively.

b) Wolframite-cassiterite (-quartz) lodes occur in greisenised (quartz-mica-topaz) metasedimentary roof pendants within granites of S. Stewart Island (Williams 1934). No tourmaline was noted.

c) Scheelite (and minor chalcopyrite, pyrite, molybdenite and galena) occurs in quartz veins associated with I-type Cretaceous Separation Point granite at Canaan, close to (and also within) the host marble (Williams 1974).

Compared with granites from cassiterite-wolframite producing areas K/Rb and Li/Mg values suggest the known type a) New Zealand granites are not as

highly evolved (Table 2). Fluorine values are also much lower in New Zealand granites and biotites. The low F is reflected in the scarcity of topaz and fluorite (and cassiterite?) and is consistent with the formation of scheelite in preference to the wolframite more commonly found in griesens (Burt 1981). Biotite  $\text{TiO}_2$  tends to be relatively high as does whole-rock  $\text{TiO}_2$ ; whole rock Sn and W tend to be lower.

Evaluation of the Sn/W potential of granites should take account of the  $\text{TiO}_2$  content of the granite or biotite. Relatively high  $\text{TiO}_2$  (Table 2) leads to the development of secondary Ti-phases (sphene, anatase, rutile) which hold in situ at least some Sn/W presumably released from biotite during chloritization (Tulloch, 1985). The Sn/W content of these secondary phases is proportional to their Ti-content, and Sn/W in excess of that which they can accommodate under the relevant fluid conditions is required.

Table 1. Whole rock analyses of New Zealand Granites associated with scheelite.

	Barrytown 1	2	Doctor/Falls 3	4	Bateman 5	6
$\text{SiO}_2$	71.80	67.83	71.45	73.39	75.70	75.70
$\text{TiO}_2$	0.37	0.82	0.30	0.17	0.05	0.11
$\text{Al}_2\text{O}_3$	14.36	14.58	14.23	13.42	13.60	12.70
$\text{Fe}_2\text{O}_3$	0.33	0.66	2.50	2.11	1.22	1.60
FeO	2.00	3.68			0.72	0.92
MnO	0.02	0.05	0.05	0.03	0.10	0.03
MgO	0.71	1.49	0.64	0.36	0.20	0.38
CaO	0.57	1.38	1.40	1.35	0.36	0.48
$\text{Na}_2\text{O}$	3.19	2.54	2.78	2.88	5.44	3.33
$\text{K}_2\text{O}$	5.06	4.37	4.32	5.01	1.05	3.74
$\text{P}_2\text{O}_5$	0.14	0.27	0.07	0.05	0.36	0.08
LOI	1.69	2.15	1.34	0.85	0.85	1.29
Total	100.24	99.82	99.08	99.59	99.65	100.36
Rb	314	275	211	253	150	190
Sr	68	113	102	79	37	99
Ba	311	480			47	308
U	9	6				
Th	25	27	28			
Nb	18	20	12	10		
Zr	155	259	141	131	40	66
Cu	15	48	5	13	17	18
Zn	86	98	45	43	12	25
Pb	41	30	38	39	2	11
Y	31	44	45	45	6	20
B	40	80	167		1025	200
F			512		760	866
Li	124		78		15	48
W			4	<3	<10	10
Sn	15	15	<1	<1	60	17

1/2 represent core and rim of pluton, 3/4 and 5/6 are averages of 2 main granite groups.

Table 2. Comparative data for W/Sn granites from New Zealand and producing areas.

	K/Rb	Li $\times 10^3$ Mg	B	F	Nb	Bio. F	Bio. $\text{TiO}_2$	Bio. Fe/Fe + Mg	W	Sn	References
S. China	78	337		3716	29-43	1.2-2.4	2.10	>62	4-13	28-32	1, 2,
Cornwall	65	83-7048	50-1200	3000-15,000	25-45	1.35			20-30	10-58	3, 4, 5, 12
Malaysia (M. Range)	78				8				4	7	6
(E. Belt)	140				6				2	5	6
Australia (Anchor)	73			5800		2.70	1.66			29	7
Australia (Ardlethan)	55	>93		2825		2.79	0.98	>82	<11	37	8
Japan (Kyushu)						1.26					9
World-av. Sn granite	67	141		3700					7	40	10
World-av. low Ca granite	247	25	10	850	21				2	3	11
NZ Barrytown	145	16	53	<500	19	<0.45	3.61	66	9	10	
NZ Doctors Ck	171	20	167	512	12	<0.45	2.52	81	3		
NZ Bateman Ck	133	20	475	830	?				7	19	
NZ barren	190						3.16				

1 Liu Yingjun et al. 1984, 2 Sun Nai et al. 1984, 3 Hawkes 1984, 4 Exeley et al. 1983, 5 Puge 1977, 6 Hutchison 1977, 7 Groves 1972, 8 Scott and Rampe 1984, 9 Nedachi 1980, 10 Tischendorf 1977, 11 Turekian and Wedepohl 1961, 12 Jackson 1979.

- Adams, C.J., 1974, Institute of Nuclear Sciences Rept R-140.  
 Burt, D.M., 1981, *Economic Geology*, **76**, 832-843.  
 Exeley, C.S., et al., 1983, pp. 153-177 in *The Variscan Fold Belt in the British Isles*, ed P.L. Hancock.  
 Fuge, R., 1977, *Contrib. Min. Petrol.*, **61**, 245-249.  
 Groves, D.L., 1972, *Economic Geology*, **67**, 445-457.  
 Hawkes, J.R., 1984, p. 571-593 in *Geology of Granites and their metallogenetic relations*, ed Xu Keqin and Tu Guangchi.  
 Hutchison, C.S., 1977, *Bull. Geol. Soc. Malaysia*, **9**, 187-208.  
 Jackson, N.J., 1979, *Bull. Geol. Soc. Malaysia*, **11**, 209-238.  
 Liu Yingjun, et al., 1984, pp. 753-770 in *Xu Keqin and Tu Guangchi, ibid.*  
 Mackenzie, I.F., 1983, MSc thesis, Victoria University of Wellington.  
 Nedachi, M., 1980, *Mining Geol. Special Issue*, **8**, 39-48.  
 Pirajno, F., Bentley, 1985, *N.Z. J. Geol. Geophys.*, **28**, 97-110.  
 Price, G.D., 1984, CRA Exploration, Papanos Report no. 12676.  
 Scott, K.M., Rampe, M., 1984, *Jl. of Geochem. Expl.*, **20**, 337-354.  
 Sun Nai, et al., 1984, p. 223-240 in *Xu Keqin and Tu Guangchi, ibid.*  
 Taylor, R.G., 1979, *The Geology of Tin Deposits*.  
 Tischendorf, G., 1977, in *Metallization Associated with acid magmatism*.  
 Tulloch, A.J., 1983, *Geol. Soc. Amer. Memoir*, **159**, 5-20.  
 Tulloch, A.J., 1985, *Proc. IGCP 220 Chiang Mai Symposium* (in press).  
 Tulloch, A.J., Brathwaite, R.L., 1986, *N.Z. Geological Survey Record*, **13**, 65-92.  
 Turekian, K.K., Wedepohl, K.M., 1961, *Geol. Soc. Amer. Bull.*, **72**, 175-192.  
 Williams, G.J., 1934, *Economic Geol.*, **29**, 411-434.  
 Williams, G.J., 1974, *Economic Geology of New Zealand*.

Comments on this work by R.L. Brathwaite are appreciated.

11

## FRACTIONATION AND MINERALISATION IN THE BOGGY PLAIN ZONED PLUTON

Doone Wyborn

Bureau of Mineral Resources, Box 378, Canberra City, ACT 2601, Australia

The Boggy Plain zoned pluton is a 36 km<sup>2</sup> complex at the northern end of the Kosciusko Batholith, SE Australia, that ranges in composition from high temperature (1150°C), dioritic (50% SiO<sub>2</sub>) margin to aplitic 75% SiO<sub>2</sub> core. The mafic rocks are part of a more extensive zone of cumulate rocks at depth, derived from an andesitic liquid in a sub-volcanic magma chamber. Complementary, high temperature (1000°C), rhyolitic liquids (72% SiO<sub>2</sub>) accumulated at the top of the chamber, probably above a double diffusive interface. They most likely escaped to the surface to form a centred volcanic complex. The more felsic rocks of the pluton formed from the residue of the original magma when the rhyolitic liquid was no longer able to escape up the margins of the pluton adjacent to the crystallisation front by boundary layer flow. Closed system fractionation then proceeded in the felsic rocks. The fractional crystallisation behaviour of this originally aphyric magma is in marked contrast to that seen in most granite plutons, where it is suggested that the presence of abundant (perhaps up to 60%) suspended solid (primary restite, altered restite and early crystallised solids) prevents fractional crystallisation from taking place.

In the most felsic rocks of the complex, water pressure reached total pressure and high temperature hydrothermal alteration produced low grade disseminated scheelite mineralisation. The alteration had little effect on the silicate mineralogy of the original rocks, with feldspars remaining unaltered. The alteration is mainly expressed in the accessory minerals, with HREE enrichment in apatite and sphene, formation of metamict rims on zircons, (with the rims enriched in HREE, U, Th, Y and Hf) and the growth of a complex U, Y, Ta, Ti, Nb oxide of the clinocllore group. The hydrothermal solutions carried high field strength elements such as W, U, Th, Y, HREE's, Nb, Ta, Zr, and Hf, but not LIL elements such as Rb, Li, La, and Ce. They had some similarities to the solutions (?magmas) that generate heavy metal pegmatites.

PRIMARY MAGMATIC CONTROL ON THE DISTRIBUTION OF Sn DEPOSITS  
OF THE LACHLAN FOLD BELT IN N.S.W. AND VICTORIA

L.A.I. WYBORN<sup>1</sup>, B.W. CHAPPELL<sup>2</sup>, AND D. WYBORN<sup>1</sup>

1. Bureau of Mineral Resources, Canberra

2. Australian National University, Canberra

A synthesis of the regional granite geochemistry of the Lachlan Fold Belt in N.S.W. and NE Victoria has shown that it is possible to divide the S-types into three supersuites; that associated with the Wagga Metamorphic Belt; that from the Kosciusko Belt including the Kosciusko, Berridale, Young, Wyangala, and Murrumbidgee Batholiths; and the Cooma supersuite, the latter of which is derived exclusively from Ordovician sediments and is volumetrically insignificant. Most of the Sn deposits of the Lachlan Fold Belt in N.S.W. and Victoria are related to S-type granites. The more significant deposits are concentrated in a NNW trending belt between Nymagee and Albury, and are associated with the Wagga Belt granites.

Above 69 SiO<sub>2</sub>% the Wagga Belt granites differ significantly from those in the Kosciusko Belt in two groups of elements. The first group of elements, which consist of Al, K, Rb, Nb, Ga, P, and U, increase with increasing SiO<sub>2</sub> in the Wagga Belt and have higher values at similar SiO<sub>2</sub> contents than those of the Kosciusko Belt. Rb values can be up to 1330 ppm (Ardlethan Granite) and P<sub>2</sub>O<sub>5</sub> values are up to .34 wt %. The second group of elements, which include Fe<sup>3+</sup>, V, Th, Y, and Ba, decrease with increasing SiO<sub>2</sub> and are lower at similar SiO<sub>2</sub> values. Below 69 SiO<sub>2</sub>% the differences between granites from the two Belts are more subtle, and the Wagga Belt granites have more Al, Ti, P, Ca, Sr, Pb, and Zr, and lower Mg and Fe.

The differences above 69 SiO<sub>2</sub>% reflect magmatic processes with the differences in the Wagga Belt granites reflecting fractionational crystallisation, as opposed to the Kosciusko Belt granites in which the chemical variation is controlled by separation of restite. In the Wagga Belt granites, Al increases with increasing SiO<sub>2</sub>, and P, Ga, and Nb increase whilst Fe<sup>3+</sup> and V decrease as a function of the resulting increasingly peraluminous nature of the liquid. These trends suggest that aluminosilicate is not an early crystallising phase in felsic peraluminous liquids, but that fractionation of quartz and feldspar drives the liquid to an even more peraluminous composition. K and Rb increase with fractionation and there is a complementary decrease in Ba, Sr, and the K/Rb ratio. These chemical changes are not found in the Kosciusko Belt granites until at least 73 SiO<sub>2</sub>%, as at lower values compositional variation is dominated by separation of restite crystals. This implies that the initial melt composition was 73 SiO<sub>2</sub>% for the Kosciusko Belt granites, in contrast to a more mafic value of 69 SiO<sub>2</sub>% for the Wagga Belt granites.

It is possible to speculate on the cause of the two distinct trends. The chemical differences between the two granite types below 69  $\text{SiO}_2\%$  suggest a higher detrital content of feldspar, apatite, and zircon and an illite-rich clay fraction for the source of most of the Wagga Belt granites. Hence a greater percentage of melt can be obtained at lower temperatures and with a higher water content. Further, a comparison of the geothermal gradient from the Wagga Metamorphic Belt with that of the Cooma region, suggests that the western geothermal gradient was lower and that melting and dehydration occurred simultaneously in upper amphibolite grade. In contrast, in the eastern Belt, dehydration occurred prior to the onset of melting, and hence most melting took place under granulite conditions, as shown by the mineral assemblages in the S-type volcanics comagmatic with granites of the Kosciusko Belt. The resulting water-rich, relatively maric (69%  $\text{SiO}_2$ ), low-viscosity melts of the Wagga Belt would favour early separation of the restite component, and an early onset of fractional crystallisation. In contrast, in the water-poor, felsic (73%  $\text{SiO}_2$ ), high-viscosity melts of the Kosciusko Belt, separation of restite from the melt was inhibited. Thus, in systems where there is early onset of fractional crystallisation, the melt has a greater chance of concentrating ore producing elements such as Sn. In a dominantly restite controlled melt system, it is not possible to obtain a greater concentration of any element other than that which is in the source or the melt.

We suggest that distinction between granite melts which have evolved by fractional crystallisation as opposed to those which have formed by separation of restite from a constant-composition melt component is important in differentiating between mineralised and non-mineralised granites. Fractionation of peraluminous melts is important in the generation of Sn deposits, and unusual chemical features such as those found in the Wagga Belt granites, viz. high Rb, P, K, and the low  $\text{Fe}^{3+}$  contents of these granites are a function of primary magmatic processes, not of alteration or wall rock interaction. Similiar chemical parameters to the felsic Wagga Belt granites are found in tin-related S-type granites in Cornwall, Malaysia, and western Tasmania. However, only in the Wagga Belt granites is it possible to observe the petrological processes below 69%  $\text{SiO}_2$ , and confirm that the major and trace element concentrations are controlled by fractional crystallisation of a peraluminous melt.

## A General Survey of Tungsten Deposits of China

Xu Keqin, Sun Mingzhi, Cheng Hai

Tungsten deposits of China can be divided into 3 categories and 6 types as follows:

- A. Tungsten deposits genetically related to granitic rocks:
  1. Hypothermal wolframite-quartz vein deposits.
  2. Pyrometasomatic scheelite-bearing skarn deposits.
    - a. Deposits related to transformation type granites.
    - b. Deposits related to syntexis type granitoids (W-deposits, W-Mo deposits, W-Cu deposits).
- B. Tungsten deposits related to sub-volcanics, volcanics, granite porphyries, and granites of shallow emplacement:
  3. Epithermal and mesothermal tungsten vein deposits (with scheelite, ferberite or hubnerite as the ore mineral, and may be associated with stibnite, gold or other sulphides).
  4. Porphyry tungsten deposits, including tungsten-bearing breccia-pipes (W-deposits, W-Mo deposits, W-Sn deposits).
  5. Submarine exhalative deposits with tungsten absorbed in iron or manganese oxide bed.
- C. Stratabound tungsten deposits in metamorphic rocks not directly related to granitic or subvolcanic rocks.
  6. Stratabound scheelite, or scheelite-stibnite-gold, or other stratabound tungsten deposits.

Of the above 6 types, the most important are the hypothermal wolframite-quartz vein deposits and pyrometasomatic scheelite-bearing skarn deposits, which together constitute more than 90% of the total production or reserves. Porphyry tungsten deposits, as discovered in recent years, may prove of importance in future.

In different tectonic environments in China, tungsten deposits occur in different geologic periods, such as Late Proterozoic (Shuefengian), Caledonian, Hercynian, and Yanshanian, but most industrial deposits occur in the early Yanshanian time. They are distributed mainly in Jiangxi, Hunan, Guangdong and Guangxi provinces. In other provinces they are only sparsely distributed.

Different genetic types of granitoids bear different relations to tungsten deposits, as shown in the following table.

Types of deposits	Transformation type granite	Syntexis type granitoids
Hypothermal wolframite -quartz vein deposits	very important	rare, unimportant
Pyrometasomatic scheelite deposits	very important	very important
Porphyry tungsten deposits	unimportant	important
Epithermal and mesothermal tungsten veins	important	important
WO <sub>3</sub> absorbed in submarine	not known	important

hematite beds

Associated metal elements	Sn, Be, Bi, Nb, Ta, REE	Mo, Cu (Fe, Pb, Zn)
---------------------------	----------------------------	---------------------

Although pyrometasomatic scheelite deposits can be associated with both types of granitoids, they have, however, somewhat different characteristics. The skarn deposits related to transformation type granites are often superimposed by greisenization phase, and possibly associated with wolframite-quartz veins; and the mineral assemblages are often characterized by abundant idocrase, fluorite, lithium micas and alkaline feldspars. All these features are uncommon to those associated with syntexis type granitoids. The latter may contain Cu, Mo, or less commonly, Fe, Pb, Zn ores of industrial importance. Both types of skarn deposits are important, but several large deposits in South China are associated with transformation type granites.

As regard the tectonic environments for the formation of tungsten-bearing granitoids, several examples can be given:

1. SE China is a wide geosynclinal region, with different periods of orogenic movements, accompanied by corresponding granite formation. From NW to SE, occurs a successive shifting of fold zones in such sequence: the Middle to Late Proterozoic folded basement, the Caledonian folded basement, the Hercynian-Indosinian folded basement (along the seacoast) and the Yanshanian folded basement. During the Hercynian time, the SE China crust began to differentiate, and there occur a series of SE-trending fault depression zones incising the well-developed continental crust. During the Late Mesozoic time (Yanshanian), when the subduction of the Pacific plate toward the Asian plate was intensified, these tensional deep fault zones were the sites of intensive volcanism and intrusion of syntexis type granitoids, with elevated Moho surface below these depression zones. Outside of these zones, volcanism was much weaker, but the transformation type granites are widespread. Therefore, Mesozoic granitoids of SE China are probably related to the subduction of Pacific plate. The syntexis type granitoids are directly related, with part of the source materials coming from the upper mantle, whereas transformation type granites only indirectly related, mainly from the heat affect.

2. In E. Qinling region (W. Henan province) the Nannihu W-Mo deposits of the Yanshanian age occur in tectonic environment quite different from that of SE China. They are located on the Middle to late Proterozoic active margin of the N. China plate. Through later geologic processes, the crust had been much thickened. The Yanshanian block movements led the intrusion of granodiorite porphyries, which are associated with W-Mo mineralization. Therefore, the W-Mo-bearing granitoids have no connection with plate movements.

3. The W- (and Sn-) bearing granites in W. Yunnan province are probably related to the collision of continental plates.

In general, it seems that, the different properties of the basement rocks may control the types of granitoids, and that, all tungsten-bearing granitoids have been derived mainly from continental crust. The authors believe that a preliminary concentration of tungsten in some horizons of the basement strata is an important controlling factor for tungsten deposits.

# GEOLOGICAL, PETROLOGICAL AND GEOCHEMICAL CHARACTERISTICS OF GRANITOID ROCKS IN BURMA: WITH SPECIAL REFERENCE TO THE EMPLACEMENT OF W-Sn MINERALISATION

Khin Zaw

Geology Department, Rangoon University, Thamaing College P.O. Thumaing,  
Rangoon, Burma

The granitoid rocks in Burma extend over a distance of 1450 km from Putao Kachin State in the north through Mogok, Kyaukse, Yamethin and Pyinmana in Mandalay Division to Tavoy and Mergui area, Tenasserim Division at south. The Burmese granitoids can be subdivided into N-S trending, three main belts viz. western granitoid belt, central granitoid belt and eastern granitoid belt. The western belt granitoids are characterised by high-level epizonal intrusions associated with Porphyry Cu-related, younger volcanics. They are thought to have been emplaced as a magmatic-volcanic arc (inner magmatic-volcanic arc) above an east-dipping, but westwardly migrating subduction zone related to the prolonged plate convergence which occurred during Late Mesozoic and Cenozoic.

The central granitoid belt is characterised by mesozonal, mostly Late Cretaceous to Early Eocene granitoid plutons associated with abundant pegmatites and aplites, numerous vein-type W-Sn deposits, and almost lack of comagmatic volcanics. The country rocks are structurally deformed, metamorphic rocks of greenschist to upper amphibolite facies ranging in age as early as Late Precambrian to upper Palaeozoic and locally of fossiliferous, metaclastic rocks (Middle Jurassic to Lower Cretaceous). Available K/Ar radiometric data indicate a significant and possibly widespread thermal disturbances in the central granitoid belt during Tertiary.

Present geological, petrological and geochemical evidences demonstrate that the W-Sn related, central belt granitoids are mostly quartz monzonite and granodiorite with minor granite gneiss formed from a source of continental, sialic materials rather than from the mantle or oceanic crust. Highly potassic character and high initial  $^{87}\text{Sr}/^{86}\text{Sr}$  ratios ( $0.717 \pm 0.002$ ) and Rb/Sr ratios (0.4-33.07) with an average value of (6.70) further add support that the granitoid magma was derived from a well established continental, sialic basement. None of the present evidence argue that the granitoid magma was generated by the remelting of the regionally metamorphosed, Late Precambrian through Upper Palaeozoic to Early Mesozoic, metasedimentary country rocks. The close association of the W-Sn bearing quartz veins and the granitoid rocks also suggests that the metals were derived from a similar crustal source. The central belt granitoids are considered to have been emplaced during the continent-arc collision of inferred Late Triassic-Jurassic magmatic-volcanic arc with continental foreland to the east at the early stage of westward migration of the east-dipping subduction zone to the west. The W-Sn related, central belt granitoids of Late Mesozoic-Early Eocene are notably different from those of mainly Triassic granitoids from northern Thailand and Permo-Triassic granites of Malay Peninsula, and thus the central belt granitoids were emplaced in a uniquely distinct geologic and tectonic setting in SE Asian region.

Na-K-Ca plots of the compositions of the central belt granitoids which are associated with either minor W-Sn occurrences or lode type W-Sn deposits fall within the field of Sn-mineralising granites of Juniper and Kleemann (1979) but outside that field on a  $\text{SiO}_2\text{-CaO-MgO-FeO-Na}_2\text{O+K}_2\text{O+Al}_2\text{O}_3$  plot.



Trace elements abundances of the central belt granitoid rock suggest that Sn content of the granitoids alone should be used with great cautions to discriminate W-Sn bearing (mineralized) granitoid plutons from W-Sn poor (barren) plutons in search for W-Sn deposits in Burma, but trace elements data reveal the tendency that the granitoid plutons which bear W-Sn mineralization are comparatively more enriched in Be, Bi, Cu, Mo, Pb, Sn, Y, and Zn but less depleted in Ba and Zr than those plutons in which no W-Sn occurrences were recorded.

The eastern belt granitoids are still largely unknown but characterized by medium- to coarsely porphyritic texture and the country rocks of regionally metamorphosed, turbiditic sediments of Chaung Magyi Group (Late Precambrian). This eastern granitoid belt lies immediately north of mostly Triassic granitoids in northern Thailand, and Sn-W bearing, mesozonal, Permo-Triassic, Main Range granitoids in the eastern part of Malay Peninsula, which were considered to have been emplaced during continental collision. Alternatively, present available geological evidences can not rule out the possibility that the eastern belt granitoids were emplaced in a continental margin above an eastward subducting ocean floor during Early Palaeozoic.

Using the criteria of Chappell and White (1974), the porphyry Cu-related, western granitoid belt pluton are I-type while W-Sn related, central granitoid belt contains both hornblende-bearing I-types as older intrusive phases and W-Sn bearing, S-types as younger plutonic phases. The eastern belt granitoids can not be demonstrated as either I-types or S-types as petrochemical data are still lacking.

# Preliminary Studies on Geology and Geochemistry of two types of Porphyry Tin Deposits in Southern China

Zhu Jinchu, Xu Keqin, Zhu Zhengshu

(Department of Geology, Nanjing University, China)

There exist two types of porphyry tin deposits related to transformation series (similar to S-type) and syntexis series (similar to I-type) granitoids in southern China, both of them are of economic importance.

Porphyry tin deposits related to transformation series granitoids are usually associated with small stocks or dikes of granitic porphyries, which are differentiates of granitic magma derived from anatexis of metasedimentary rocks. Yinyan porphyry tin deposits is typical of this kind.

It occurs in an uplift area of the Caledonian geosynclinal foldbelt. The tin-bearing granite porphyry, as a blind pipe-like stock of about 92 Ma (by K-Ar whole-rock dating), intruded into late Precambrian metamorphic rocks. Except for some quartz porphyry dikes exposed on surface, no Mesozoic volcanic rocks and plutonic batholiths are found around the deposit area. Tin mineralization in form of cassiterite accompanied by wolframite is disseminated and veinlet-disseminated within the greisenized porphyry. The least altered porphyry (observed from drill cores) is fleshred. The grain size of phenocrysts (30-40% in volume) is 1 to 3 mm, which are composed of quartz, oligoclase ( $An=12-25$ ), orthoclase (including perthite) and Fe-biotite (<5%). Petrochemically, the porphyry is peraluminous, with  $SiO_2 > 74\%$ . It is rich in Li (258 ppm), Rb (1291 ppm), Cs (24 ppm), U (20 ppm), <sup>2</sup>Th (33 ppm), Y (94 ppm), F (5475 ppm), as well as ore-forming element Sn (107 ppm), but depleted in Sr (13 ppm), Ba (42 ppm), Co (2 ppm), Ni (2 ppm). Zr and Nb contents are 75 ppm and 48 ppm respectively, relatively lower as compared with alkali granites. REE patterns exhibit marked negative Eu anomalies ( $Eu/Eu^*=0.03$ ) and V-shaped flat curves with  $\Sigma REE$  (14 elements) 213 ppm and La/Yb ratio 1.5. The  $\delta^{18}O$  value of whole rock is 9.55%. All above-mentioned characteristics suggest that the ore-bearing porphyry is produced by fractional crystallization of anatectic magma from metasedimentary rocks.

Wall rock alterations from the deeper level upwards can be identified and divided into following vertical zones: (1) less altered granite porphyry (with weak K-feldspathization, (2) protolithionite (10-35%) - quartz greisenization, (3) topaz (10-40%) - quartz greisenization (4) sericite-quartz sericitization, and (5) massive quartz core silicification. The tin mineralization is mainly associated with topaz-quartz greisenization. There is no leaching zone of ore-forming elements. The presence of large amount of F-rich minerals such as topaz and protolithionite indicates that fluorine, rather than chlorine, plays a predominant role in tin transportation. Interactions of ore-forming fluid with country rocks destroy the stability of F-bearing tin complex, and result in deposition and mineralization of tin.

Fluid inclusion studies and oxygen isotope analyses of cassiterite (1.47%) - quartz (9.33%) mineral pair show that ore-forming temperatures range 320-350°C with  $fO_2$  about  $10^{-34.3}$  b. Therefore, the metallogeny of transformation series porphyry tin deposits should be the result of both geochemical heritage and magmatic differentiation.

Syntexis-series porphyry tin deposits, such as Tashan and Xiling, occur in Mesozoic volcanic belt. Tashan tin-bearing porphyries are late-stage quartz-porphyry dikes which are distributed along fractures in strata. The  $\delta^{18}\text{O}$  values range 4.8-7.1%. The  $\delta^{18}\text{O}$  value of cassiterite is 1.3%. Xiling tin deposit is related to volcanic rocks (rhyolitic ignimbrite) which grade downwards into quartz diorite porphyrite with copper-sulfide mineralization. The tin-bearing rock has low Li (<20 ppm) and Rb (<250 ppm) contents. REE patterns of the ore bearing rocks show LREE enrichment and HREE depletion, with  $\Sigma\text{REE}$  (14 elements) ranging 119-204 ppm and  $\text{Eu}/\text{Eu}^*$  0.41-0.79. The  $\delta^{18}\text{O}$  values are in range 9.1-10.0%, and the initial Sr ratio is 0.7081.

Based on the petrochemical, geochemical and isotopic characteristics it is proposed that both tin and copper-polymetallic mineralizations are genetically related to the hydrothermal systems differentiated from the same magma chamber at different stages. The tin bearing acidic volcanic rock falls into syntexis series granitoids. Sericitization is the main wall rock alteration in the tin deposit.

In addition, because this type of porphyry tin deposit usually occurs in volcanic or metasedimentary strata with higher tin content, it is possible that the ore-forming process is not only related evolution of magma, but also associated with tin-bearing strata.

#### Comparison between two types of porphyry tin deposits

	Yinyan type	Xiling type
Tectonic setting	Geosynclinal foldbelt inside the continental plate	Volcanic belt near deep fault along continental margin
Petrology	Associated with transformation series granitoids, differentiated as small stocks from granite magma	Associated with syntexis series granitoids occurring as volcanic-subvolcanic rocks
Alteration	K geldsparthization-greisenization-sericitization-silicification. Mineralization mainly associated with topaz greisen	K feldsparthization-sericitization-silicification. Mineralization associated with sericitization
Ore mineral association	Sn-W-Mo-Bi less sulfides	Sn-Cu more sulfides
$\text{Nb}_2\text{O}_5 + \text{Ta}_2\text{O}_5$ in cassiterite	> 0.05%	< 0.05%